Center for
Materials Science

Metallurgy Division

Technical Activities 1984

NBSIR 84-2995
January 1985

U.S. Department of Commerce
National Bureau of Standards

Center for
Materials Science

Metallurgy Division

Dr. Louis R. Testardi, Chief
Dr. Gilbert Ugiansky, Deputy Chief

Technical Activities 1984

NBSIR 84-2995
January 1985

DEPARTMENT OF COMMERCE · NATIONAL BUREAU OF STANDARDS

U.S. Department of Commerce
National Bureau of Standards

METALLURGY DIVISION

CHIEF

Louis R. Testardi
Phone: (301) 921-2811

DEPUTY CHIEF

Gilbert M. Ugiansky
Phone: (301) 921-2811

GROUP LEADERS

Structure Characterization
Masao Kuriyama
Phone: (301) 921-2986

Metallurgical Processing
John R. Manning
Phone: (301) 921-3354

Wear and Mechanical Properties
Arthur W. Ruff
Phone: (301) 921-2966

Chemical Metallurgy
Kirit J. Bhansali
Phone: (301) 921-2982

Corrosion
E. Neville Pugh
Phone: (301) 921-2094

Electrodeposition
David S. Lashmore
Phone: (301) 921-2958

Nondestructive Characterization
Haydn N. G. Wadley
Phone: (301) 921-2956

ABSTRACT

This report summarizes the FY 1984 activities of the Metallurgy Division of the National Bureau of Standards. The research centers upon the structure-processing-properties relations of metals and alloys, and on the methods of their measurement. Task efforts comprise studies of synchrotron radiation research for materials characterization, metallurgical processing, wear and mechanical properties, chemical metallurgy, corrosion and protection of metals, electrodeposition, and nondestructive characterization.

The work herein described includes three cooperative data programs with American professional societies and industry: the American Society for Metals-NBS Alloy Phase Diagram Program, the National Association of Corrosion Engineers-NBS Corrosion Data Program, and the American Iron and Steel Institute-NBS Steel Sensor Program.

New facilities include specialized hardware for the National Synchrotron Light Source, Hot Isostatic Pressing apparatus, gas atomizer for rapidly solidified powder production, a 300 kV transmission electron microscope, and a thermal wave measurement system.

The scientific publications, invited talks, committee participation, and other professional interactions of the 95 full-time and part-time permanent members of the Metallurgy Division and its 30 guest researchers are identified.

TABLE OF CONTENTS

METALLURGY DIVISION (450)

L. R. Testardi, Chief
G. M. Ugiansky, Deputy Chief
A. M. Marinoff, Secretary

The Metallurgy Division conducts fundamental research on the structure-properties-processing relations of metals and alloys, and on the methods of their measurement. It also evaluates data, compiles data bases, and produces standard reference materials. It performs these activities for the benefit of American industry, government, and universities. Within the Division the work is carried out in seven discipline or interest-oriented groups.

The National Bureau of Standards/Center for Materials Science (NBS/CMS) part of the National Synchrotron Light Source (Brookhaven) is now instrumented. The specialized and unique hardware was designed and built by the Structure Characterization Group and will provide microstructural analytic techniques including Extended X-ray Absorption Fine Structure (EXAFS), Small Angle X-ray Scattering (SAXS), monochromatic and white beam tomography, microradiography, and diffractometry. An experimental program has been simultaneously carried out at Cornell's High Energy Synchrotron Source (CHESS) and its accomplishments, as well as those of all groups, are noted below. An important new research thrust into interface studies is now being established. This will couple new material forms (thin films, epitaxial layers, and modulated structures) with research into establishing new x-ray techniques for the structural characterization of interfaces.

A new kind of solid phase, intermediate between a crystal and a liquid and formed by rapid solidification, has been shown to exhibit long range orientational order but possesses 5 fold point group symmetry which cannot be consistent with translational periodicity.

Major hardware acquisitions for metals processing have now been completed. The Hot Isostatic Pressing (HIP) apparatus has been undergoing its initial runs. The e-beam surface melting equipment has been refined to yield better control and measurement of operating performance. An inert gas atomization system capable of producing up to 50 pound lots has also been installed. This provides excellent new facilities to support our major effort in rapid solidification, and the relation of processing variables to phase occurrence, microstructure, and performance. Peter Voorhees, following his completion of a National Research Council Postdoctoral appointment, has joined our permanent staff and will be collaborating with the Metallurgical Processing Group.

A technique for automated, electronically controlled, nonoptical, microhardness measurement with dynamic response capabilities has been developed in our Wear and Mechanical Properties Group. A 300 kV transmission electron microscope with improved resolution and depth penetration over older models was installed at CMS during the past year and is being currently used (among other programs) in our wear studies. New work in wear and mechanical properties has been initiated for the Bureau of Engraving and Printing, and the Consumer Product Safety Commission. An Industrial Research Associate position is being established in the galling wear area with Deere and Co., Moline, IL. A new materials characterization technique, thermal wave imaging, has been installed during the past year and is already incorporated in a 1985 research program. We are very pleased that A. William Ruff received the American Society for Metals 1984 George Kimball Burgess Award.

The American Society for Metals (ASM) has essentially reached their planned goal of raising four million dollars to support the ASM/NBS Alloy Phase Diagrams Program. The NBS output and responsibilities have continued to grow. Eighteen Ti-, eight Al-, and five Fe-based binary systems have been evaluated by NBS scientists. The Bulletin of Alloy Phase Diagrams is now published bimonthly (instead of quarterly). The bibliographic data base is nearly current, the prototype computerized phase diagram data base and graphics system are under continued development. The first book and hard cover published outputs of the program are being planned for late 1985. NBS is playing a major role in expanding the ASM/NBS program into full international cooperation. A new Research Associate from ASM has joined us during the past year.

Activities of the Corrosion studies group have developed greater focus in the two areas of greatest interest to us; fundamental studies on localized corrosion and corrosion data. A highly successful workshop in environmentally-induced cracking was organized and held at NBS. The new Corrosion Data Center, in support of the recent National Association of Corrosion Engineers-NBS (NACE-NBS) Cooperative Data Program, has continued to increase its internal staffing support and its interactions with the external community of potential data users and suppliers. A new NACE-supported Research Associate has joined the program. Michael Kaufman has also joined our staff and has initiated activities in fundamental studies. We are particularly pleased that E. Neville Pugh has received the 1984 Willis Rodney Whitney Award from the National Association of Corrosion Engineers.

Our work in the production of Standard Reference Materials by electrodeposition is continually augmented by new requests from American industry. Development of microhardness standards in the range 800 - 1000 (Vickers and Knoop) is in progress. New corrosion "step test" standards have been requested by the automotive industry and are currently being researched. Other new areas include theoretical modelling of alloy electrodeposition and experimental work in electrodeposited "matrix" coatings on fibers for use in metal matrix composite materials. Patents on our process, and the application, of ultra-black coatings have been granted. The Bureau of Engraving and Printing is funding a new program to study the coating technology of engraving plates.

Cooperative work with the American Iron and Steel Institute to develop sensors for steel processing continues to be a major activity of the Nondestructive Characterization Group. New high temperature electromagnetic acoustic transducers (EMATS) have been obtained and are now undergoing evaluation. Theoretical work coupling the temperature measurement problem with classical heat flow has shown how the complexity of the task can be reduced. Ultrasonic imaging, acoustic emission, and eddy current techniques are receiving major attention in our goal to develop in-situ measurement capability for materials processing.

The Division was staffed in 1984 by 95 full-time and part-time permanent people. In addition, there were 30 guest researchers and research associates in residence during the past year who collaborated with us on our studies.

The activities of the Division are formally identified in seven tasks which largely parallel the objectives of the seven groups. These tasks are listed below. The major accomplishments associated with each of these tasks, and a fuller description of task-related activities follow.

Task 26105--SYNCHROTRON RADIATION RESEARCH FOR MATERIAL SCIENCE. Relates to joint NBS/Naval Research Laboratory x-ray instrumentation complex at the National Synchrotron Light Source, and its use to perform microstructural characterization.

Task 15442--STRUCTURE CHARACTERIZATION. Addresses activities in the application of synchrotron radiation to materials science, with particular emphasis on microstructural details for evaluation of materials quality processing, and new materials design. Also addresses the activities on analytical electron microscopy to complement the evaluation performed by radiation.

Task 15443--METALLURGICAL PROCESSING. Contains most of the Division's competence in rapid solidification, surface modification, interface stability and measurement, and the Diffusion in Metals Data Center.

Task 15444--WEAR AND MECHANICAL PROPERTIES. Focused on measurement methods, understanding, and predictive methodology of tribology. It also includes research on synthetic metal implants.

Task 15445--CHEMICAL METALLURGY. Contains all activities related to the ASM/NBS Alloy Phase Diagrams Program including data/bibliographic base compilations, graphics, phase system evaluations, and modelling, and the publication of the Bulletin of Alloy Phase Diagrams.

Task 15446--CORROSION AND PROTECTION OF METALS. Relates to major focused effort on study of corrosion in metals, including predictive models and measurement methods. Now contains all activities related to NACE/NBS Cooperative Program for Corrosion Data.

Task 15447--ELECTRODEPOSITION (ELECTROCHEMICAL PROCESSING). Covers all Division activities in electrodeposition, and its processing/structure/ properties relations. Also covers electrodeposited Standard Reference Materials for hardness, thickness, and crack dye-penetrant.

Task 15448--NONDESTRUCTIVE CHARACTERIZATION. Addresses activities in nondestructive evaluation and processing control. Includes work on acoustic sensing, including that related to the new cooperative American Iron and Steel Institute (AISI) program.

FY 84 Significant Accomplishments

Task 15442--ADVANCED MICROSTRUCTURE CHARACTERIZATION.
Task 26105--SYNCHROTRON RADIATION RESEARCH FOR MATERIAL SCIENCE.

- Completed the *in situ* observation of Al-Sn alloys (3 to 30 wt% Sn) during the liquid phase sintering and coarsening processes. Data were sought to test recent theoretical work on statistical coarsening of two-phase mixtures at high volume fraction liquid. Detailed features of the formation of liquid phase regions have been analyzed.

- Studied the recrystallization process using pure Al and Al-Sn alloys under improved temperature control. Also, using monochromatic topography, grain boundary motion during recrystallization has been observed *in situ* on lead bi- and multi-crystals.

- Completed the study of the roles of Cr and H in the passive film on iron using various EXAFS techniques. The structure of a tantalum oxide film has been studied by EXAFS using the L-absorption edge of Ta.

- Initiated the study of single interfaces between various films and different substrates and within multilayered materials using EXAFS, topography and a new diffraction technique.

- Developed cooperative programs with Lawrence Berkeley Laboratory for the *in situ* characterization of materials using topography, with Lawrence Livermore Laboratory for the interface study of multilayered metals, and with industry for the characterization of compound semiconductors for process and quality control.

Task 15443--METALLURGICAL PROCESSING.

- Rapid solidification theory and experiment were extended to NiAl-Cr quasibinary alloys. The observation that ordered crystalline structures rather than disordered crystalline structures were obtained under rapid quenching conditions in this system was explained by theory developed in this work.

- Unique precipitate phases and microstructures were produced in rapidly solidified Al-Cr alloys.

- Fluid flow which occurs during directional solidification was investigated. Unexpectedly vigorous flow, apparently caused by Marangoni (surface tension gradient) forces, was found when gas bubbles were introduced at the solid-liquid interface.

- Signal averaging by a rotating transducer method was shown to provide greatly improved measurements of solidification interface motion in iron and steel by ultrasonic techniques.

- Careful measurements were made of the temperature variation of the surface tension of liquid silicon, a quantity that previously was only poorly known despite the technological importance of silicon.

Task 15444--WEAR AND MECHANICAL PROPERTIES.

- A dynamic microindentation test system has been constructed and used in a series of micromechanical studies of several well characterized metals. This system can provide dynamic mechanical properties data over five decades of strain rate and obtained from regions of the order of 10 μm in size.

- Wear and friction studies of "break-in" phenomena were completed with an emphasis on uni-direction and reversed-direction sliding contacts using a series of well characterized copper alloys.

- A new test method has been developed to study wear due to abrasive contaminants in lubricating greases. The test is now being extended to investigations of other fluids and different types of abrasives.

- Task personnel handled arrangements for the largest, most comprehensive biomaterials meeting ever held with 823 attendees from 25 countries. NBS research results were presented in two papers concerned with corrosion and mechanical properties.

- A non-destructive eddy current test technique was devised to reliably detect cracks in the neck threaded regions of pressure gas cylinders fabricated from aluminum-fiberglass composite.

Task 15445--CHEMICAL METALLURGY.

- Six issues of the Bulletin of Alloy Phase Diagrams were published which contained approximately 100 new phase diagram systems. Graphics were prepared at NBS and computer files for the published systems are maintained. This meets the newly set goal of six issues a year.

- Eighteen Ti-, five Al-, and five Fe-binary systems each have been evaluated. Systems completed include; Ti-Be , -Al, -Ga, -In, -Si, -Ge, -Sn, -Pb, -P, -As, -Sb, -Bi, -Sc, -Y, -La, -Ce, -Th, -U, Al-Bi, -As, -Sb, -Pd, -Pt, Fe-Ag, -Au, -Rh, -Mg, -Ta.

- Calculations have been performed of T_0 curves and metastable extensions of solid solutions in the Al-Cu systems of interest for rapid solidification, age hardening and metastable precipitates. Results were presented at the Annual TMS-AIME meeting in Los Angeles.

- An interactive computer program was developed for applying cluster variation calculations of order-disorder transitions to binary alloy systems, in collaboration with Dr. Ryoichi Kikuchi (Hughes Aircraft). Results are to be published in CALPHAD.

- Great progress has been made in the development of the computerized phase diagram database in three main areas: (1) the design of the search technique and data structure, (2) the development of algorithms for extracting salient numerical metallurgical information from graphical data, and (3) the development of standardized file formats for data update and data portability.

- Experimental proof of the existence of an $\alpha \rightarrow \alpha_2 + \gamma$ eutectoid in Ti-Al alloys near 45 at.% Al, and detection of the probable existence of a new intermetallic compound, Ti_2Al, were obtained.

Task 15446--CORROSION AND PROTECTION OF METALS.

- Mechanistic studies of stress corrosion cracking have led to the recognition of the controlling role of cleavage-step formation in the propagation of transgranular cracks, suggesting a new approach to increasing resistance to this technologically important failure.

- International Conference on the Durability of Steel Piling in Soil and Coastal Marine Environments organized by the Corrosion Group and held at NBS in October 1983.

- The NACE-NBS Corrosion Data Center increased its staffing support with both NBS employees and with the addition of a full-time NACE-supported Research Associate. Interactions with the external community of both potential contributors and users of corrosion data have continued to increase while also initiating several new pilot projects.

- Microcomputer controlled systems were developed to automate _in situ_ measurements of corrosion rates of steel reinforcing bars in concrete.

Task 15447--ELECTRODEPOSITION (ELECTROCHEMICAL PROCESSING).

- A process and electrolyte was developed for electrodeposition of Ni-Cr alloys by both dc and pulse plating techniques. A U.S. patent, 4,461,680, was assigned to the U.S. Government on July 24, 1984.

- Corrosion studies in "Hank's" solution have revealed that electrodeposited Ni-P alloys do not exhibit severe breakdown like 316L stainless steel or nickel. At potentials above 300 mv, the Ni-P alloy outperforms 316L SS and nickel and only Ti seems superior.

- Electrodeposition technology has been used as a rapid and precise method of applying a uniform "matrix" coating to silicon carbide fibers for use as precursors for metal matrix composites. Electrodeposites of copper and nickel have been applied and evaluation of these coatings will be made to investigate the use of fibers electrodeposited with aluminum, aluminum alloys, and titanium.

- A theoretical model based on mass transport and kinetic considerations was developed for alloy deposition. It predicts the concentration profile of ionic species in solution under dc and pulse electrodeposition on a rotating disk electrode and hence the alloy composition.

- An automatic measuring system for microhardness testing was designed to improve the accuracy of microhardness standards. This system involves a new principle of determining hardness from displacement of the indenter into the test material (dynamic) rather than optical measurement of an indentation after withdrawal of the indenter from the test material (static).

- A demand for special coating thickness standards has resulted in the availability of two new standards for next year.

Task 15448--NONDESTRUCTIVE CHARACTERIZATION.

- Two techniques were developed for reconstructing the spatial distribution of source intensity of acoustic emission. One technique is an exact solution to the three dimensional inverse random source problem. A second applies a backprojection method commonly used in tomography.

- A theory of the acoustic emission from martensitic transformations has been developed based upon the equivalent inclusion method. It has been shown that the acoustic signal is approximately proportionally related to (a) the volume that transforms, and (b) the transformation strain.

- Acoustic emissions from martensitic transformations of shape memory alloys have been measured and used to determine the kinetics of transformation during heating and cooling. These data together with electron microscopy, electrical resistivity and ultrasonic velocity measurements have enabled unequivocal identification of pre-martensitic transformation above Ms.

- A standard method for measuring calibration curves of ultrasonic velocity as a function of temperature in solids has been developed and tested on 304 stainless steel up to 1200 °C.

- New tomographic algorithms have been developed to deduce internal temperature distributions in square or rectangular cross section samples from ultrasonic time of flight measurements. The algorithms make maximum use of a-priori heat flow information to minimize data requirements.

National Bureau of Standards
Center for Materials Science
Metallurgy Division
Organizational Chart

Codes:
● - Student
+ - Consultant
Ø - Guest Worker or Research Associate
† - Post Doc.
* - Building 231
** - Building 224

450 METALLURGY DIVISION

Division Chief: L. R. Testardi
223, B268, x2811

Deputy Division Chief: G. M. Ugiansky
223, B262, x2811

Secretary: A. M. Marinoff
223, B266, x2811
Clerk Typist: S. L. Neal
223, B260, x2811/2991
Student: D. Y. Hutcherson
223, B266, x2811

Administrative Officer

M. L. Slusser
223, B260, x2991

Center Scientist

J. W. Cahn
223, A265, x2960

Structure Characterization

Group Leader: M. Kuriyama
223, A161, x2986

Secretary: Vacant
223, A163, x2986/2956

ØBechtoldt, C. J.	A157	2944
ØBendersky, L.	B116	2944
Black, D. R.	A159	3603
Burdette, H. E.	B164	2970
ØCarrick, D. G.	B116	2944
Dobbyn, R. C.	A157	2952
Long, G. G.	A159	3603
+Moss, S. C.	A161	2986
ØOosterhuis, W.	A161	2986
ØShechtman, D.	B163	2973
Spal, R. D.	B164	2952

Metallurgical Processing

Group Leader: J. R. Manning
223, A149, x3354

Secretary: S. L. Candore
223, A153, x3350

Biancaniello, F. S.	B156*	2323
Boettinger, W. J.	B168	2973
Butrymowicz, D. B.	A151	3353
Coriell, S. R.	B166	2962
Early, J. G., Jr.	A129	2976
†Handwerker, C. A.	A147	2997
Hardy, S. C.	B160	2985
Parke, R. L.	B156*	2323
Parker, R. L.	B162	2961
Ridder, S. D.	B156*	2323
Schaefer, R. J.	B118	2985
+Sekerka, R. F.	B166	2962
Voorhees, P. W.	B118	2985
ØYoon, D. N.	A155	3351
●Dang, D. T.	A129	2976
●Stockton, K.	B109*	2323

Wear and Mechanical Properties

Group Leader: A. W. Ruff
223, B114, x2966

Secretary: J. D. Nichols
223, B266, x2991

Blau, P. J.	B110	2974
Boyer, P. A.	A112	2943
Fraker, A. C.	B128	2992
Harris, J. S.	B108	2945
ØImam, M. A.	B106	2126
Ives, L. K.	A121	2943
Mattamal, G. J.	B106	2126
Olaon, C. D.	B116	2126
Polvani, R. S.	B112	2944
ØPoulose, P. K.	B106	2126
Smith, J. H.	A127	2945
ØSung, P.	B106	2126
VanOrden, A. C.	B108	2992
Whitenton, E. P.	B110	2974
●Tai, A.-J.	B112	2944
●Yau, A.	B106	2126

Chemical Metallurgy

Group Leader: K. Bhansali
223, B152, x2982

Secretary: R. V. Drew
223, B150, x2981

Bennett, L. H.	B154	2914
ØForsen, R.	B148	2981
Harris, J. F.	B144	2917
Hayes, R. M.	B142	3356
Kahan, D. J.	B145	2917
+Massalski, T. B.	B146	2917
McAlister, A. J.	B156	2955
Murray, J. L.	B140	2917
Read, M. E.	B142	3356
+Reno, R. C.	B154	2913
Shull, R. D.	B150*	2323
ØSims, J.	B148	2913
Swartzendruber, L. J.	B158	2955
●Bise, T.	B150	2981
●Pillai, N.	B145	2917

Corrosion

Group Leader: E. N. Pugh
223, B254, x2094

Secretary: N. J. Wilkin
223, B266, x2094/2811

Bertocci, U.	B242	2556
ØClausen, D.	B244	2556
Derr, C. F.	B246	2556
Escalante, E.	B250	2556
Fink, J. L.	B248	2556
Interrante, C. G.	A245	3662
Kaufman, M. J.	B244	2556
Mathews, D. E.	B250	2556
ØOiu, F.	B254	2556
Rodriguez, M. J.	B246	2556
Smit, J.	B248	2556
Ugiansky, G. M.	B262	2811
●Devadas, A.	B250	2556
●Harriaon, S.	A245	3662
●O'Connor, S.	A245	3662

Electrodeposition

Group Leader: D. S. Lashmore
224, B164, x2958

Secretary: M. M. Wykes
224, B162, x2958

ØBeauchamp, C. R.	B168**	2958
Brown, H. J.	B160**	2957
Johnson, C. E.	B158**	2954
Kelley, D. R.	B158**	2954
Mullen, J. L.	B156**	2954
ØNamgoong, E.	B168**	2957
+Ogburn, F.	B166**	2957
ØRatzker, M.	B166**	2958
●Lewis, S. P.	B160**	2957
●Oberle, R. R.	B156**	2957
●Rutledge, K.	B162**	2954
●Van Vechten, R.	B162**	2954

Nondestructive Characterization

Group Leader: H. N. G. Wadley
223, A165, x2956

Secretary: Vacant
223, A163, x2956/2986

ØBerlinsky, Y.	A167	2965
Clough, R. B.	A125	2965
ØDroney, B.	A367	3663
ØElkind, B.	A167	2965
ØGvishi, M.	A167	2965
Kahn, A. H.	A117	3355
Linzer, M.	A119	2611
ØMartinez, J.	B170	3663
Mauer, F. A.	A225	2910
Norton, S. J.	A145	2611
ØRogers, D.	B170	3193
ØRosen, M.	A167	2956
ØRudolph, R.	A367	3663
Simmons, J. A.	A263	3355
ØSmith, J.	A167	2965
●Hsieh, T.	A167	2965
●Kim, W. D.	A125	2965
●Long, K.	A117	3355
●Ryckebusch, S.	A147	3355
●Sandstrom, K.	A119	2611
●Turner, C.	A125	2965

ADVANCED MICROSTRUCTURE CHARACTERIZATION
Task 15442 and

SYNCHROTRON RADIATION RESEARCH FOR MATERIALS SCIENCE
Task 26101

Currently many important new materials are emerging in industry. These materials are produced by far more sophisticated control and processing methods than heretofore utilized. Coupled with increased industrial emphasis on quality control and automation for increased productivity, these advanced materials require a new, wide range of nondestructive microstructural characterization methods. The objectives of Task 15442 and Task 26101 are to address this challenge through the development of measurement methods and standards for the advanced quantitative characterization of metallurgical microstructures.

In the past year, the scientists from the Structure Characterization Group have been working on a nearly regular basis at NSLS to assist NSLS scientists to align the NBS/CMS front end for the CMS synchrotron radiation beamlines. Hardware for the CMS beamlines is complete, awaiting approval of the installation of our beamlines and experimental stations from NSLS.

In the meantime, the scientists from this group have been using the synchrotron radiation source at CHESS to perform various experiments in materials science. This group's highlighted accomplishments in FY 1984 are:

- We have completed the *in situ* observation of Al-Sn alloys (3 to 30 wt% Sn) during the *liquid* phase sintering and coarsening processes. Data were sought to test recent theoretical work on statistical coarsening of two-phase mixtures at high volume fraction liquid. Detailed features of the formation of liquid phase regions have been analyzed.

- We have studied the recrystallization process using pure Al and Al-Sn alloys under improved temperature control. Also, using monochromatic topography, grain boundary motion during recrystallization has been observed *in situ* on lead bi- and multicrystals.

- The study of the roles of Cr and H in the passive film on iron using various EXAFS techniques has been completed. The structure of a tantalum oxide film has been studied by EXAFS using the L-absorption edge of Ta.

- We have initiated the study of single interfaces between various films and different substrates and within multilayered materials using EXAFS, topography and a new diffraction technique.

o Cooperative programs have been developed with Lawrence Berkeley Laboratory for the in situ characterization of materials using topography, with Lawrence Livermore Laboratory for the interface study of multilayered metals, and with industry for the characterization of compound semiconductors for process and quality control.

The details of these activities are described under each Subtask.

Study of the Structure of the Interface between the Film and the Substrate in Layered Materials
Subtask 1 of Task 15442 and
Subtask 1 of Task 26101

R. C. Dobbyn, D. R. Black, H. E. Burdette, G. G. Long, and M. Kuriyama

We have initialed the study of single interfaces in various films on various substrates and in multilayers using EXAFS, topography, and other diffraction techniques. Our objective is first to find the most suitable technique for obtaining data solely from the interface between the film and the substrate or between the various layers.

As seen in Figure 1a, a (400) topograph on a 1 μm thick CdTe film shows almost no features, as if the film were as perfect as the substrate, when the diffracting plane is parallel to the substrate surface and the interface. To obtain the information on atomic displacements or irregularity within the interface, the momentum transfer of x-rays, that is the reciprocal lattice vector relating to the diffracting planes, must be out of the interface plane. Using synchrotron radiation in extreme grazing incidence, a (444) topograph was obtained. As seen in Figure 1a, this shows the real structure of the film or interface. Topographs from the InSb substrate could not be obtained for this beam condition because the radiation could not penetrate through the film to reach the substrate.

Figure 1b shows the structural variations of films or interfaces for various film preparation conditions. What we need is a new method to reveal the interface structure only. We have started a preliminary experiment using single-interface metals, such as Pd or Ag (f.c.c.) metal on Cu (f.c.c.) and Nb (b.c.c.) on Cu (f.c.c.).

In-Situ Observation of the Coarsening Effect by Synchrotron Radiation Microradiography
Subtask 2 of Task 15442

W. J. Boettinger, H. E. Burdette, P. Voorhees, and M. Kuriyama

In situ observation of the coarsening of a two-phase liquid plus solid mixture has been achieved by microradiography using the intense x-ray radiation available at the Cornell High Energy Synchrotron Source (CHESS). The alloy, Al-5 wt% Sn, was chosen for study following classical work on the three dimensional shape of grains [1]. Above the melting point of Sn, the alloy will consist of grains of almost pure Al with a Sn-rich liquid between the grains. This provides excellent x-ray absorption contrast. Data is sought to test recent theoretical work on statistical coarsening of two-phase mixtures at high volume fraction liquid by Voorhees and Glicksman. Also possible is the observation of the details of liquid film migration and other microscopic coarsening mechanisms.

Microradiographs were taken using 8 keV x-rays selected from the synchrotron beam by a flat crystal monochromator. Al-5 wt% Sn samples were cast and rolled to a thickness of 0.25 mm. In situ heating was provided by clamping the sample between plates which were attached to an annular resistance heating element. Microradiographs were recorded in real time using an x-ray sensitive vidicon with a spatial resolution of ~50 μm. High resolution images were recorded on film with a 5 s exposure.

Figure 2 shows microradiographs from the latter stage of the coarsening of Al-5 wt% Sn at 620°C. Here the recrystallization of the alloy is complete and the grain growth is primarily two-dimensional. Stereo pairs can be taken to determine the three-dimensional structures which occur at shorter times (smaller grain size). In the figures many features can be seen. Large grains grow at the expense of small grains (marked A). Quadruple junctions are seen to be unstable (point Q). A few grain boundaries wet with only a thin layer of liquid are also seen (boundary S). Presumably these are small angle grain boundaries. Future work will be directed at measurement of the orientation relation between adjacent grains during coarsening.

[1] W. M. Williams and C. S. Smith, J. Metals, p. 755 (1952).

X-Ray Strain Measurements with Energy Dispersive Spectroscopy
Subtask 3 of Task 15442

D. R. Black, C. J. Bechtoldt, R. C. Placious, and M. Kuriyama

Five years ago we demonstrated, using a curve fitting technique and low energy x-rays, the ability of Energy Dispersive X-ray Diffraction (EDXRD) to measure residual strains in thin materials accurately and reproducibly [1]. The capabilities of this technique were then extended to real, thick materials by use of a 250 keV radiographic x-ray source [2]. With this system, the distribution of strains across a weld zone in a section of Alaskan pipeline was measured [2]. This result demonstrated the potential of EDXRD for the in-situ evaluation of strains in industrial materials. As the continuation of the application of this technique to industrial materials, the purpose of this year's work was to demonstrate that EDXRD can be used to obtain 3-dimensional mapping of strains.

The success of past work relied on the ability of the curve fitting routines to determine diffraction peak positions two orders of magnitude better than the energy resolution of the solid state detector. Single peak curve fitting was used which required that the various diffraction peaks be well separated in energy. To accomplish this, small scattering angles, $2\Theta \leq 5.7°$, had to be used for high energy x-rays; see figure 3. These values of 2Θ imply that the x-ray probe spans the entire sample thickness. For the purpose of 2-dimensional mapping of strains, e.g. across the surface of a plate, this allows the maximum volume of sample to be used and hence improves the count rate. For 3-dimensional mapping, the loss of resolution in this direction is unsatisfactory. While the former method is adequate for rapid inspection of materials on-site to identify which section of the material has flaws, the improved spatial resolution of the latter method is required for pinpointing flaw locations and for strain evaluation.

To establish the necessary resolution in the direction of sample thickness, the scattering angle must be increased. Unfortunately, this causes the number of diffraction peaks in a given energy range to increase. To compensate for this we have developed a multiple peak curve fitting routine which will maintain the necessary accuracy of peak determination with $2\Theta = 10$.

The system has been used to measure the strain gradient through the thickness of a 9.5 mm thick cantilevered steel bar. Three points have been measured through the sample and six different diffraction peaks for each point have been fitted. Satisfactory spectra could be obtained in six hours with the x-ray generator operating at 250 keV and 4.5 mA of current. It should be noted that acquisition times can be dramatically reduced by utilizing existing higher efficiency detectors (currently we use an inferior detector for these x-ray energies) and more powerful x-ray sources.

Figure 4 shows the measured strains for these three points. Due to the shape of the x-ray probe, the volume from which diffraction occurs for the front and back positions is centered approximately 1.5 mm below the sample surface. Extrapolation to the surface yields a strain value of 1×10^{-3}. Using elementary beam theory, the calculated value is 1.4×10^{-3}.

We have demonstrated the ability of EDXRD to measure the strain distribution through the thickness of a material. This result, coupled with previous work measuring strain distributions across a sample, constitute a demonstration of the capability of an EDXRD system to map 3-dimensional strains in real materials.

[1] M. Kuriyama, W. J. Boettinger, and H. E. Burdette, X-ray Residual Stress Evaluation by an Energy Dispersive System, Proceedings of Symposium on Accuracy on Powder Diffraction, NBS Special Publ. 567, pp.479-487 (1980).

[2] C. J. Bechtoldt, R. C. Placious, W. J. Boettinger and M. Kuriyama, X-ray Residual Stress Mapping in Industrial Materials by Energy Dispersive Diffractometry, Advances in X-ray Analysis 25, pp.329-337 (1982).

Observation of Two Structurally Distinct States in Ni-P Glasses Using EXAFS

Subtask 4 of Task 15442

G. G. Long, A. I. Goldman, L. H. Bennett, and M. Kuriyama

Structural relaxation, as a function of time or temperature, is responsible for appreciable changes in many of the physical properties of metallic glasses. It has therefore become customary to explain different results in the literature concerning the same material by saying that some of the samples may not have been measured in the "fully relaxed" state. Application of this approach overlooks the possibility of a more fundamental transition between structurally distinct glassy states that may occur, in addition to structural relaxation, in many systems.

Nuclear magnetic resonance (NMR) experiments detected two distinct glassy states in NiP glasses for compositions between 14 and 25% phosphorous. Fig. 5 shows the measured Knight shifts as a function of the atomic percent phosphorous for glasses prepared by different methods where the various methods are indicated with different symbols. Knight shift measurements on crystalline samples are also shown for reference. Of particular significance is the fact that these measurements all fall along two (or at most three) lines. Furthermore, density measurements collected from the literature similarly demonstrate that the results fall along two linear curves.

Samples for EXAFS measurements were taken from the upper curve (type I) of the NMR and from the lower curve (type II). Annealing experiments have identified II as the lower energy state. The Ni-K near edge regions of the absorption spectra for the glasses and pure Ni show that the edge of the type I specimen is shifted n1 eV (where the uncertainty in the scale is <0.5 eV) relative to that of type II, and the detailed edge shapes are different. This is suggestive of differences in the chemical bonding between the two structures. Comparison of the EXAFS data with the Ni and P backscattering amplitudes indicates that the signal from the type II specimen exhibits predominantly P backscattering whereas that from the type I specimen appears to be dominated by the Ni backscatterers.

Fourier transforms of the EXAFS data are shown in Fig. 6. The first peak in the Fourier transform of the type II data is significantly broader than that of the type I data. Holding the number of nearest neighbors fixed, and using the amplitude reduction factor S_0^2 and the relative Debye-Waller factor σ^2, the function $D = S_0^2 \exp(-2k^2\sigma^2)$ is an inverse measure of the number of different bond lengths contributing to the peak. Our results show that Ni-Ni in type I is much narrower than in type II (D(I)/D(II) = 1.5) and Ni-P in type I is significantly broader than in type II (D(I)/D(II) = 0.67).

A local fluctuation theory was previously used to predict that the distribution of atomic distances become narrower in the relaxed state. Our data, in contrast, suggest that the lower energy state (II) shows a greater distribution of atomic distances around the central Ni atoms. A second neighbor peak is also seen for the higher energy (I) state which is not evident for the lower energy glass. This indicates that there is greater structural ordering in the higher energy state than in the lower energy state. The better structural definition (i.e., narrower peaks and more peaks in the Fourier transform) is seen in the higher energy glass; the greater distribution of atomic distances (a single broad peak) is seen in the lower energy glass.

These results cannot be reconciled using a continuous structural relaxation mechanism, but can be understood in terms of two distinct structural environments. The linear curves for the NMR and the density data, throughout this compositional range, suggest that the two structural types persist, even in the phosphorous deficient range far from perfect stoichiometry.

X-Ray Absorption Study of Tantalum Oxide Films on Silicon
Subtask 5 of Task 15442

G. G. Long and M. Kuriyama

Thin films of noncrystalline tantalum oxide are widely used as dielectric films in capacitors, as waveguides in integrated optics, and as antireflective coatings. Regarding their use as capacitors, it has been noted that they should be noncrystalline so as to avoid the defective grain boundary regions typical of polycrystalline materials. So far, however, results from the existing techniques such as optical measurements and electron diffraction/microscopy have been insufficient to characterize completely the tantalum oxide films. What is required is a method which can be used to give direct structural information on short range order and on the nature of the chemical bonds to complement the existing measurements. One such technique is extended x-ray absorption fine structure (EXAFS) spectroscopy combined with x-ray absorption near edge structure (XANES) measurements.

In this work, the XANES and EXAFS spectra of thin (~60 nm) $Ta_{.286}O_{.714}$ (where this notation represents 28.6 atomic percent Ta, or the stoichiometry of Ta_2O_5, without representing the crystalline structure) films on single crystal silicon were measured near the tantalum L_{III} absorption edge, and compared with spectra from polycrystalline β-Ta_2O_5. The density of the crystalline powder is 8.73 g cm^{-3} whereas that of the glass is 8.3 g cm^{-3}.

A comparison of near edge L_{III} structure in the crystalline material and in the thin film is shown in Fig. 7. These spectra were normalized to each other at a point about 100 eV above the edge by assuming that the L_{III} atomic absorption for a tantalum atom is independent of its environment. The area under the white line (first peak near the edge) for the film is larger than that for the crystalline material. This may be due to increased covalency as a result of changes in the d band.

The magnitudes of the Fourier transforms of the data in Fig. 8. The first broad peak in the crystalline data represents the Ta to O distances in the pentagonal bipyramid-like and octahedron-like settings of the Ta. A much narrower Ta-Ta peak is also seen, corresponding to the better defined Ta to Ta distance. The thin film result shows a Ta-O peak that is (within 2%) the same as the polycrystalline result--both in distance and coordination. The Ta-Ta coordination, however, was reduced in the film by a factor of one-half the crystalline result. The lower coordination in the second shell is evidence of reduced long range order in the film.

These results demonstrate that the polycrystalline and the glassy forms of tantalum oxide are based on essentially invariant short range order. The only addition to this is the probable tendency toward greater covalency in the bonding of the glassy material.

Direct Conversion X-Ray Imaging Detectors

Subtask 6 of Task 15442 and
Subtask 2 of Task 26101

R. D. Spal, H. E. Burdette, and M. Kuriyama

This report covers our progress in the development and characterization of x-ray imaging detectors. Several features should be considered when comparing imaging detectors. The two most obvious are sensitivity and spatial resolution as a function of energy; others are geometric distortion, decay lag, lifetime, active area, and total size. For photon counting detectors, energy resolution may also be considered.

Our previous report studied a detector in which x-rays are converted to a video signal by the following four stage process: 1) a phosphor converts the x-rays to visible light; 2) a photocathode converts the visible light to electrons which are amplified by a microchannel plate; 3) a phosphor converts the electrons back to visible light; and 4) a solid state CID (charge injection device) image sensor converts the visible light to a video signal. Stage 1 is coupled by fiber optics to stage 2, as is stage 3 to 4. The latter coupling requires bonding a fiber optic to the CID image sensor. Because strain at this coupling can easily damage one of several fine wires also bonded to the sensor, the detector is rather fragile. For 8 keV radiation, this system has sufficient sensitivity for photon counting, a point spread function with a FWHM of 450 micrometers, and negligible geometric distortion and decay lag.

In this report, two different detectors are considered for increased spatial resolution and ruggedness. They both directly convert the charge carriers generated by x-rays striking a target into a video signal, without any intervening stages to provide carrier multiplication. Thus, one might expect increased spatial resolution but decreased sensitivity.

One direct conversion image detector under study is a commercial x-ray vidicon camera (Hamamatsu model C790-01).[1] In this device, the x-rays generate charge carriers in a PbO photoconductor target, which is scanned by an electron beam at 60 Hz over an active area of 1.0 cm X 1.2 cm to produce a video signal. For 8-keV radiation, the measured minimum detectable intensity is 10^8 photons/cm^2/s, while the spatial resolution is 25 micrometers. The geometric distortion is 3 percent, and the decay lag is 0.1 s for a 90 percent decay. Since the specified dark current of 1 nA is equivalent to about 10^7 photons/cm^2/s at 8 keV, it may be possible to decrease the minimum detectable intensity by an order of magnitude by scanning the target at 6 Hz. However, since the video monitor must be refreshed at 60 Hz, a buffer memory is required to hold the vidicon output and drive the monitor. This capability is being developed. Further improvement in detectability is possible by cooling the vidicon tube to reduce the dark current, but is awkward due to the large tube size.

Another direct conversion image detector is the CCD (charge coupled device) image sensor. In this device, the x-rays generate charge carriers in a depletion layer in silicon, and the carriers are collected in potential wells or pixels under gate electrodes. Charge packets may be shifted from one pixel to the next by applying a sequence of voltages to the gate electrodes. In this manner, all charge packets may be shifted serially to an output amplifier. While no commercial CCD image sensors intended for x-rays are available, several studies have been reported on the x-ray response of commercial devices intended for visible radiation, and of research devices optimized for x-rays (refs. 1-4 are some recent studies). A major performance limitation of commercial devices with hard x-rays is the thickness of the depletion layer, typically 10 micrometers. Only 13 percent of 8 keV radiation is absorbed in 10 micrometers of silicon, so the remainder is absorbed in the substrate. While carriers generated in the substrate may diffuse to the depletion layer and be collected by the pixels, they may be spread out over many pixels since

----

[1]"Certain commercial equipment, instruments or materials are identified in this paper in order to adequately specify the experimental procedure. Such identification does not imply recommendation or endorsement by the National Bureau of Standards, nor does it imply that the materials or equipment identified are necessarily the best available for the purpose."

they also diffuse laterally. Thus, a thin depletion layer may degrade spatial resolution as well as quantum efficiency. A research device with a 254 micrometer depletion layer fabricated on high resistivity silicon has demonstrated high quantum efficiency and negligible charge spreading for 1-10 keV radiation (ref. 2). Another solution to the charge spreading problem is to heavily dope the substrate so that carriers recombine before diffusing to the depletion layer. A research device implementing this solution, having a 10 micrometer depletion layer and a 15 μm X 15 μm pixel size, has demonstrated at 5.9 keV a spatial resolution of 15 micrometers, quantum efficiency of 34 percent, and energy resolution of 250 eV FWHM (ref. 4). A similar device is commercially available (Texas Instruments model TC201).[2]

We have begun evaluation of the TC201 CCD. It has an active area of 6 mm X 8 mm, containing 245 X 328 pixels measuring 24 μm X 24 μm. The pixel capacity is 100,000 electrons or, equivalently, 50 photons at 8 keV. The electronic noise is 100 electrons per pixel, giving a dynamic range of 1000. The room temperature dark current is 5 nA, or 400,000 electrons/pixel/s. Photon counting is possible if the device is cooled to reduce the dark current. Since the device is small and consumes little power, thermoelectric cooling is convenient. The device may be scanned at 60 Hz for a standard video signal, or more slowly to improve the signal-to-noise ratio for low signal levels. Unfortunately, the necessary circuitry to drive the gate electrodes and process the floating gate amplifier output is not commercially available. The former circuitry has been completed, while the latter, along with the cooling stage, is in preparation. Preliminary tests have verified sensitivity to visible and x-ray radiation.

[1] Griffiths, R.E. et. al., SPIE 244, 57 (1980)

[2] Peckerar, M.C. et. al., Appl. Phys. Lett. 39, 55 (1981)

[3] Janesick, J.R. et. al., SPIE 290, 165 (1981)

[4] Stern, R.A. et. al., Rev. Sci. Instrum. 54, 198 (1983)

Collaborative Synchrotron Radiation Research with Lawrence Berkeley Laboratory for Material Characterization using Topography
Subtask 7 of Task 15442

R. C. Dobbyn, D. R. Black, and M. Kuriyama

---

[2] "Certain commercial equipment, instruments or materials are identified in this paper in order to adequately specify the experimental procedure. Such identification does not imply recommendation or endorsement by the National Bureau of Standards, nor does it imply that the materials or equipment identified are necessarily the best available for the purpose."

In collaboration with scientists from Lawrence Berkeley Laboratory, we have tested how effectively synchrotron radiation topography, particularly monochromatic topography, performs in real time for the characterization of crystals. The capability of testing crystals in real time is required for possible industrial use to feed back information from final products to the processing (growth) stages. Figure 9a shows real time TV images of topographs taken from various Si-doped GaAs crystals. These views were compared with still topographs taken on high resolution, special photographic films. These TV images show dislocations, small angle subgrain boundaries, precipitates and dislocation network. Also shown in Fig. 9b are the formation of various dislocations in Ge grown under different conditions.

Another interesting application of real time TV imaging is shown in Fig. 10. The top photograph on the left shows a TV image of the microradiograph of a Si device. The image clearly displays the device structure on the crystal. When this device sample is rotated around some axis, the sample, being a single crystal, may satisfy a Bragg condition. Then the topographic images from crystal defects appear in addition to the microradiographic image. Note that dislocations are revealed under the pad, indicating a particular alignment.

CdTe on InSb

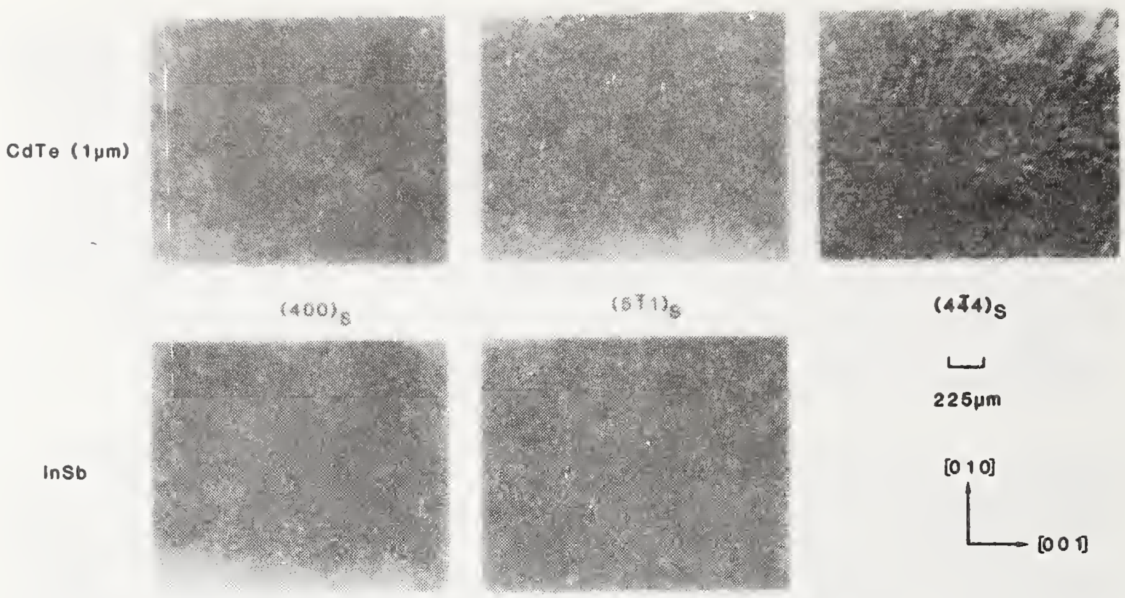

Figure 1a. Synchrotron radiation (monochromatic) topographs of a CdTe film on an InSb substrate. This series shows the detectability of microstructural disorder within the interface as the momentum transfer of x-ray photons varies.

STRUCTURAL VARIATIONS IN CdTe FILMS

(4 4̄ 4)S

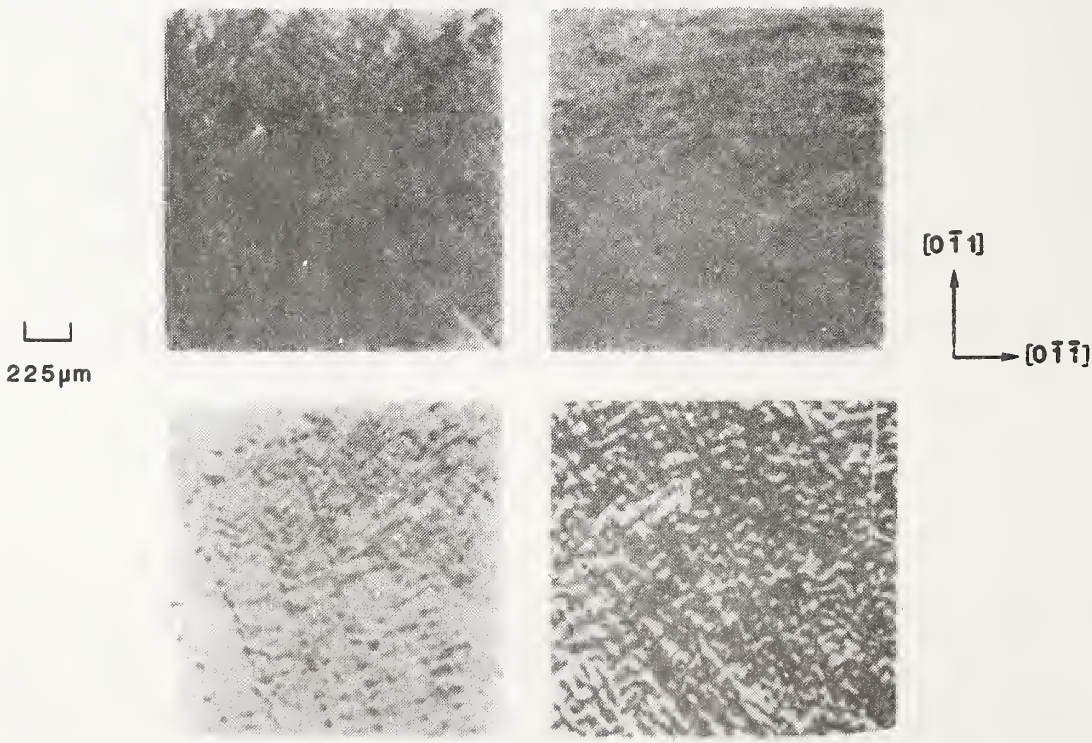

Figure 1b. A series of (444) synchrotron topographs showing structural variations in CdTe films for various preparation conditions.

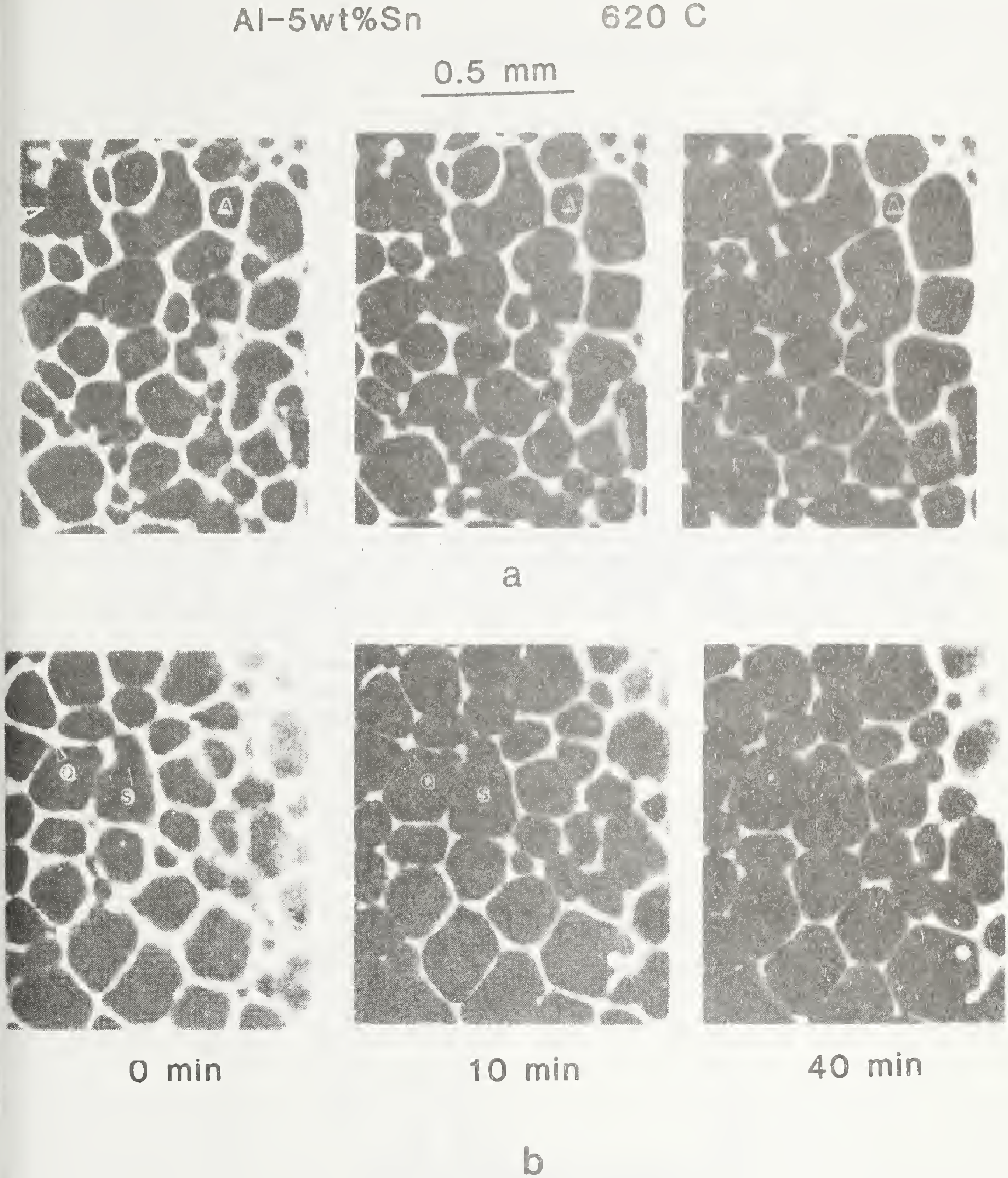

Figure 2. Microradiographs showing the coarsening effect of Al-5 wt% Sn at 620°C.

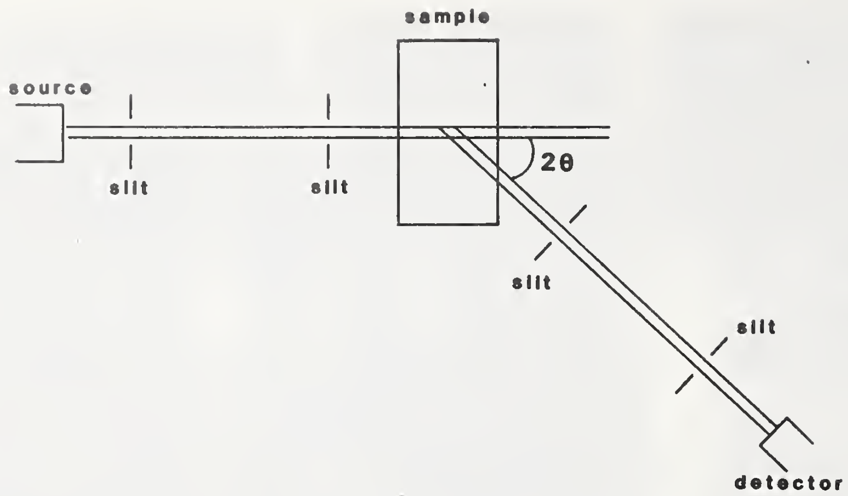

Figure 3. Schematic of the experimental geometry for Energy Dispersive X-Ray Diffraction.

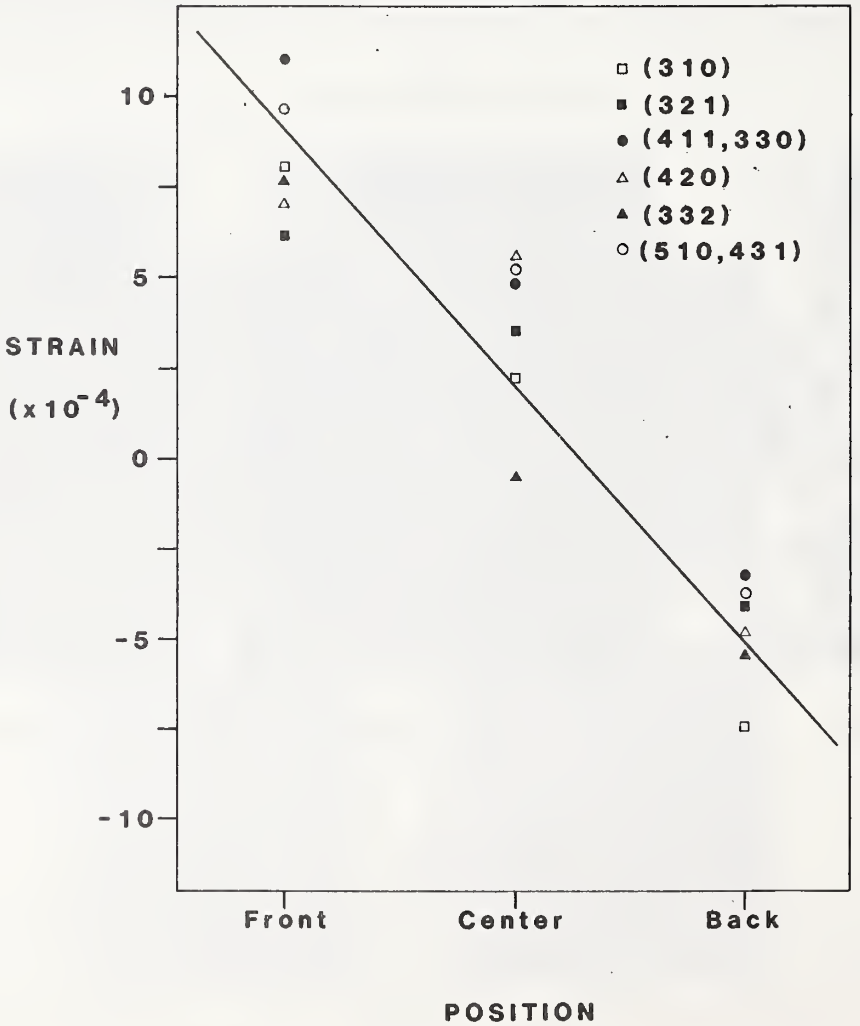

Figure 4. Plot of measured strain for six different peaks, as a function of position through the thickness of a 9.5 mm thick steel bar.

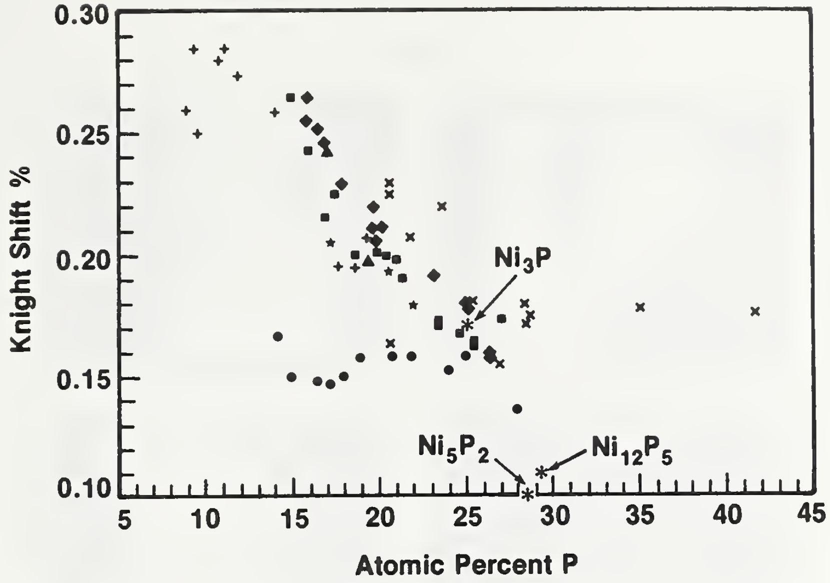

Figure 5. NMR Knight shifts in Ni-P amorphous alloys prepared by different techniques. These techniques include dc electroplated, pulse plated (99.9% on time), pulse plated (95% on time), splat quenched, electroless (NBS), and electroless (European), represented by different symbols. Also included for comparison are data for three crystalline alloys: Ni_3P, Ni_5P_2 and $Ni_{12}P_5$.

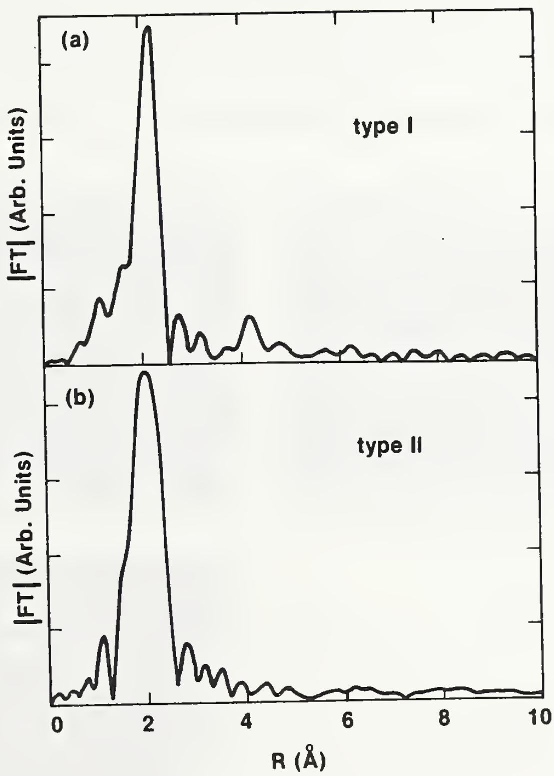

Figure 6. Magnitude of the Fourier transform, |FT|, for the (a) type I and the (b) type II Ni-P glasses. R is uncorrected for phase.

REAL TIME TV IMAGES

(220) T

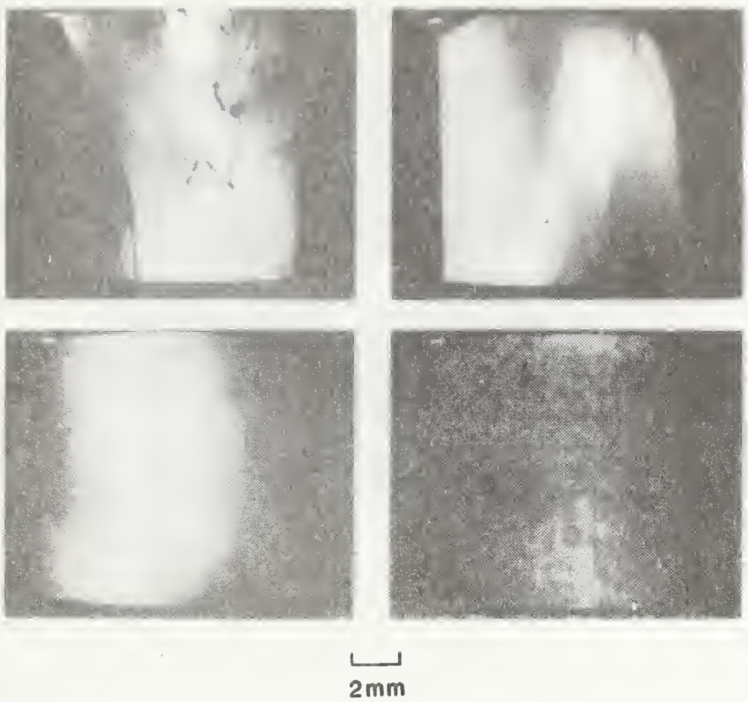

Figure 9a. Real time TV images of topographs from (a) GaAs (Si-doped) crystals and (b) Ge crystals.

HIGH/LOW DISLOCATION DENSITY IN Ge

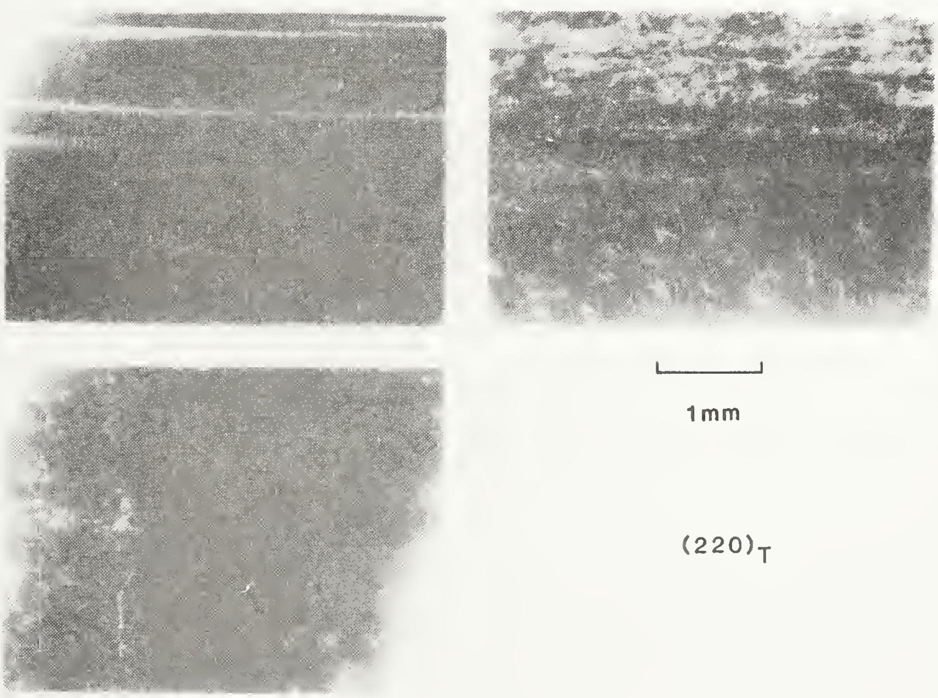

Figure 9b. Various dislocation images obtained from Ge crystals under various processes.

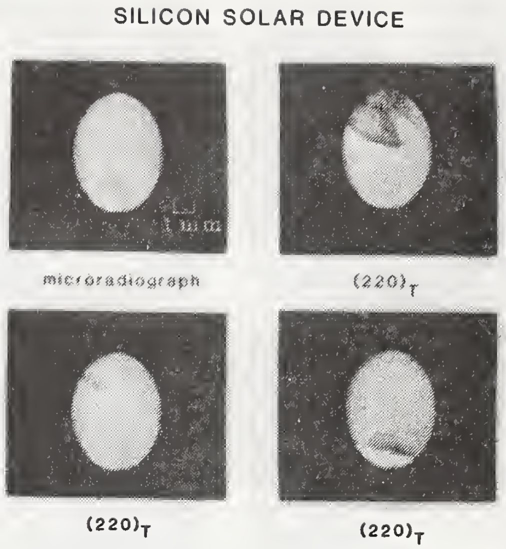

Figure 10. Microradiography with topography (real time view of a Si device). Crystalline defects are revealed in a microradiograph, when the sample, being a single crystal, satisfies a Bragg condition.

METALLURGICAL PROCESSING
Task 15443

The properties of alloys depend on their processing history. Solidification processes, solid state transformations, diffusion, and other kinetic changes that alloys undergo during their production and achievement of final form determine the microstructures and compositional distributions in the alloys. These features in turn decide the properties and performance of the alloy. The objective of this task is to develop measurements and predictive models to allow prediction of the effects that processing conditions have on alloys. Increased reliability, cost-savings and higher performance of final products can be expected from the resulting improved control of metallurgical processing.

This task includes the NBS activities on rapid solidification. Special Congressional appropriations allowed the capabilities of the NBS Metals Processing Laboratory to be enhanced in the past few years to provide a wide variety of rapid solidification techniques. The equipment for electron-beam surface melting of alloys has been refined during the past year to provide improved control and measurement of electron-beam energy profiles, an inert gas atomization system to produce rapidly solidified powders has been installed, and an improved melt-spinning system is now in operation. These techniques are being applied to test predictive models for these high technology materials.

A new program on powder processing has been started during the past year, associated with the rapid solidification work. Relations between powder particle size and powder microstructure in rapidly solidified Al-Fe and Al-Cu powders were developed. Here the smallest particles solidify most rapidly. Work is underway to relate the original microstructures to coarsening rates observed during consolidation of such rapidly solidified powder. This work is important for development of high temperature precipitate-strengthened alloys.

Other new activities include theoretical studies of alloy microstructural coarsening as affected by stress and investigations of boundary migration processes. In this work, it was found that stresses from elastically interacting precipitates can change the diffusion fields that influence coarsening behavior. As part of the boundary migration studies, driving forces for liquid film migration and diffusion-induced grain boundary migration were compared. This work provided new understanding of interface processes and new techniques for modifying alloy microstructures and surface compositions.

Other significant accomplishments during the past year include:

- Rapid solidification theory and experiment were extended to NiAl-Cr quasibinary alloys. The observation that ordered crystalline structures rather than disordered crystalline structures were obtained under rapid quenching conditions in this system was explained by theory developed in this work.

- Unique precipitate phases and microstructures were produced in rapidly solidified Al-Cr alloys.

- Fluid flow which occurs during directional solidification was investigated. Unexpectedly vigorous flow, apparently caused by Marangoni (surface tension gradient) forces, was found when gas bubbles were introduced at the solid-liquid interface.

- Signal averaging by a rotating transducer method was shown to provide greatly improved measurements of solidification interface motion in iron and steel by ultrasonic techniques.

- Careful measurements were made of the temperature variation of the surface tension of liquid silicon, a quantity that previously was only poorly known despite the technological importance of silicon.

Strong interactions have been established with industry, universities, and other government agencies. Visiting scientists from industry come to NBS to participate in production of rapidly solidified alloys for purposes of exploratory research. Scientists from Harvard University, University of Wisconsin, University of Connecticut, Johns Hopkins University, Technion (Israel) and the Korean Advanced Institute for Science and Technology spent periods of weeks to months at NBS during the past year cooperating in investigations with the metallurgical processing task scientists. A Massachusetts Institute of Technology (MIT) co-op student is participating in joint MIT-NBS work in rapid solidification. Powder processing work on rapidly solidified Al-Fe is supported by the Naval Air Development Center and other major studies on rapid solidification are funded by the Defense Advanced Research Projects Agency. Studies of convection during directional solidification and silicon surface tension measurement work were sponsored during the past year by the National Aeronautics and Space Administration. Diffusion-induced grain boundary migration investigations directed toward surface alloying are supported by the Army Research Office.

Group members participated during the past year on advisory panels for the Department of Energy, the National Aeronautics and Space Administration, and the Consumer Products Safety Commission. Task members are active on national standards committees for resource recovery and powder alloys, have a leadership role in the AIME Solidification Committee, served as chairman of a conference held in May 1984 at NBS on failure mechanisms in high performance materials, including rapidly solidified alloys, and serve as deputy principal editor of the International Journal of Crystal Growth.

Powder Processing for Rapidly Solidified Alloys
Subtask 1 of Task 15443

J. G. Early, F. S. Biancaniello, W. J. Boettinger, and S. D. Ridder

Facilities for production and consolidation of rapidly solidified alloy powder have been installed in the Metals Processing Laboratory. In addition to the electrohydrodynamic microparticle processor, which produces small amounts of rapidly solidified powder for laboratory analysis, an inert gas atomizer capable of producing larger amounts of rapidly solidified powder, up to 30 pounds per run, has recently been installed. The inert gas atomizer produces and rapidly cools small droplets by impingement of inert gas and liquid metal emerging from a carefully designed die. Powder handling equipment and a hot isostatic press have been installed to help process this powder into bulk specimens.

The consolidation of the rapidly solidified powder into a fully dense product, typically carried out at elevated temperatures is a critical processing step in controlling the ultimate properties of the material. The use of rapidly solidified powder complicates the selection of proper processing conditions because of the lack of knowledge as to whether microstructures obtained by high rate and supposedly "nonequilibrium" solidification can be retained during the various high temperature consolidation processes. Two aspects of the general microstructural advantages of rapid solidification are important in powder processing: (a) Elimination of macrosegregation and second phase particles (segregates)--obtained in some superalloys, tool steels and traditional aluminum alloys. (b) Extension of the solubility range of alloying additions or development of metastable phases - obtained in aluminum-base transition metal alloys.

Alloys whose microstructures are influenced only by aspect (a) can be consolidated without significant loss of microstructural advantages provided by rapid solidification; however, for alloys whose microstructures include aspect (b) as well as (a), the situation is less clear. These alloys, particularly the aluminum-base transition metal alloys, are of interest because their lack of equilibrium will significantly affect the choice of processing path to produce full density. Generally, these microstructures will respond to thermal processing through the nucleation and growth of precipitates or dispersoids.

A systematic study of the microstructural response of several rapidly solidified aluminum-base alloys to consolidation conditions typical of those which occur during hot pressing and/or HIP cycles has been initiated. The approach being followed includes: characterization of the as-solidified powder; thermal stability experiments to determine coarsening behavior and its dependence on temperature and as-solidified microstructure; and the selection of the consolidation processing variables based on the coarsening results and densification models. The goal is to formulate processing rules which will combine the requirements for densification with the requirements of minimal precipitate (dispersoid) coarsening.

To provide baseline measurements for this work, rapidly solidified Al-8 w/o Fe powder was obtained and characterized according to size and microstructure. Electron microscopy of the alloys was performed in collaboration with L. Bendersky of The Johns Hopkins University, Center for Materials Research. A strong correlation was found between powder particle size and the type of microstructures present for particles in the size range 5 μm to 45 μm diameter. The microstructure of the as-solidified aluminum alloy powder is non-uniform within individual powder particles. This non-uniform structure results from changes in solidification rate due to latent heat evolution. Four general types of microstructure were observed: microcellular α-Al, cellular α-Al, α-Al and metastable Al_6Fe eutectic structure, and α-Al and Al_3Fe primary intermetallic structure. The microcellular structure contained fine-scale cells of α-Al (cell spacing of 25 nm to 100 nm) with a yet-to-be identified precipitate within the cell walls. The cellular structure had a cell spacing 10 times coarser with the same unknown precipitate in the cell walls. The presence and fraction of each microstructure found in a given powder particle is strongly dependent on particle size. Thus the microstructural response of different regions within individual powder particles could vary significantly under different consolidation conditions.

The characterization of the as-solidified Al-8 wt% Fe powder showed: the microstructure of particles smaller than 5 μm was almost entirely microcellular; particles larger than 30 μm were predominantly α-Al and Al_3Fe intermetallic; particles between 5 and 30 μm contained microcellular, cellular and eutectic structures in various proportions (see table 1).

The thermal stability of the various microstructures was investigated by a series of annealing experiments during which powder samples were held at fixed temperatures for different lengths of time. The microstructural changes resulting from the thermal treatment were followed by optical and transmission electron microscopy. Substantial variations in coarsening behavior of the four microstructural types were observed for the range of annealing temperatures and times studied. Some microstructural features disappeared while others were unaffected.

Table 1. Approximate Volume Fraction of Various Microstructures in Different Size Fractions

Size (μm)	Microcellular	Cellular	Eutectic	Primary Intermetallic
< 5	~ 1.0	--	--	--
5-10	0.34	0.59	--	0.07
10-20	0.11	0.83	--	0.06
20-30	--	0.33	0.33	0.34
30-45	--	--	0.05	0.95

Rapid Solidification
Subtask 2 of Task 15443

W. J. Boettinger, F. S. Biancaniello, S. R. Coriell, S. D. Ridder, R. J. Schaefer, and J. W. Cahn

The control of microstructure by rapid solidification processing and subsequent thermomechanical processing constitutes an important new approach to alloy design and property improvement. High rate solidification requires numerous modifications of solidification theory which involve more refined analyses of heat and solute diffusion as well as non-equilibrium interfacial conditions. This project is focused on the kinetic processes that govern the evolution of microstructure during rapid solidification processing of crystalline alloys and their subsequent thermal treatment.

(1) Extended Solubility

The extension of solid solubility by rapid solidification is common, yet the relationship between alloy composition, growth rate, and thermodynamic constraints has not been significantly investigated. Experiments have been performed on NiAl-Cr and Al-Cu alloys for this purpose. The electron microscopy of these alloys was performed in collaboration with D. Shechtman of The Johns Hopkins University, Center for Materials Research.

NiAl-Cr Quasibinary Eutectic Alloys

The microstructure of rapidly solidified NiAl-Cr quasibinary eutectic and the nature of the thermodynamic restrictions on solubility extension in this system have been determined. Under slow solidification conditions the alloy microstructure consists of rods of α-Cr in a matrix of β-NiAl. These two phases have BCC and ordered BCC(B2) structures respectively. They have nearly identical lattice parameters and differ crystallographically only by ordering. Because of these factors, significant solubility extension of these phases was anticipated. The major microstructural constituent of the rapidly solidified eutectic alloy produced by melt spinning or electron beam surface melting are columnar grains of eutectic composition containing a fine spinodal-decomposition structure and a much larger scale anti-phase domain structure. The scale of the domain structure suggests that the columnar grains formed from the melt as the ordered β-NiAl phase but supersaturated to the eutectic composition. The fine spinodal structure is produced during the solid-state cooling after solidification. In order to understand why the supersaturated ordered β-NiAl phase solidifies from the eutectic melt rather than a supersaturated disordered α-Cr phase, an analysis of the T_0 curves for this system was performed. Figure 1 shows the stable phase diagram (solid lines) along with a probable set of metastable extensions of the solvus curves (dashed) and the T_0 curves (long-short dashed). The lower part of the figure shows the associated schematic free energy composition curves for two temperatures. The most important feature which sets the topology of the T_0 curves is the assumption of the existence of a metastable tricritical point at the intersection of the solvus curves. Such a tricritical point is known to exist in the similar FeAl-Fe system. At the eutectic composition the T_0 curve for the β-NiAl phase is higher in temperature than the T_0 curve for α-Cr. Hence rapid solidification of the eutectic composition should favor the formation of supersaturated β-NiAl over supersaturated α-Cr. This prediction is consistent with the observed results.

Al-Cu Alloys

Fine Al-Cu powder particles with compositions between 0.5 and 20 wt% Cu were produced by electrohydrodynamic (EHD) atomization in the size range between 3 nm and 2 μm. The particles produced were divided into two types; ones which exhibited segregation-free microstructure, and ones which exhibited a segregated, cellular microstructure. Some of the particles show a transition from partitionless solidification to a segregated, cellular solidification mode. The type of microstructure observed depends on the particle size and the composition as shown in figure 2 with the smallest particles free of segregation.

The size dependence can be interpreted in terms of bulk supercooling of individual particles prior to nucleation. Although partitionless solidification is possible without undercooling the liquid, it is reasonable to assume that larger undercoolings will be achieved in the smallest particles where cooling rates due to radiation are on the order of 10^5 K/s and the isolation of heterogeneous nucleation sites is high. Considering the case of growth into undercooled melts, partitionless solidification requires an interfacial temperature below the $T_0^{L/\alpha}$ temperature of the alloy (the $T_0^{L/\alpha}$ temperature is that point at which the α-solid and liquid have the same free energy) and an interfacial velocity in excess of the diffusive velocity of solute in the liquid in front of the interface. For powder particles, the latter conditions can only be achieved through substantial bulk supercoolings prior to solidification. In the absence of such supercoolings, the rate of external heat extraction limits achievable solid/liquid interfacial velocities to below that required for partitionless solidification. The data on the concentration dependence of the maximum particle size where cell-free structures are observed is unique. Detailed mechanisms for this dependence have been proposed as part of the present work.

(2) Microsegregation Theory

Rapid solidification of binary alloys often occurs with a cellular non-planar interface, exhibiting periodic structure and segregation transverse to the growth direction. This periodic structure, especially the segregation pattern, strongly affects the ultimate properties of rapidly solidified materials. In collaboration with G. B. McFadden of the NBS Center for Applied Mathematics, numerical methods for calculating steady state two-dimensional non-planar interface shapes were previously developed. This method of calculation is now being extended to the much more complex three-dimensional problem. The calculations utilize local equilibrium concepts which are valid for rates below ≈ 10 cm/s. For a specified interface shape, the temperature fields in the solid and liquid are found which satisfy energy conservation and temperature continuity at the solid-liquid interface. Similarly, the concentration field in the liquid is found which satisfies solute conservation at the solid-liquid interface. In general, the temperature, concentration, and specified interface shape will not satisfy the local equilibrium condition including the Gibbs-Thomson Effect at the interface. A self-consistent interface location is computed by an iterative procedure that effectively introduces an artificial time dependence in the problem. This procedure reproduces the correct linear instabilities for the planar interface and computes non-planar steady state solutions in the limit of large artificial time.

(3) Microstructure and Precipitation in Rapidly Solidified Al Alloys

In cooperation with D. Shechtman of The Johns Hopkins University, precipitation at 450°C was studied in melt-spun ribbons containing up to 15 wt% Mn in solid solution in Al. The as-spun ribbons were microsegregation-free at compositions up to 5 wt% Mn, but in more concentrated alloys a cellular microstructure was present. Upon annealing, four precipitate phases are observed, some of them being found preferentially on cell boundaries and others being found within the cells. Al_6Mn, G and the G" phase can coexist for long times at 450°C, but the G phase appears to be slightly more stable. A less stable T phase was detected in Al-5 wt% Mn foils following short annealing periods. The supersaturation of the Al matrix can persist for many hours in alloys containing up to 3 wt% Mn, but is essentially gone after 1 hour in alloys with 5 wt% Mn or more.

The solid solubility of chromium in alumium cannot be extended to as large an extent as can that of manganese. When melt-spun ribbons of Al containing up to 15 wt% Cr were examined it was found that the more concentrated alloys contained multi-phase spherulites embedded in an α-Al matrix: chemical microanalysis showed the average composition of the spherulite core to be 22 ± 2 wt% Cr. The kinetics of precipitation at grain boundaries and within the matrix were determined by TEM and x-ray diffraction. Three very similar Al-Cr intermetallic phases are present in the equilibrium phase diagram, but most of the precipitates in the melt-spun ribbons could be identified as Al_7Cr. Because of the several possible intermetallic phases it is difficult to reconstruct with certainty the exact sequence of solidification and decomposition events which lead to the spherulitic structure in Al-Cr. This work was carried out in conjunction with L. Bendersky of The Johns Hopkins University.

(4) Techniques for Experimental Rapid Solidification Research

Electron Beam Surface Melting

Electron beam surface melting has been used to produce a wide variety of alloys with known rapid solidification velocities. For these experiments the electron beam system has been upgraded by the development of improved computer control, beam characterization, and operating procedures. An example of the effect of focus current on the electron beam is shown in figure 3. A program has been started to study Al-Fe and Al-Mn alloys with controlled electron beam melting. These results will be compared to previous results using melt-spinning and/or atomization. In the alloys containing Mn, the expected transition from primary Al_6Mn to cellular aluminum was found as a result of increasing growth velocity, and a very narrow intermediate region of coupled eutectic growth has been seen. Analysis of the Al-Fe melts is still preliminary: they show a wider range of solidification microstructures than do the Al-Mn alloys.

Melt Spinning

A new melt spinner has been designed and constructed which incorporates several improved features. The controlled atmosphere chamber is 1 m long, permitting a four-fold increase in flight path. This feature eliminates the tendency for some alloys to agglomerate on the side of the chamber while still hot. The chamber can also be used with either inert gas or vacuum environment. New melt ejection tubes have been fabricated from zirconia and alumina for melt spinning of alloys which react with quartz. Finally an induction coil has been used which levitates the alloy during melting inside the tube before ejection. The resulting reduction of contact between the tube and the molten metal permits the melt spinning of refractory alloys. Several Nb-based alloys have been processed by this method.

<u>Convection During Directional Solidification</u>
Subtask 3 of Task 15443

R. J. Schaefer and S. R. Coriell

In this research, the fluid flow which occurs during solidification is studied with emphasis on understanding how this flow affects the shape of solid-liquid interfaces and how it affects solute segregation. Of specific interest are gravity-driven flows due to density variations in the fluid, which can arise from differences in temperature, composition, or both. When such flows are present they can significantly affect the homogeneity of the solidified material, and for critical applications the material performance may be significantly degraded. Both theoretical and experimental investigations of the interactions between solidification and convective flow are in progress.

Recent experiments by Glicksman and colleagues at Rensselaer Polytechnic Institute have demonstrated a remarkable coupling between hydrodynamic and morphological instabilities. In collaboration with Glicksman and colleagues and G. B. McFadden and R. F. Boisvert of the NBS Center for Applied Mathematics, we have carried out a linear stability analysis of this phenomenon. In the experiments, a long vertical cylindrical sample of high purity succinonitrile was heated by passing an electrical current through a long, coaxial, vertical wire, so that a vertical melt annulus formed between the coaxial heater and the surrounding crystal-melt interface. The outer radius of the crystal was maintained at a constant temperature below the melting point (58.1°C). With this arrangement, the temperature increases in the melt and decreases in the crystal with distance from the crystal-melt interface, and consequently the interface would be morphologically stable in the absence of fluid flow. The flow between two vertical infinite coaxial cylinders containing succinonitrile is unstable to an axisymmetric perturbation above a Grashof number of 2150 and the wave speed of this perturbation is comparable to the unperturbed flow velocity. When calculations are carried out with the outer rigid cylinder replaced by a crystal-melt interface, quite different results are obtained. The onset of instability occurs by an asymmetric mode at a Grashof number of 176, which is in agreement with experiment. The calculations predict that the period of oscillation (time for the wave to traverse one wavelength) is proportional to the fifth power of the gap width (the difference between the radius of the crystal-melt interface and the wire radius). This has been verified experimentally with the period of oscillation ranging from 300 to 60000 s.

In order to understand better the "coupled mode" of instability, we have also used linear stability theory to analyze a simpler geometry, viz., we consider the stability of the parallel flow between a vertical crystal-melt interface and a vertical wall held at a temperature above the melting point of the crystal. Three modes of instability occur: (1) a buoyant mode, (2) a shear mode, and (3) a coupled crystal-melt mode. The buoyant and shear modes are similar to those that occur for flow between two vertical rigid walls held at different temperatures.

For Prandtl numbers greater than approximately two, the coupled crystal-melt mode occurs at a lower Grashof number than the other two modes. Specific results have been obtained for succinonitrile and lead. It has been found experimentally that during unidirectional upward solidification of succinonitrile containing ethanol, convective flow of 10-30 μm/s was typically present as a result of horizontal components of the temperature gradient within the liquid. While these flows were sufficiently rapid to obscure the effect of the thermo-solutal convection which is expected in this system, it was observed that still more vigorous convection was induced by the accidental presence of a gas bubble at the solid-liquid interface. This flow was at least an order of magnitude faster than that due to the radial temperature gradients and was especially rapid immediately adjacent to the bubble surface. It was, however, erratic in nature. It appears to be Marangoni (surface energy gradient driven) flow, and it would thus be especially significant in low-gravity processing where a primary objective is to reduce convective flow but where the location of gas bubbles is difficult to control. Additional experiments are therefore being carried out to more thoroughly characterize the origins of this type of convection.

Ultrasonic Measurement of Solid/Liquid Interface Position During Solidification and Melting of Metals
Subtask 4 of Task 15443

R. L. Parker and J. R. Manning

Ultrasonic techniques are being developed to provide real-time, in-situ, nondestructive measurement of the position, motion and shape of solidification interfaces in opaque materials.

The use of pulse-echo ultrasonic flaw detectors to detect the presence and location of cracks, voids, and other flaws in metals and non-metals is well known. The solid-liquid interface in a melting or freezing metal should also produce a reflected echo, in that there is a measurable difference in both sound velocity and density across the interface. For normal incidence of longitudinal waves, about 10% of the pressure amplitude, or 1% of the energy, would be expected to be reflected from a planar solid-liquid interface in a pure metal. Such a technique would be useful for feedback and closed-loop process control of solidification to achieve improved quality control and productivity--such as in warning of potential breakouts in continuous casting of steel. The technique can be regarded as real-time ultrasonic metallography.

Results from the present work show that the melting and freezing of pure iron can be followed satisfactorily by this technique; however, for 304 stainless steel at 1 MHz, weaker signals were obtained resulting from (1) attenuating effects on beam strength caused by Rayleigh scattering from enlarged grains produced by rapid grain growth in the solid portion of the specimen, and (2) weaker reflection from the solid-liquid mushy zone due to its more gradual change in acoustical impedance compared to the sharp solid-liquid interface for pure iron. Thus 304-SS (or any other concentrated alloy) requires signal processing to improve the signal/noise ratio. Such signal processing also will be essential for use with EMAT transducers.

To help achieve signal enhancement for the 304-SS alloy, a transducer rotation system was developed that can render incoherent the reflection from the grains while preserving the backwall or solid-liquid reflection. With this system, signal averaging significantly improved the signal/noise ratio. One-half of a split, dual transducer (of PZT) was used and oscillated at the base of the cylindrical Bridgman-type specimen.

During the past year, software was developed for rapid averaging and display of these signals by interfacing a Biomation 8100 digital waveform recorder with an S-100 computer system. A system developed with the assistance of Professor N. C. Peterson of the Polytechnic Institute of New York, was able to average and display 256 scans of the waveform in 7 seconds with 8 bit vertical resolution and 512 sample intervals, with the sample intervals as small as 0.01 microsecond. A series of measurements on hot 304-SS have been initiated to test this system. It is expected that such averaging techniques will be of considerable use in any hot steel measurement system where grain sizes are large. Further signal processing development will be needed, especially when EMAT transducers, which have less sensitivity than PZT transducers but seem well-suited for on-line applications, are used. To that end, work is underway to reduce the above 7 second time to about 1 second.

Surface Tension Measurements
Subtask 5 of Task 15443

S. C. Hardy

The surface tension of silicon and its variation with temperature have not been known accurately, despite its technological importance in the processing of silicon. These data are of increasing interest because it is now thought that surface tension driving forces contribute significantly to fluid flow in the Czochralski and float zone crystal growth of silicon. Fluid flows arising from surface tensions are referred to as Marangoni or thermocapillary flows. The driving force for Marangoni flow is the surface tension gradient rather than the surface tension itself. Thus the flow depends sensitively on the value of the surface tension temperature coefficient $K = d\gamma/dT$. For silicon, estimates of K have ranged from approximately -0.1 mJ/m^2K to -0.4 mJ/m^2K. Recent modelling of the Czochralski process for silicon found that this variation in K gave significantly different flow patterns. Thus a quantitative understanding of silicon processing is to some extent dependent on accurate measurements of the temperature variation of the surface tension. We have measured the surface tension of liquid silicon in purified argon atmospheres as a function of temperature using the sessile drop technique. We find a temperature coefficient near -0.28 mJ/m^2K. Our experiments show a high sensitivity of the surface tension to what we believe are low concentrations of oxygen as shown in figure 4. Thus we cannot rule out some effect of low levels of oxygen in our results. However, the highest surface tension values obtained in conditions which minimized the residual oxygen pressure are in good agreement with a previous measurement in pure hydrogen which did not study the temperature variation. We therefore believe that the depression of the surface tension by oxygen is insignificant in these measurements.

Diffusion-Induced Boundary Migration
Subtask 6 of Task 15443

D. B. Butrymowicz, J. W. Cahn, C. A. Handwerker, and J. R. Manning

When a polycrystalline metal is exposed at temperatures one-third to one-half of its melting point to an alloying element that forms a solid solution with the metal, diffusion down the grain boundaries is consistently found to produce diffusion-induced grain boundary migration (DIGM) and provide alloying, but only in regions swept by moving grain boundaries. Without the grain boundary migration, alloying does not occur, since diffusion from the surface directly into the bulk is slow at these temperatures. A similar boundary translation and alloying process occurs when a new component is added to a system consisting of two grains separated by a liquid film, as occurs in some cases of liquid phase sintering. Although the two grains are separated by a liquid, the microstructural and chemical changes are analagous to those changes which occur in the solid state. In response to the addition of the new component, a solid solution forms on one grain surface and the other surface dissolves leading to a film translation. In current work, DIGM and liquid film migration are being investigated to test whether driving forces for both these effects arise from the same source. One theory has emerged which can explain the experimental observations in both interface migration situations, namely a theory based on stress differences from coherency strains which are produced on the unalloyed side of the boundary.

Scientifically, these phenomena are important because they are examples of a set of related kinetic problems, which include discontinuous precipitation, for which the thermodynamics and kinetics are not completely understood. Technologically, DIGM and liquid film migration are important since the microstructural and compositional changes that are produced can be used to modify the physical properties of the original solid in such processes as diffusion coating, sintering and interface interactions in composites.

The theory of this effect assumes that, when the metal is exposed to a diffusion alloying source, fast transport paths (grain boundaries or liquid layers) allow penetration of alloying elements into the boundary layer between grains and incipient alloying occurs on both sides of this layer. If the lattice parameter of the alloyed region is different from the unalloyed bulk metal, a stress will result. If stress relief occurs in the grain on one side of the boundary, there will be an incoherent unstressed layer adjacent to a coherent stressed layer. This situation will produce a driving force that makes the boundary migrate. Using the full thermodynamic expressions for free energy, the equalities of chemical potentials in phases at equilibrium, diffusion theory, and anisotropic elasticity, we have calculated for liquid film migration both the compositions of the equilibrium phases and the velocities of migration that should be produced by this effect. For the first time in this field, velocities and compositions derived from first principles are available with which experimental results can be compared. From this theory, the conditions for avoiding boundary migration and concomitant alloying are clearly spelled out. In addition, differences in stress and, hence, migration velocity are predicted for different crystallographic orientations of the stressed solid due to anisotropic elasticity.

Measurements of chemical composition (SIMS, electron microprobe), migration velocity, crystallographic orientation (selected area electron channelling), and lattice parameter were performed during the past year on Au-Ag (DIGM), Fe-Zn (DIGM), and W-Ni (liquid film migration) to test the predictions of the coherency stress theory. The condition of no coherency stress and the orientation dependence of migration were confirmed using the Au-Ag and the Fe-Zn systems, respectively. In the Au-Ag system, where the lattice parameter change with composition can approach zero, we observed, using quantitative analytical techniques, that the extent of alloying and migration decreased as the lattice-matching compositions were approached. In the Fe-Zn system, the shapes and orientations of the dissolving stressed regions corresponded to those predicted based on orientation-dependent stress and migration velocity.

A new phenomenon was observed with addition of O_2 to Cu-As during DIGM. Discontinuous oxidation, producing Cu-As-O compounds, occurred only in regions swept by moving boundaries. However, the rate of boundary migration was observed to be independent of the degree of discontinuous oxidation. Internal oxidation during DIGM adds a new and technologically important dimension to surface modification of metals by DIGM since it provides the opportunity of precipitation hardening of metal surfaces at temperatures that are typically one-third of the melting point.

<u>Microstructure Transformations--Coarsening; Liquefied Grain Boundaries</u>
Subtask 7 of Task 15443

P. W. Voorhees, R. J. Schaefer, and C. A. Handwerker

Within two-phase alloy systems at elevated temperatures, microstructural changes can occur even if the system is superficially at equilibrium, i.e., if the system consists of the equilibrium phases appropriate to the prevailing temperature and composition. The driving forces for these changes can include many types of differences or gradients within the system, for example, interfacial curvature, coherency stresses, solute concentrations or temperatures. In this subtask, the dynamics of this type of microstructural change are investigated theoretically and experimentally.

(1) Ostwald Ripening--Solute Distributions Surrounding Elastically Interacting Precipitates

Ostwald ripening, or the coarsening of particles under the influence of interphase surface energy, has long been recognized as an important mechanism of microstructural change in technologically important alloy systems. While the general nature of the effect is well known, the quantitative understanding of the influence of factors such as volume fraction of the coarsening phase or coherency stresses generated by the growing particles is extremely limited. These effects are currently under investigation.

In collaboration with Professor W. C. Johnson of Carnegie-Mellon University, an investigation was undertaken into the interaction between the stress and composition fields surrounding two spherical coherent precipitates. The precipitates were assumed to have different elastic constants than the matrix, and either be in a matrix subject to an applied tensile or shear stress or have identical isotropic stress-free transformation strains. The solute fields were calculated using the open system elastic constants approach of Larché and Cahn. As a result, the effects of the self-stress arising from the non-uniform composition field, as well as the stress field induced by the precipitates was included in the calculations to first order in the composition change. It was shown that the solute distribution surrounding two elastically interacting precipitates must be non-uniform at equilibrium (fig. 5). The magnitude of the concentration changes, with respect to an unstressed system, can easily exceed 50 percent under normal conditions. For two misfitting precipitates the composition field was highly localized near the precipitates, i.e., the composition field varied as R^{-3}, where R is the radius of the precipitate. Under an applied tensile stress, the solute field depended strongly on the orientation of the axis connecting the centers of the two precipitates with respect to the direction of the applied tensile stress. The predicted solute distributions surrounding two misfitting precipitates appears to be consistent with those observed by Piller et al. in a field ion microprobe. A central result of this investigation is that under conditions commonly occurring in many alloy systems significant concentration gradients can exist which do not engender mass flow. These large changes in solute composition can be expected to have an impact on many of the physical properties of two phase alloys.

(2) Migration of Liquefied Grain Boundaries

At elevated temperatures near the bulk solidus temperature, a layer of liquid can be produced at the grain boundaries of a polycrystalline alloy. When such a liquated boundary migrates, as it will do under the influence of curvature or temperature gradients, it leaves behind a modified microstructure. Measurements of this type of boundary migration have been carried out in two systems; succinonitrile containing 0.15 mole percent acetone and 2024 aluminum alloy. The former system, which is a transparent metal analogue, was strictly isothermal and the migration was induced by curvature effects, while in the latter system the migration was induced by the extreme temperature gradients present in the heat affected zone of electron beam surface melts. In addition to these migrations attributed to curvature and temperature effects, migrations of liquid boundaries have been observed in experiments on liquid phase sintering in W-Ni, where the driving force appears to be stress differences caused by compositional changes, as in diffusion-induced grain boundary migration. The wide range of alloys and disparity in driving forces in which wetted grain boundary migration has been observed implies that the phenomenon may occur in many alloy systems at temperatures near the solidus temperature. The microstructure generated by the moving boundaries depends primarily on the stability of the solidifying interface. In the case of the 2024 aluminum in the temperature gradient, the solidifying interface was cellular and a characteristic spacing could be measured, while in the succinonitrile the instability was much less but one could observe in detail how the boundary left behind occasional individual liquid inclusions in the solidifying crystal. A result of the droplet shedding process is that a homogeneous solid is transformed to an inhomogeneous mixture of solid plus liquid droplets. Therefore, upon freezing the solid will have a highly non-uniform solute segregation pattern with the accompanying poor physical properties.

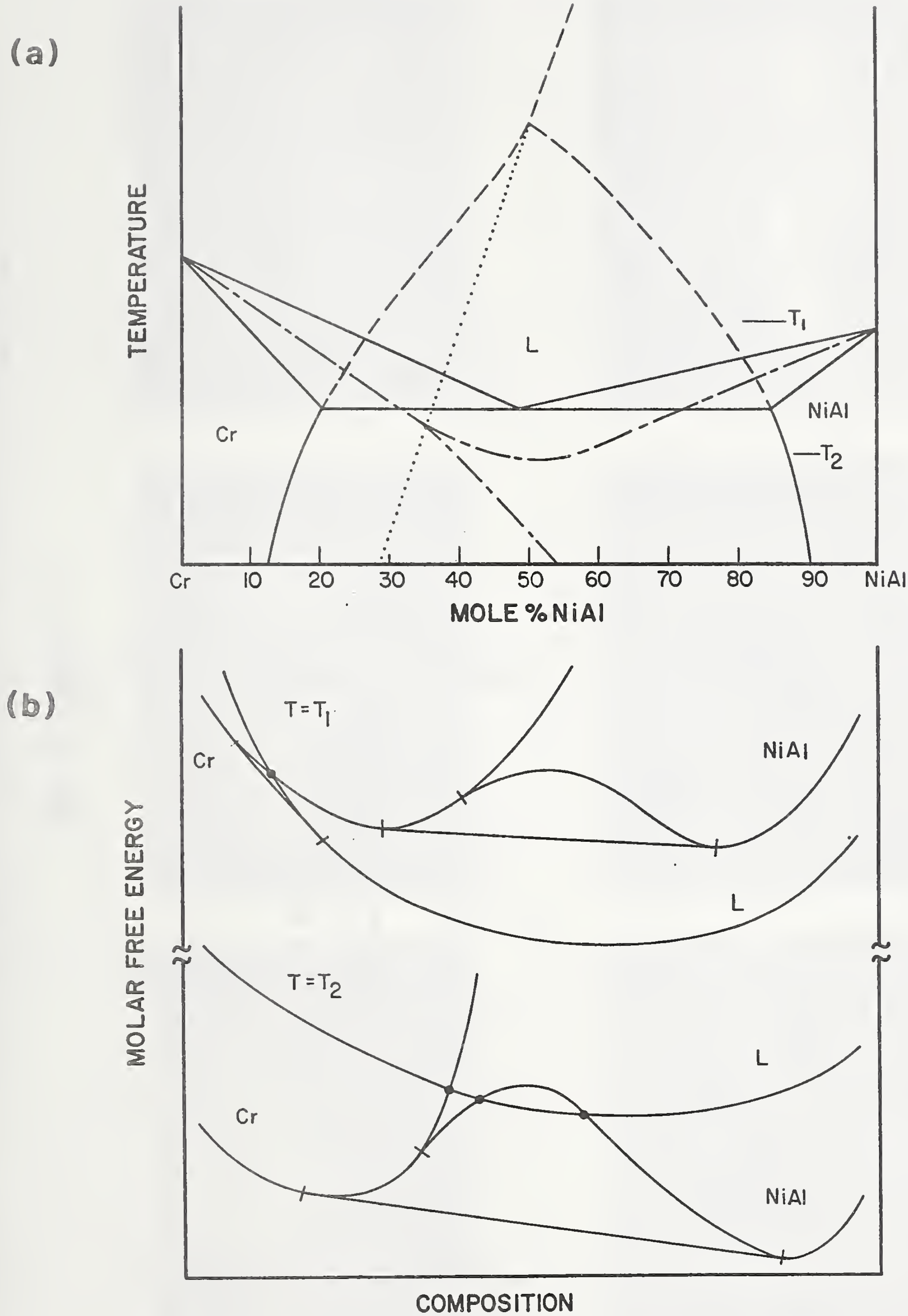

Figure 1. (a) NiAl-Cr phase diagram (solid lines), schematic metastable extension of solvus curves (dashed) to tricritical point and beyond where the ordering reaction is not first order, T_0 (dot-dashed lines) curves for α-Cr and β--NiAl and spinodal curve (dotted line) which determines point at which the α-Cr T_0 curve splits. Partitionless solidification of the NiAl structure is energetically favored over the Cr structure to the right of the point where the Cr T_0 curves split.

(b) Schematic free-energy vs. composition curves for NiAl-Cr system..

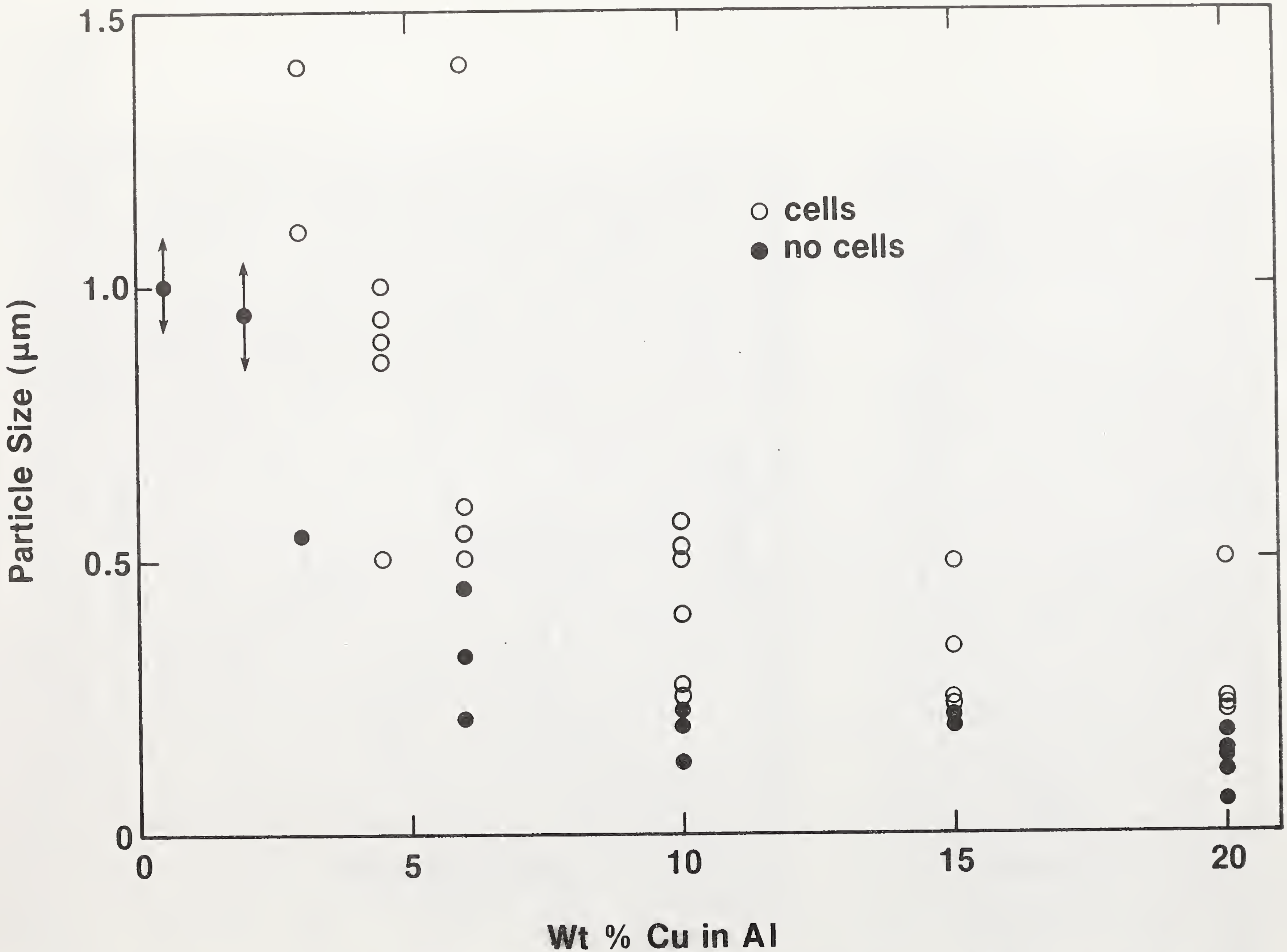

Figure 2. Results of microstructural study using electrohydrodynamic atomization of Al-Cu particles indicating size, composition and microstructural type observed. The maximum size where cell-free particles are observed is strongly composition dependent.

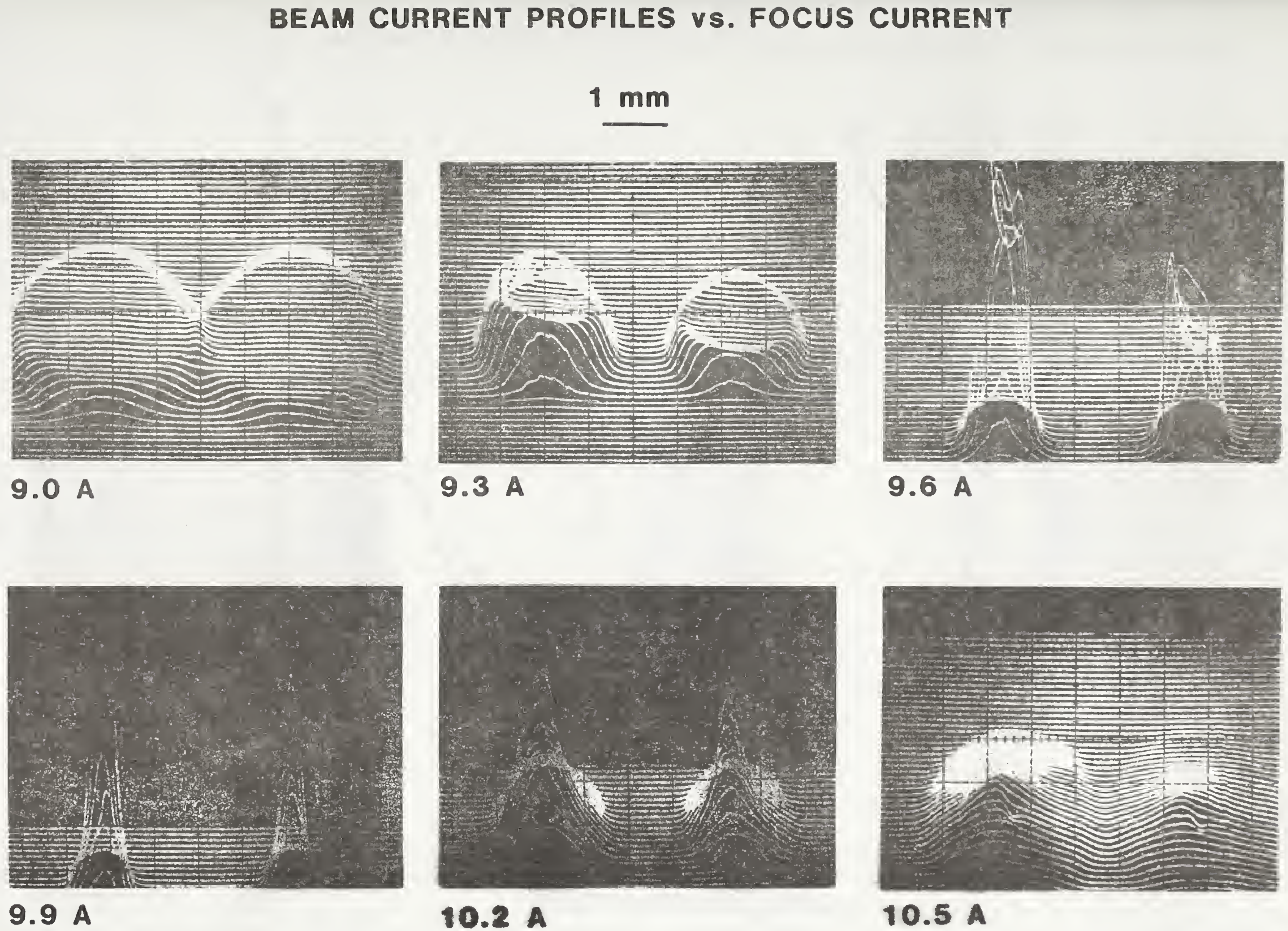

Figure 3. The distribution of current density in a 25 kV electron beam at different focus lens currents. The detector produces two images of the beam current profile separated by 3 mm.

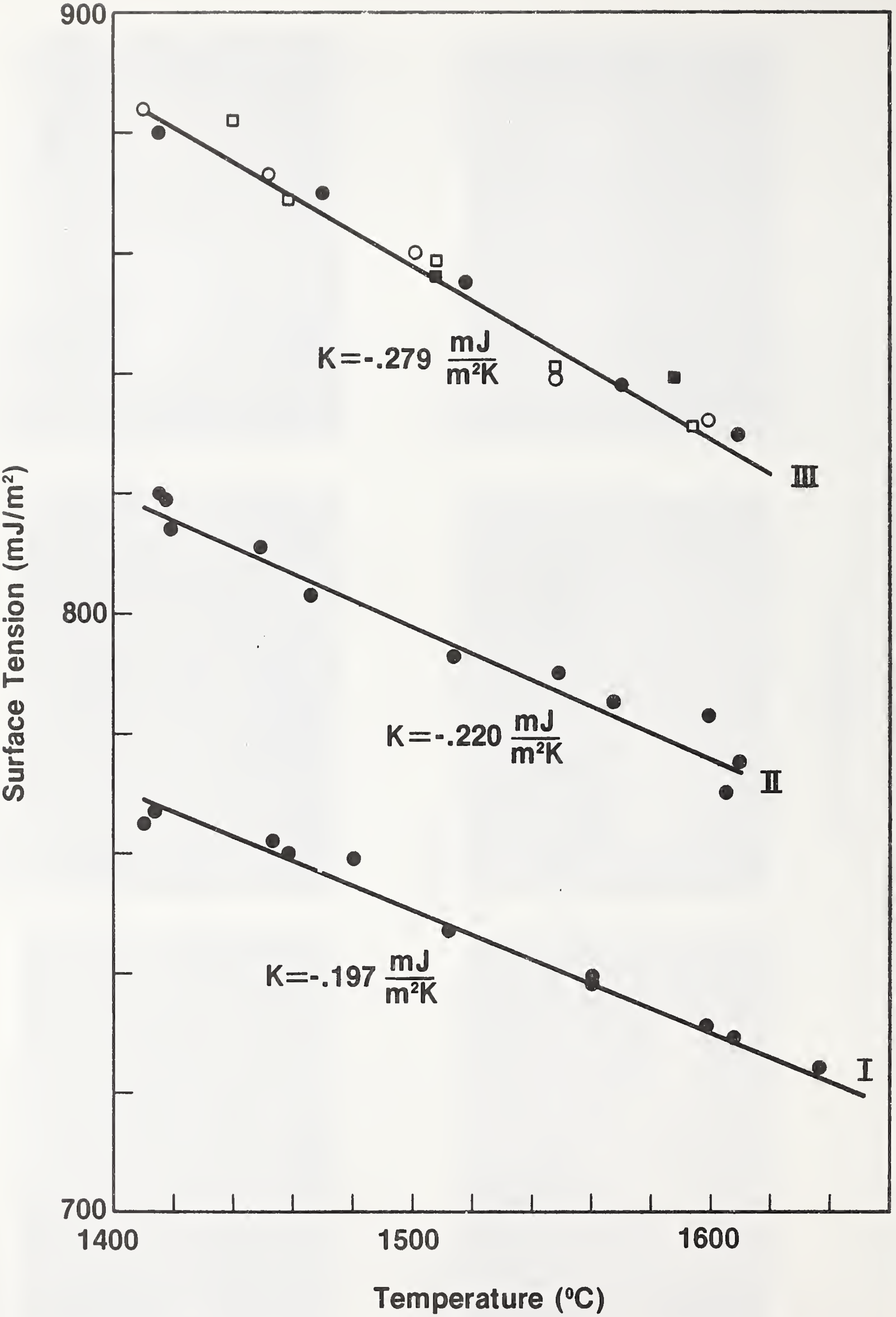

Figure 4. The surface tension of silicon as a function of temperature. The surface tension and K variations in the three groups of data are attributed to different concentrations of impurities. Data set III is for highly purified silicon, whereas data sets II and I are for silicon with increasing amounts of oxygen present.

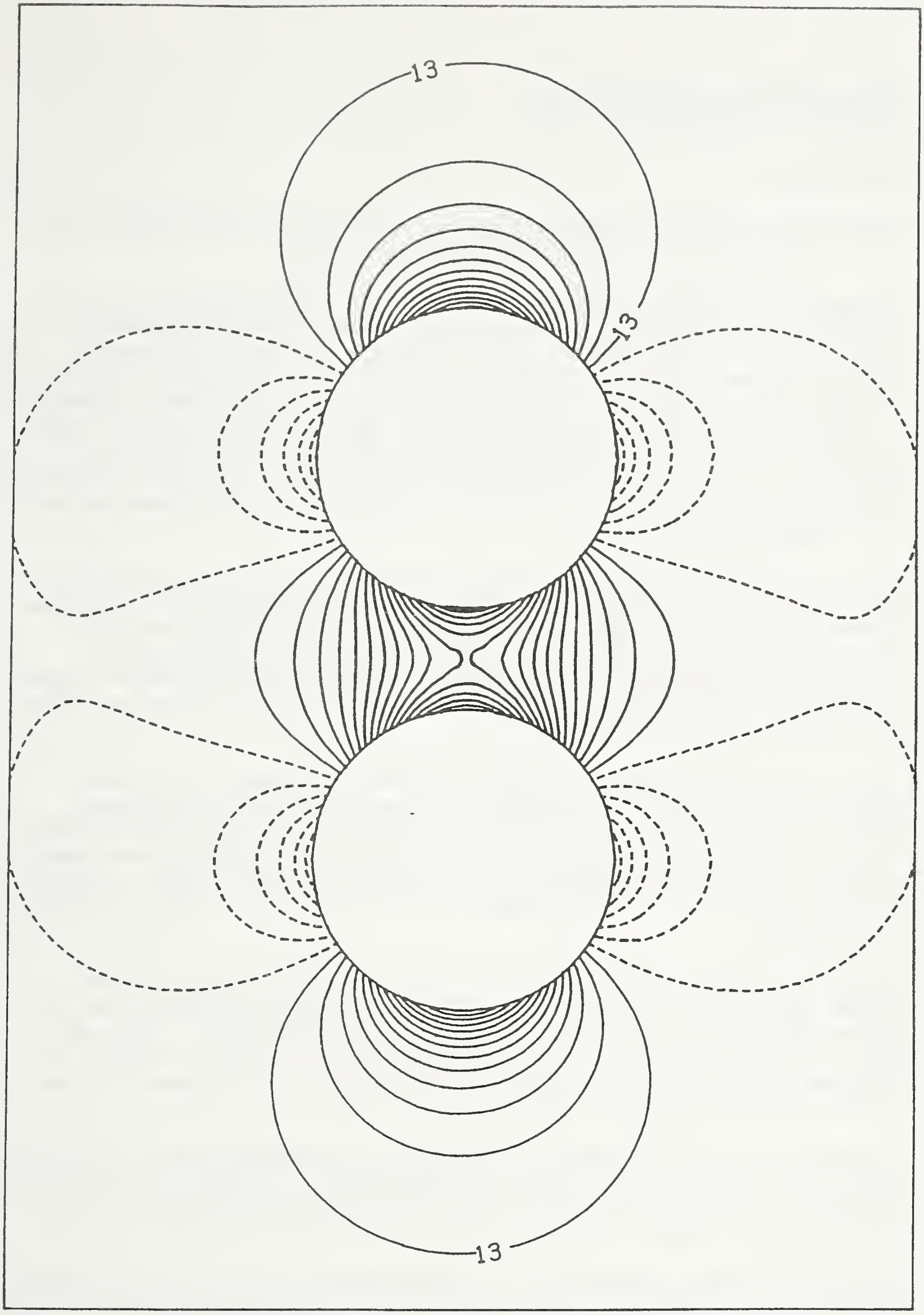

Figure 5. Dimensionless isoconcentrates surrounding two elastically interacting coherent misfitting precipitates. The dimensionless scale depends on the relative misfit and elastic properties of the precipitate and the matrix, as well as the relative atomic volume of the solvent and solute species. Dashed and solid lines represent deviations with opposite signs from the average matrix concentration.

Theoretical Materials Stability
Subtask 2 of Task 15401

John W. Cahn

This work addresses fundamental factors in the stability of materials. It is carried on with a wide variety of colleagues.

In support of the phase diagram activity, statistical mechanical calculations of phase equilibria and ordering in hexagonal close packed metals are being carried out. The usefulness of various metastable curves on phase diagrams in predicting sequences of metastable equilibria and phase change mechanism has been explored. Rules for the occurrence of higher-order critical points have been formulated, and several rules derived for their shapes on phase diagrams. A new understanding of coherent phase equilibria has revealed a theoretical basis for unexpected differences in experimental results that may resolve discrepancies that have plagued evaluators.

A new kind of solid phase, intermediate between crystal and liquid, has been formed by rapid cooling of molten aluminum alloyed with transition elements. The phase shows long range orientational order, but its point group symmetry, $m\bar{3}5$-icosahedral, can not be consistent with crystalline translational periodicity. The phase forms from the liquid by nucleation and growth, and is quite resistant to transforming to the equilibrium crystal structures.

A solid-state thermodynamics theory has been developed which takes properly into account that surface or interface stress is different from surface or interfacial free energy and is being extended to complex crystal structures with complex point defects. The results have shed insight into coherent phase equilibria and diffusional creep, including the discovery that there are stressed solids that can't creep by diffusion of vacancies.

General principles of surface, interface, and grain boundary phase changes have been developed. One important theorem indicates that such changes generally result in faceting to new orientations. Congruent phase changes in which a planar surface change to a planar surface of the same orientation with a new structure occur only for specific, and usually highly symmetric, orientations.

A formulation of multicomponent diffusion was developed which incorporates obvious invariances with respect to some arbitrary changes in definition. The result seems to be a simplification that may be important in data gathering and in applications.

Inclusion or solid precipitates in solid matrices give rise to an elastic distortion whose energy is shape dependent. Shape bifurcations have been shown to occur if interfacial energy is considered.

WEAR AND MECHANICAL PROPERTIES
Task 15444

The goal of the research carried out in this task is to improve measurement methods and to develop standards appropriate for problems involving wear and mechanical properties of metals. Supporting research also is carried out addressing the mechanisms involved in wear and mechanical performance, for example, in abrasion, microplasticity, and dimensional stability. The approaches used in the various subtasks are described in the following sections. The methods used include wear and mechanical testing, optical and electron microscopy, microindentation measurements, surface analyses, metallography and particle and surface film analyses. An additional activity concerns corrosion and fatigue behavior of alloys used in synthetic implants.

Wear and mechanical related failures occur in all areas of material applications, from large scale structures to small scale mechanical devices, even including microcircuits. Avoidable wear losses to the U.S. economy have been estimated to be as high as $50 billion annually. A recent NBS study on the costs of fracture in the U.S. concluded that even larger costs are found in that area. It is believed that improved measurement and test methods can assist in selecting materials and developing new materials having superior wear properties. Data obtained using well controlled test methods can be utilized in developing analytical models of wear and mechanical behavior. In this way, predictive capability can gradually develop to assist the design of improved mechanical systems.

Highlights of the technical program in this task over the past year include the following:

- A dynamic microindentation test system has been constructed and used in a series of micromechanical studies of several well characterized metals. This system can provide dynamic mechanical properties data over five decades of strain rate and obtained from regions of the order of 10μm in size.
- Wear and friction studies of "break-in" phenomena were completed with an emphasis on uni-direction and reversed-direction sliding contacts using a series of well characterized copper alloys.
- A new test method has been developed to study wear due to abrasive contaminants in lubricating greases. The test is now being extended to investigations of other fluids and different types of abrasives.
- Task personnel handled arrangements for the largest, most comprehensive biomaterials meeting ever held with 823 attendees from 25 countries. NBS research results were presented in two papers concerned with corrosion and mechanical properties.
- A non-destructive eddy current test technique was devised to reliably detect cracks in the neck threaded regions of pressure gas cylinders fabricated from aluminum-fiberglass composite.

A considerable portion of the staff efforts in this task involves collaboration with outside groups, industry, academia, and other federal agencies. These efforts are listed later in this report, however, several are worth special attention here. A new Industrial Research Associate position is being established in the galling wear area with Deere and Co., Moline, IL. The interaction may also broaden next year to include wear data evaluation involving key personnel in both organizations. Discussions are underway with the American Society of Mechanical Engineers (Tribology Division) and the Department of Energy to support a new wear data effort within this task. The aim of the work will be to evaluate wear data from standard tests on many materials as possible, and to examine the potential for analytical modeling of wear in terms of material properties. Other important interactions of the past year involved 3 guest worker assignments, numerous industrial consultations, and some critical assistance provided to the Department of Transportation concerning pressure gas cylinder failures.

Metallic Wear
Subtask 1 of Task 15444

A. W. Ruff, P. J. Blau, L. K. Ives, C. Olson, J. Harris, E. Whitenton

Studies have continued in the application of surface melting techniques followed by rapid solidification to develop wear resistant microstructures in tool steels and other alloys. Dry sliding block-on-ring wear studies have been completed using electron beam surface melted O-2 tool steel against 52100 bearing steel. All tests were done at 20 cm/s sliding speed in an argon gas atmosphere at 23°C using loads from 1N to 500N. Since previous studies had shown that reduced wear resulted from the refined, martensitic microstructure produced in the surface melted material, it was important to determine the load dependence to examine the mechanisms involved. As the load increased from 1 to 500N, the wear coefficient first decreased and then increased above 100N. The initial decrease is believed to reflect a transition from wear of the oxide film to wear of the O-2 steel itself. In the first case the wearing stresses are contained primarily in the region of the the surface film (which is continually replaced by oxidiation during wear). As load increases, more of the stresses are transferred deeper into the wear resistant steel and wear coefficient decreases. Above 100N the wear coefficient increases again. This is thought to be a result of increasing stress and plastic deformation within the steel that finally exceed the inherent resistance of the microstructure. Confirming evidence is being sought through studies of the wear debris from these tests. Debris particle size, shape, and amount of oxide present are being measured. Recently, electron beam surface melting was conducted with R. Schaefer on a set of 4 Cu-Al alloys that are also being studied at Vanderbilt University. These alloys show a variation in wear rate that is associated with metallurgical characteristics such as composition, stacking fault energy, and microstructure. Dry sliding wear studies are being done at Vanderbilt and polishing abrasion studies will be done at NBS for comparison.

A new abrasive wear test method is being developed and applied based on previous work by Rabinowicz at MIT. The method involves a water/slurry of fine abrasive (<40μm particle size) fed continously to a rotating, cloth covered wheel on which 9 individual specimens are rotating independently under light load. The method seems to be reproducible so long as uniform motion and abrasive feed rate are maintained. The flow of abrasive from the wheel center out to the rim seems to uniformly distribute the abrasive and continually feed fresh abrasive into the contact zones of the 9 specimens. This test may be suitable for evaluating surface modification treatments of metals since mild abrasive wear conditions can be reproducibly maintained. Studies are underway on an abrasion resistant tool steel and a stainless steel, since abrasive wear values are available for those alloys using the ASTM G-65 wear test. A group has been formed in ASTM Committee G-2 on polishing abrasion; the chairman is from this task. Seven other individuals from industrial companies are involved. A liaison has been established with the Naval Engineering Center, Philadelphia, where there is need for a test for metal polishes.

An analysis has been completed of interlaboratory test data on solid particle erosion of several metals using the new ASTM standard G-76, Erosion by Solid Particle Impingement using Gas Jets. The data were obtained at NBS and seven other laboratories in four rounds of measurement under NBS leadership. The new standard was developed as part of this effort. The overall precision of measurement was found to be 3% within-lab average and 17% between-lab average. The use of an agreed-upon reference material for calibration of the test system is presently being explored. The overall reproducibility is felt to be adequate to justify using the method in quantitative laboratory studies of erosion performance of materials and coatings.

Since metallic wear occurs by progressive deformation, damage accumulation, and fracture, another project is studying particular aspects of the wear process. These include the response of the microstructures in the contact zone to the stress conditions imposed by the geometry of the contact and the loads being applied. An investigation of the effects of unidirectional and reversed sliding was performed with computer-controlled sphere-on-flat tribometers using fixed 52100 steel balls sliding dry on flats of Cu-3.5 wt.% Al, Cu-5 wt.% Sn, and Cu-15 wt.% Zn alloys. Both the friction coefficient dependence on number of strokes and the type of damage observed on the wear tracks differed between unidirectional and reversed sliding in all three alloys (see Fig. 1). This effect is believed due to the difference in crystallographic texturing, debris distribution, and workhardening structures which develop early in the break-in period. Implications to simulating machine component wear and friction behavior using laboratory tests are that there can be significant differences in operative wear processes unless the appropriate sliding motion for a given application is provided during the simulation. Additional studies involving thin oxide film effects on these same materials are under way. The new technique of thermal wave microscopy is being applied to provide more microstructural information on the metal/oxide mechanical behavior under wear conditions. The equipment has been added to our SEM and is being used in this and other projects to detect flaws, cracks, and certain subsurface microstructures.

In February 1984 a transmission electron microscope was installed as a Center for Materials Science facility in the Materials Building. This microscope is designed for routine operation at 300 kV. It is one of the first of its type to be delivered in this country. It offers several advantages over existing lower voltage instruments. The shorter electron wavelength leads to an increased resolution which makes it possible to obtain structure images in the 0.15 to 0.2 nm range. In addition to improved resolution, the increased accelerating voltage allows the study of thicker specimens. Thus a better representation of bulk microstructures can be obtained. Specimen preparation problems can be reduced and in a given specimen much larger regions may be available for study. It also is expected that improvement in chemical analytical capabilities will be obtained with the new instrument.

Galling of Metals
Subtask 2 of Task 15444

L. K. Ives, M. B. Peterson, K. J. Bhansali

This project is supported primarily by the Department of Energy Fossil Energy Materials Program. Its purpose is to develop a better understanding of galling wear of metals. Particular emphasis is placed on developing measurement methods to characterize galling damage and on determining the influence of metallurgical variables on the severity of galling. Galling is an extremely severe form of wear on sliding surfaces that tends to occur suddenly. Galled surfaces are very rough as a result of local plastic deformation, tearing, fracture, gouging, and often material transfer between the mating surfaces. Austenitic stainless steels and many high temperature corrosion resistant alloys which find application in energy conversion systems are particularly susceptable to galling. Valves and actuating linkages are particular relevant components.

A unique test apparatus capable of operating at high loads and elevated temperatures has been developed here. Tests have been carried out on a number of different metals including a series of pure metals having fcc, bcc, and hcp crystal structures. The interest has been in relating plastic deformation properties of the simplest and best understood materials to galling behavior. Other more complex alloys selected on the basis of particular mechanical, microstructural, or elevated temperature properties have also been studied. Results so far indicate that microstructural features or plastic flow characteristics that tend to restrict the spread of deformation result in less severe galling damage. This is best demonstrated in a two phase structure such as leaded brass which contains a soft phase (lead) together with a hard phase (brass). The concept concerned with the localization of deformation damage was demonstrated in a simple way involving surface finish. When machining grooves were parallel to the sliding direction the spread of damage was constrained. With the machining grooves perpendicular to the sliding direction, deformation was less localized and galling was greater.

Investigations of galling that have been reported in the past have not attempted to characterize galling in terms of the degree of severity. Developing methods to measure the amount of galling also has been a major focus of this project. Athough further evaluation is needed, a measure based on the maximum peak to valley roughness appears to be an appropriate parameter for galling damage. Galling is recognized as a problem of widespread importance in industry. Task personnel have worked in the ASTM Committee G2 on Erosion and Wear to develop test methods to measure galling. Interest in the NBS program has lead to the identification of an Industrial Research Associate from Deere and Co. A scientist from the Technical Research Center will work at NBS to further develop methods to characterize galling damage.

Lubricated Wear
Subtask 3 of Task 15444

L. K. Ives, M. B. Peterson, P. Boyer

This project, supported by the Office of Naval Research, has been concerned with defining the effect on wear of the solid additive compound, antimony thioantimonate ($SbSbS_4$), and determining its mechanism of action. The purpose of the final stage of the study has been to investigate the effect of the compound on wear by abrasive contaminants in lubricating greases. The presence of abrasive contaminants is often cited as a primary cause of wear in lubricated systems. In spite of this, relatively little fundamental work has been published in this area. In the work that has appeared in the literature there is considerable disagreement on the effect of additives on abrasive wear. On the basis of our studies it appears that the disagreement is probably related to the use of different test methods and conditions as well as to some confusion as to whether the additives directly affect the efficiency of abrasion or prevent adhesive wear which is caused indirectly by abrasion. Our studies indicate that under mild wear conditions antimony thioantimonate and molybdenum disulfide, which was studed for comparison, tend to increase the rate of wear in the presence of abrasives (see Fig. 2). In addition to these findings an important contribution of the project has been the development of a wear test device for the measurement of wear by abrasive contaminants under grease lubricated conditions. A second part of this subtask, initiated during the current year, is studying the influence of metallurgical variables on the transition from mild to severe wear. The study so far has focused on pure metals sliding at low speeds under lubricated conditions. Under these conditions deformation processes can be more easily understood and complications due to thermal effects are minimized. The investigation utilizes optical, scanning electron, and transmission electron microscopy. Both subsurface microstructures and surface films are studied using specimen preparation techniques that were developed previously in this project.

Wear Standardization and NDE
Subtask 4 of 15444

A. W. Ruff, P. J. Blau, L. K. Ives, R. Polvani, P. Boyer

Measurements are underway to improve the specifications for the Tool Steel Abrasive Wear SRM (#1857) which had been developed here previously.

While employing the SRM in the calibration of dry sand/rubber wheel tests it was recognized that opposite test faces of the standard gave small but systematic differences in wear rate. It was found that this difference could be correlated with differences in roughness of the worn surfaces which could be related to the location of the specimen in the original bar material. Experiments are currently underway to measure wear rate as a function of position in the specimen. As a result of this work it is expected that the abrasive wear value for the SRM can be specified with greater precision. A request has been received from ASTM to consider the development of a second wear SRM with properties closer to those of less wear resistant materials.

A unique load-displacement microindentation hardness testing device with high precision penetration measuring capabilities was used to investigate the response of Cu and Ni microhardness standards to a range of loading rates and load application wave forms. The purpose of this work was: (1) to determine whether load-displacement techniques would give similar microhardness numbers to conventional optically measured and calculated values, (2) to determine whether existing SRM's produced by NBS would be certifiable for computer-controlled microindentation devices in the future, and (3) to see whether the additional load-displacement information obtained by the new type of machine could be used to extract additional information about elastic-plastic behavior of metals. Initial results are encouraging in demonstrating that comparable microhardness values can be obtained by the new device, and that load-displacement curves are very reproducible. Work continues on the detailed interpretation of these curves. Support from the NDE office is anticipated next year to expand this project and improve our capability for microindentation testing.

A project on standardization of wear debris analysis methods, particularly ferrography, is being completed. Interlaboratory studies have shown that quantitative analyses on wear particle size and density can be obtained using magnetic recovery methods from lubricating fluids; however, closer agreement between laboratories is dependent on better measurement of particle densities. We have proposed a method for calibrating optical reader systems used in this type of work, and are finishing development of that method. It will then be tested in four other laboratories to determine the improvement that is possible.

Microdeformation Studies
Subtask 5 of Task 15444

R. Polvani, E. Whitenton

Designers of equipment and structures face a variety of end uses. They need access to a range of mechanical properties data for design purposes, particularly on a dynamical scale. As examples, structural supports and piping are creep strength limited, while bearings, cams and gears are wear, fatigue, and impact strength limited. A rate-sensitive strength is characteristic of all materials; it can be thought of as having two components, elastic and plastic, the magnitudes depending on loading rate. At low rates of deformation, plasticity dominates, while at high rates the response is largely elastic. Complementing this engineering need for data is a research need to understand the particular mechanical behavior. An example would be the mechanical differences between ordered versus disordered regions in a nickel base superalloy, or between the matrix region and the fiber of a metal matrix composite.

A new non-destructive approach to mechanical testing is being implemented in this project. Although derived from conventional hardness testing, the method of dynamic microindentation has two important innovations. First, while indenting a sample a load/displacement curve is obtained similar in concept to the stress-strain diagram from a tensile test. Second, indentation may be performed over a broad range of loading times, from hours on down to milliseconds. The range of loading times means that a variety of test conditions--creep, tensile yield, impact--can be established using a single apparatus. The test frame and instrumentation package are shown schematically in Figure 3. An electromagnetic driver is interfaced to a dedicated microcomputer permitting close control over the loading waveform. The computer system can also plot and do statistical analyses of the data. A hardness number comparable to conventional practice is one measurement result. By using the load/displacement curve, we can separate out the elastic versus plastic components of ductile materials and elastic versus fracture components of brittle materials. The relative magnitude of these various components are being measured for lead, 6061,2024 and 1100 aluminum, copper, glass, 1020 steel, titanium, and nickel. We are also trying to extract a true compressive yield stress directly from indentation testing using the load/displacement curve. With a small ball indenter the task is straightforward but the spatial resolution is unacceptably large. An alternative, being investigated is based on small ball indentation and extrapolation of the Meyers' "mean pressure" to zero applied load.

<u>Mechanical Properties of Metals</u>
<u>Subtask 6 of Task 15444</u>

J. H. Smith, J. S. Harris

An accurate and comprehensive understanding of the behavior of materials under a wide range of loading and environmental conditions is required to obtain adequate structural and mechanical integrity in manufactured products. The objectives of this task are to (1) accurately characterize the mechanical properties of metals and composites, particularly ductility, toughness, and formability, (2) relate these properties to the microstructural features of the materials, (3) develop reliable mechanical properties test methods, and (4) demonstrate the applicability of these test methods to specific structures and mechanical components. The emphasis of this work is both on the characterization of newly developed materials, such as rapidly solidifed metals and metal matrix composites, and on the improved characterization of conventional materials, such as steel and aluminum alloys. A study of ductile fracture is underway to better characterize fracture that occurs under large plastic deformation and multi-axial straining. A parameter has been defined which measures true strain to fracture and which appears to correlate well with fracture behavior of compliant, ductile structures. This procedure is most applicable to fracture of very compliant structures such as piping and thin walled pressure vessels.

Studies have been initiated to better understand the significance of microstructural features such as inclusions and chemical segregation on the ductility and formability of conventional and newly developed materials. The objective of this work is to better define the fundamental microstructural features controlling ductility and formability so that the effect of unique materials processing can be determined to produce acceptable materials.

Development of Test Methods for Hazardous Materials Containers

NBS has provided technical assistance and testing services to the Office of Hazardous Materials Regulations of the Department of Transportation in support of promulgating safety regulations for metallic and composite pressure vessels. The following two projects were carried out this year. (1) Standards for Metallic Cylinders and Cargo Tanks: A detailed evaluation was made of the use of a fracture mechanics criterion to ensure the structural integrity of high strength steel cylinders and to permit the use of higher strength, light weight cylinders manufactured from newly developed steel alloys. An extensive, experimental test program has been initiated to verify the use of this fracture criterion. A detailed stress analysis of a full scale intermodel cargo tank has been completed and a full scale experimental test program has been initiated to verify this analysis. The results of this program will permit the design of lighter weight cargo tanks without sacrificing any structural integrity. Tests have been completed to correlate the tensile ductility with the test specimen size and configuration for a wide range of metals used for the construction of metallic cylinders. The results of this work will permit the reliable conversion of tensile test results between common U.S. specifications and all foreign specifications. (2) Non-Destructive Evaluation (NDE) of Seamless Pressure Vessels: An assessment was made of the use of acoustic emission techniques to periodically inspect large seamless steel pressure vessels used to transport compressed gases. The use of these techniques permits much more reliable and cost effective evaluation of these pressure vessels. Extensive NDE tests were carried out on composite (fiberglass-aluminium) cylinders to develop a suitable procedure for finding cracks in the threaded necks. An eddy current method was found to be reliable and will permit the use of these cylinders in critical service applications.

Evaluation of Degradation of Metallic Chimneys

At the request of the Consumer Product Safety Commission, extensive metallurgical and mechanical properties evaluations were undertaken of metallic chimneys used for wood burning stoves. These chimneys have been found to be responsible for approximately 50,000 house fires per year and it was necessary to determine to what extent the degradation of the material is responsible for causing such incidents. Preliminary results indicate that recently manufactured chimneys constructed of type 304 stainless steel do not experience significant degradation during normal use. Chimneys manufactured from type 430 stainless steel appear to be susceptible to degradation by embrittlement under some situations.

Metallic Surgical Implants
Subtask 7 of 15444

A. C. Fraker, A. C. Van Orden, G. J. Mattamal

Metals are used extensively as implants in the human body for many purposes including orthopedics, heart pacemaker cases and leads, and dental implants. Metals and alloys selected for use as surgical implants must be biocompatable, durable, and meet special requirements for a given use such as strength in the case of orthopedic implants. Biocompatibility and durability are associated with the corrosion resistance of the metal to the body fluids. High corrosion resistance will assure that ion release into the body is limited and that failures caused by corrosion are minimized. Work on this project deals with metallurgical aspects; corrosion behavior and mechanical properties of surgical implant metals are investigated. Also addressed is the effect on corrosion and mechanical strength of alloy composition, changes in processing parameters, and other factors. A new development involves metal porous coatings applied to metal prosthetic devices in an effort to improve fixation of the device in the body. Application of porous coatings can result in different metallurgical phases, microstructures, contamination, etc., and these changes can affect corrosion and mechanical behavior. Summaries of the results of the past year's work are presented in the following paragraphs.

Corrosion Behavior of Porous Coated Implant Metals
The corrosion behavior of porous coated Co-Cr-Mo material was studied by exposure to Hanks' physiological saline solutions and anodically polarizing the material. Specimens of sintered Co-Cr-Mo spheres on a Co-Cr-Mo substrate were obtained from two different implant manufacturers. The sphere size was in the range of 200 to 800 μm. Anodic polarization measurements were made on specimens in the passivated and non-passivated condition. The unpassivated porous coated Co-Cr-Mo material and the smooth Co-Cr-Mo material showed a breakdown potential at 0.47 volts vs. saturated calomel electrode (s.c.e.) while the passivated specimens broke down at a more noble potential of 0.80 volts vs. s.c.e. Corrosion current was higher for the porous coated material but the current density of the porous specimens was the same as that of the smooth material. Second phases can be present in the necks of the sintered spheres, and this can be controlled partially by processing. The morphology of the surface films was studied using scanning electron microscopy. Films appeared to be thicker in the interstices. Energy dispersive xray spectrocopy was used to analyze the surface films which were enriched in Cr, Mo and Fe. Electron spectroscopy for chemical analysis (ESCA) was used to determine that the oxidation state of Cr in the surface film, was +3 as shown in Fig. 4.

Standard Reference Materials (SRM)
Production of the SRM 1890, 316L stainless steel, for use with the ASTM

test for pitting and crevice corrosion of implant metals has been completed. The Food and Drug Administration has purchased five more sets of these materials for the ASTM to use in another round robin test. The Co-Cr-Mo material for SRM 1981 has been obtained from an implant manufacturer, and production of the SRM is in progress.

Metal Ion Interactions with Body Fluids

Further analysis was made of data collected on the binding of the Ni(II) ion to human blood serum albumin. The experiments conducted previously utilized introduction of the nickel ion to the serum albumin by a nickel salt or by electrochemical means. This was followed by ultrafiltration and by atomic absorption analysis. Results showed that nickel was bound to the protein molecule at approximately 16 bonding sites. Data on the kinetics of the reaction and the degree of bonding were presented to the dental and biomaterials communities. Dr. George Mattamal, who has been associated with this project, at present is on assignment with the Department of State.

Titanium Alloys: Mechanical Properties, Heat Treating and Porous Coating

This area of study involves two parts. The first is an investigation of the influence of thermal treatments on the fatigue crack initiation and propogation in the Ti-4.5Al-5Mo-1.5Cr (Corona-5) alloy. This was a cooperative study with Professor Charles Gilmore, S. H. Yang, and Dr. M. A. Imam of the George Washington University. The alloy was heat treated for 30 minutes in the range of 760°C (1400°F) to 965°C (1770°F), and the resulting chemical composition of the phases and the microstructural condition were correlated with mechanical behavior. The presence of a metastable beta titanium phase can lead to a strain induced transformation to martensite. This was verified by microstructural analysis utilizing techniques of transmission electron microscopy and electron diffraction. Torsion fatigue tests conducted on the specimens from the different heat treatments showed that fatigue life was dependent on the heat treatment and the strain induced transformation. Fatigue crack growth rate measurements indicated no significant effect resulting from heat treatment or the presence of the metastable beta titanium phase.

The second area of study is an investigation of the application of a porous coating of Ti-6Al-4V or of Ti on a Ti-6Al-4V substrate for use as surgical or dental implants. This work, partially supported by the FDA, is conducted in cooperation with Henry Hahn, Artech Corporation. Coatings are applied by arc plasma spraying onto Ti-6Al-4V ELI grade specimens. Specimens are tested for interface bond strength, corrosion-fatigue life, and hardness through the cross section of the coating, interface and substrate. Corrosion-fatigue tests are conducted in fully reversible torsion with a constant applied shear strain amplitude. Specimens are held in flowing saline solution kept at body temperature, and the frequency of the test is usually 1 Hz. Results show that the application of the coating does not adversely affect the corrosion-fatigue life of the material but that (i) sintering above the beta titanium transus or (ii) introducing oxygen or (iii) causing oxygen migration reduces the corrosion of arc plasma sprayed titanium.

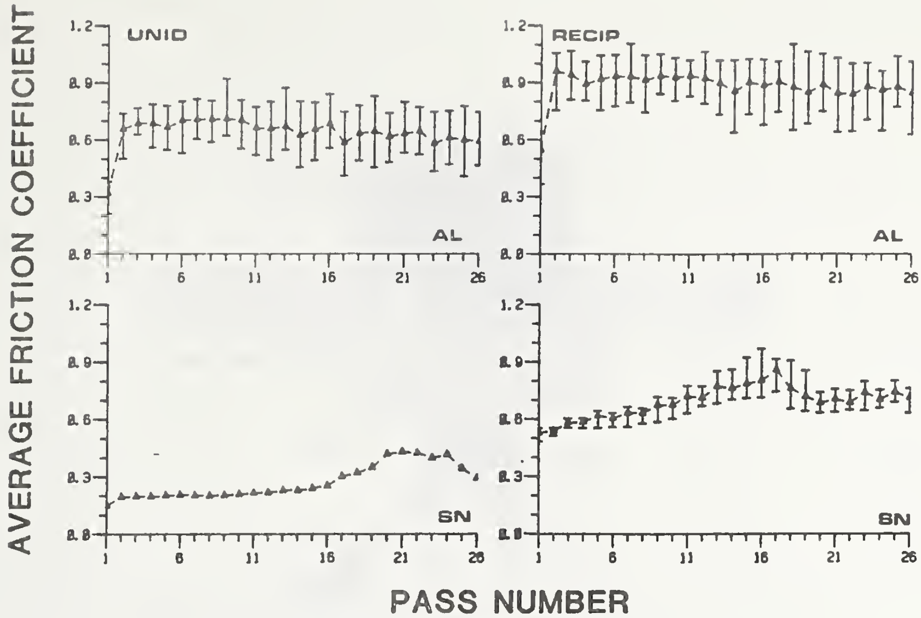

Fig. 1 Sliding friction coefficient variation with accumulated number of sliding passes for Cu containing either 3.5%Al or 5%Sn comparing uni-directional to reciprocal motion during the "break-in" phase. (500g load, 5mm/s velocity, 2 cm stroke length, lab air).

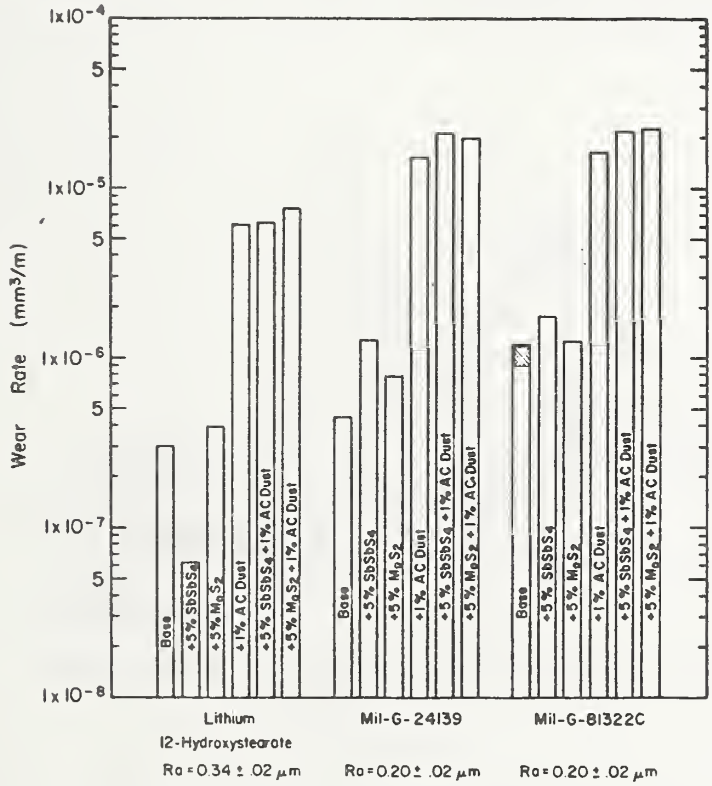

Fig. 2 Wear rates of 52100 steel vs 02 tool steel in the presence of several different grease and solid lubricant additives involving contamination by a reference test dust (abrasive).

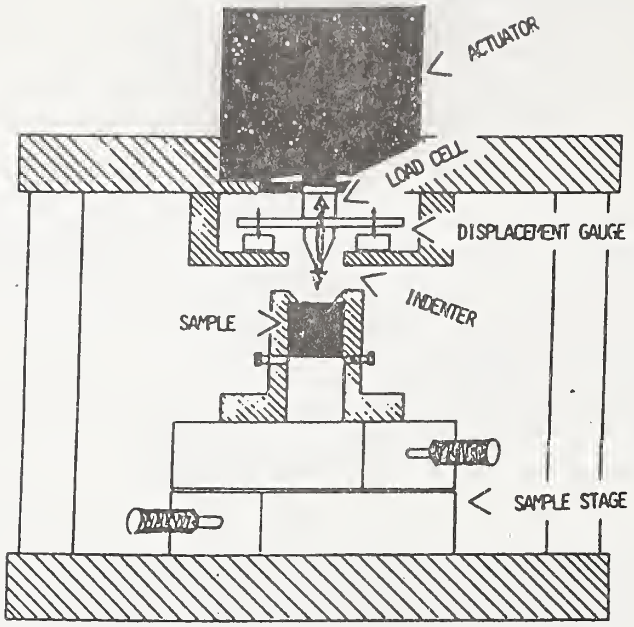

Fig. 3 Schematic illustration of NBS dynamic microindentation test system.

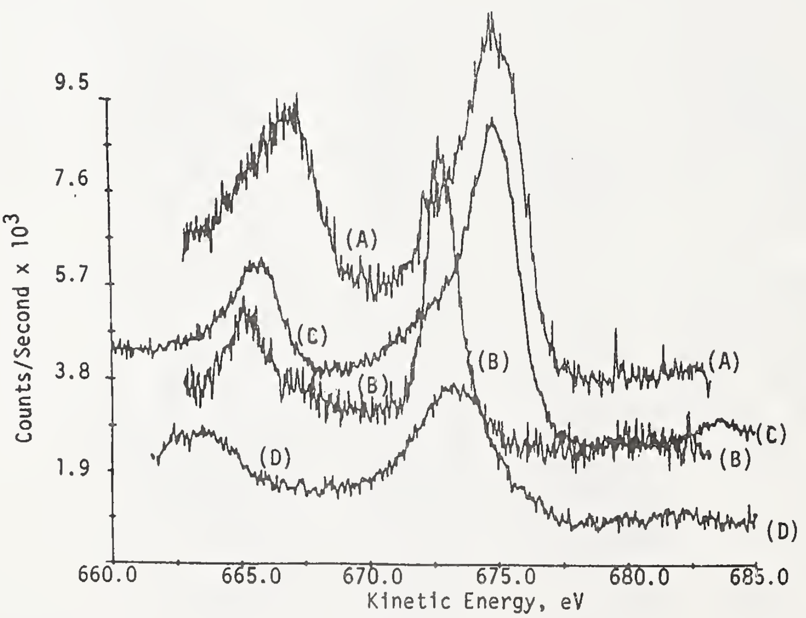

Fig. 4 ESCA spectra for (A) Cr_2O_3 standard for Cr^{+3}, (B) $K_2Cr_2O_7$ standard for Cr^{+6}, (C) Cr metal surface, and (D) oxide film on Co-Cr implant alloy specimen.

CHEMICAL METALLURGY
Task 15445

The joint program mandated by agreement between the Directors of the National Bureau of Standards (NBS) and the American Society for Metals (ASM) has continued to provide critically evaluated phase diagram and other constitution data as well as related bibliographic material. Technical oversight of this program and work on selected systems is being carried out by the Alloy Phase Diagram Data Center (supported in part under this task and by the Office of Standard Reference Data (OSRD)). ASM has increased its contribution to the program and increased its support for category editors to evaluate phase diagrams. The total number of binary category editors has now increased to 28. ASM has continued to provide two Research Associates at NBS. ASM has been successful in raising 3.9 million dollars for the 4 million dollar fund raising effort from industry. The Bulletin of Alloy Phase Diagrams is now published bimonthly under this program. The scope of the major effort to evaluate binary phase diagrams at NBS now includes iron-based and aluminum-based systems in addition to previously initiated evaluations of titanium-based systems. Thus, evaluation of all binary alloy phase diagrams based on elements of commercial and national interest like Fe, Al, Ti, is well underway. During the last year eighteen Ti-, eight Al-, and five Fe-based binary systems have been evaluated. The program has four basic and interrelated components. These include compilation and evaluation, development of bibliographic methods, thermodynamics optimization, and development of a prototype database for storage and retrieval of phase diagram and ancillary data. Category editors at NBS serve as a model for the rest of the categories in the NBS/ASM joint program on binary phase diagrams.

With the help of the ASM Research Associates and personnel from the Mathematical Analysis Division of the Center for Applied Math (CAM), considerable progress has been made in the development of the prototype database to store, search and retrieve phase diagram information. The database is aimed at providing features including invariant reactions, congruent transformations, homogeneity range, etc. The data structure is designed to provide rapid update-ability in order to manage the flow of information as evaluations progress.

Other activities in this task include theoretical work on understanding parameters important to alloy phase stability, and an experimental program to understand microstructural stability as related to alloy phase diagrams during processing of coating by the plasma arc method.

Alloy Phase Stability
Subtask I of Task 15445

K. J.Bhansali, L. H. Bennett, R. Forsen, R. M. Hayes, D. J. Kahan, A. McAlister, J. L. Murray, M. E. Read, J. Sims, L. J. Swartzendruber, R. D. Shull

We are pursuing a program of four interconnected parts: critical evaluation, compilation and thermodynamic modeling of binary phase diagram data; designing and setting up a prototype database for on-line retrieval of the bibliographic, graphic and numeric phase diagram and ancillary data (crystal structure, lattice parameters, etc.); experimental work on phase stability on alloy phase systems selected with a view to complement the evaluation program; and the theory of phase stability stressing the prediction of what intermediate compounds form in transition metal binary alloys.

Alloy Phase Diagram Data Center Activities

All activities revolve about a collaborative data evaluation program for alloy phase diagrams with the American Society for Metals. At NBS, the scope of the phase diagram program has been greatly extended. During the last year, the Alloy Phase Diagram Data Center has continued to be the focal point for the entire ASM/NBS Phase Diagram Program.

Phase diagram evaluation projects are being carried out by three category editors at NBS: Joanne Murray for Titanium alloys, Archie McAlister and Joanne Murray for Aluminum alloys, and Lydon Swartzendruber for Iron Alloys. Eighteen Ti, five Al-, and five Fe-based systems have been assessed this year including: Ti-Be, -Al, -Ga, -In, -Si, -Ge, -Sn,-Pb, -P, -As, -Sb, -Bi, -Sc, -Y, -La, -Ce, -Th, -U, Al-Bi, -As, -Sb, -Pd, -Pt, Fe-Ag, -Au, -Rh, -Mg, -Ta.

Coverage of the system includes crystal structures, metastable and constrained equilibria, and high temperature thermodynamic properties as well as the stable equilibrium diagrams. Calculations of the phase diagram from thermodynamics data are carried out using a number of computer programs available at NBS. Programs provided by Lukas, Henig and Petzow (Stuttgart, Germany) provide the capability of using Gibbs energy models such as polynomial expansions, "surrounded atom", associated liquid, and the sublattice model. Programs provided by R. Kikuchi (Hughes Aircraft) and by J. Sanchez (Columbia Univ.) model order-disorder transitions using the cluster variation technique. Programs provided by B. Sundman and M. Hillert (Stockholm, Sweden) include magnetic interactions, of importance for the Fe category. Significant improvements have been made to this program in order to improve the efficiency and the precision with which data can be evaluated. Critical calculations have been converted to double-precision arithmetic, the number of data points which could be handled at one time has been increased, and the input-output functions have been made more efficient.

Plans are being made to develop new thermodynamics algorithms for including the elastic energy associated with coherency strains. Such calculations will allow us to model and predict the metastable equilibria associated with age-hardening in solid solution phases, such as occurs widely in Al based alloys.

Great progress has been made in the development of the computerized phase diagram database in three main areas: (1) the design of the search technique and data structure, (2) the development of algorithms for extracting salient numerical metallurgical information from graphical data, and (3) the development of standarized file formats for data update and data portability.

Previously it was reported that a phase diagram graphics program had been developed at NBS and that systems being published in the Bulletin of Alloy Phase Diagrams were being entered into a graphical phase diagram database. It was also reported that a file structure, known as LEMM (Linear Encoding for Multi-Media) had been developed to enhance the portability and update-ability of the database. Software for implementing the LEMM format are completed and conversion of data to the LEMM format has been initiated.

In order to select phase diagrams for viewing in an on-line graphical database, searching techniques (known as interphase diagram searching) have been developed to select the phase diagrams based on metallurgical properties. An inter-phase diagram database has been set up to allow for efficient searching of the information embedded in a phase diagram. It contains as a separate, rapidly searchable set of data, the subset of the phase diagram data which concisely summarizes the metallurgically important features of the phase diagram. This subset is extracted from a phase diagram graphics file (containing the phase diagram data) by a program which performs a topological analysis of the curves in the phase diagram. The key to the analysis is that each curve in the graphics file has associated with it a list of the phases that the curve bounds. The curve list and the curve geometry are analyzed to find the salient metallurgical features of the phase diagram. These features include:

(1) Invariant transformations, classified by type and identified by transformation temperature and the identities and compositions of the participating phases;
(2) Congruent transformations and critical points, classified by type and identified by the names of the participating phases and the temperature and composition at which the process takes place; and
(3) Homogeneity ranges; i.e., the range of stability of the various phases in the alloy system.

In addition to the set of data obtained directly from the phase diagram by our algorithms, provisions are made to search (as part of the separate, rapidly searchable set of data) additional information characterizing the phases whose existence and range of stability the phase diagram graphically displays. This ancillary data includes information about the structure of the phases, and this structural information is frequently the key to the desirable (or undesirable) properties of the alloy in question. The program which performs the topological analysis of the phase diagram (of a particular alloy system) identifies the phases in existence and their homogeneity ranges, and this phase information is then augmented by detailed information on the crystal structures of the phases, including phase name, Strukturbericht symbol, prototype, Pearson symbol and space group. Currently about 500 entries from Ti-, Al- and Fe-based binary systems are available for on-line search at NBS.

The final requirement for rapid inter-phase diagram searching is rapid retrieval algorithms. Our prototype database uses a relational database management system (RIM) to take advantage of its efficient storage and retrieval algorithms. An applications programmer can take advantage of the efficient algorithms of a DBMS, while tailoring access and viewing of the data to specialized needs. This is exactly what we have done, writing our own software interface to RIM (which we call EZRIM) to allow us to tailor-make a "user-friendly", metallurgically-oriented, flexible environment in which a database user can (hopefully) easily search across alloy systems for the alloy systems containing the metallurgical features he/she desires.

Work at NBS on ternary phase diagrams has focussed on three dimensional representation of surfaces. This work has been done in collaboration with the Center for Applied Mathematics (S. Cramer, D. Redmiles). In order to represent a ternary diagram three-dimensionally, algorithms have been implemented to fit a surface through the data, and to clip and join the surfaces at invariant lines either on the Evans and Sutherland terminal which allows real time translation and rotation of the diagrams, or in color. In the past year color displays have been developed.

These color diagrams can be sectioned as isotherms or isopleths, and hidden surfaces displayed. This allows the user to visualize the three-dimensional structure of the diagram, and then to transform it to the isothermal sections familiar to the metallurgist.

An additional six issues of the "Bulletin of Alloy Phase Diagrams" have been published which contained approximately 100 phase diagram systems. The Bulletin is now published six times a year, up from the previously maintained quarterly schedule. The Bulletin, published by ASM, and edited at NBS, is the main method of rapid dissemination of evaluated phase diagrams. It also acts as a vehicle for open review system for the evaluations submitted by category editors. During the year, routine procedures for handling flow of material were established. Non-technical aspects of publications such as record keeping, mailing, etc. were transferred to ASM. In addition, the graphics program, which serves the dual functions of providing publication quality graphics for the Bulletin and acting as a data input program for the phase diagram database, was made fully operational. The program is now routinely used by the ASM research associates to produce final graphics for the Bulletin. These modifications have enabled NBS to concentrate on technical editing and handling the increased flow of evaluated phase diagrams from the category editors worldwide.

Experimental Phase Diagram Program

The experimental phase diagram evaluation effort is aimed at providing critical experiments to resolve uncertainties surfaced by critical evaluation.

The recent evaluation by Murray of the Ti-Al binary system points out a clear need for further study of well characterized, high purity samples in the 25 to 45 at.% Al range. We have therefore extended our earlier studies of this binary to include this composition range, with particular emphasis on: (a) the formation of the 'Ti_3Al', or α_2, phase; (b) the $\alpha \leftrightarrow \alpha_2 + \gamma$ eutectoid; and (c) the systematics of the reversible, low temperature DTA event observed in the 'single phase α_2' field below 25 at.% Al in our earlier studies of the binary and Mo-, Ta-, and Nb-ternaries based on the binary. To date, samples heat treated at selected temperatures have been studied by differential thermal analysis (DTA). These preliminary results are moot with respect to the formation of α_2, but in some aspects favor peritectoid formation; place the $\alpha \leftrightarrow \alpha_2 + \gamma$ eutectoid at (1117 ± 7) °C; and suggest that two 'α_2' phases exist, both of broad compositional range, the lower temperature form, which orders at Ti_3Al, undergoing second order transformation at a maximum of 740 °C to the higher temperature form which orders at the composition Ti_2Al. Metallographic studies of heat treated and quenched samples, as well as high temperature neutron and electron diffraction studies of α_2 samples, above and below the DTA event temperatures (the latter in collaboration with D. Konitzer of the University of Illinois) are in progress.

A very deep eutectic, liquid $\leftrightarrow$ Pd_2Al + (Pd), has been reported in the binary Al-Pd system at 1150 °C via DTA cooling studies. This interesting compositional region has never been studied by rapid quenching techniques. Further, it has been noted in the critical review of the chemically similar Al-Ni system (Singleton, Murray, Nash) that cooling DTA studies place the Ni rich eutectic at lower temperature than metallographic studies of heat treated and quenched samples. Thermodynamic modeling of the Al-Pd system by McAlister, based on the limited thermodynamic data available on the Al-Pd system, strongly suggests that here too supercooling effects result in significant error in the DTA cooling results. Both rapidly quenched and heat treated bulk samples are being prepared to better characterize the equilibrium phase diagram of Al-Pd system, and to determine the nature of the rapidly quenched product, by means of heating DTA, metallographic, and x-ray structural studies.

It should be noted that both of these projects depend on the advanced preparative techniques developed here, based on producing homogeneous samples by rapid quenching from the liquid state. This project is in part a continuation of a previously reported approach to the study of equilibrium phase diagrams through heat treatment of rapidly solidified homogeneous samples.

A new general research effort fully coordinated with our phase diagram evaluation and theoretical studies, topics already discussed at some length in the description of our Alloy Phase Diagram Data Activities, focuses on the effect of coherency in binary alloy systems. Experimental studies commenced in this area include the Al-rich end of the Al-Ag binary, a much studied but still inadequately understood classic example of metastable coherent spinodal decomposition. Samples prepared by rapid quenching from the melt and cooled from the equilibrium solid solution are under study. At question here are the coherent metastable miscibility gap and the nature of GPII to GPI transition at ~170 °C, the results to be coupled with theoretical estimates of the effect of coherency on these quantities.

The peritectic Ag-Pt system is another system where coherency strain may be very important in controlling phase equilibria in the solid state. In this system, the possible occurrence of several ordered fcc phases inside the two phase αAg + αAl region has been reported. Work (via DTA and electron diffraction) is underway to determine whether these "ordered phases" are not indeed artifacts of the locally strained regions between the fcc Al and Ag phases.

In the technologically important Al-Li system, the recent evaluation by McAlister has illustrated the inconsistency in the metastable boundary data at the Al rich end. Preliminary studies have been initiated in this laboratory to use a novel neutron profiling technique at NBS (in connection with R. Fleming, G. Downing and S. C. Carpenter of the Inorganic Analytical Research Division) to determine absolute alloy compositions, locations of Li segregation in the alloy, and the effects on the Li distribution during equilibration heat treatments.

Work has continued in the study of the Small Angle Neutron Scattering (SANS) of non-magnetic metallic glasses this year. The novel asymmetric SANS patterns observed for the $Ti_{45}Cu_{55}$ metallic glass last year were also found for a $Cu_{55}Zr_{45}$ metallic glass this year. The alloy regions (~200Å in diameter) giving rise to the small angle scattering were found in both metallic glasses studied so far to be "disc shaped" with the axis of symmetry oriented in the direction of solidification. Large angle diffraction (x-ray and neutron) confirmed in both cases the absence of any Bragg scattering peaks indicative of crystallinity. Attempts to observe these regions by electron microscopy, however, have been unsuccessful. The SANS technique was also found this year to be very useful in following the crystallization and growth process of these metastable materials during their subsequent heat treatment. Initially, a very symmetric SANS pattern is observed for the random formation of 50Å crystallites on heating the material just slightly above the crystallization temperature. On continued heating the symmetric pattern systematically converges into the center (the main beam spot). During this growth stage, the distribution and shape of the crystallites apparently remained constant while their size increased. Modifications are presently being made to the sample holder so that absolute intensity measurements may be made on the melt spun ribbons. In addition other metallic glasses are being prepared for observation. Large angle neutron diffraction measurements on the crystallized $Ti_{45}Cu_{55}$ metallic glass additionally showed the initial crystallization was into primarily the ordered tetragonal Ti-Cu phase. Subsequent decomposition into the equilibrium Ti_3Cu_4 and TiCu occurred at somewhat higher temperatures.

The recently determined structure of the Ti_4Cu_2O phase was also confirmed in this laboratory this last year. In collaboration with M. Kaufman, the structure of this phase was unequivocably determined to be diamond cubic by means of convergent beam electron microscopy.

Fundamental Theory

Further advances in the understanding of alloy phase stability have been made in a series of collaborative efforts with Dr. R. E. Watson of Brookhaven National Laboratory.
A study, initiated last year, to formulate rules for the occurrence or non-occurrence of sigma and other related brittle phases (the so-called topologically-closed-packed, or TCP, structures) in transition-metal alloys has been bearing fruit. The appearance of these phases leads to catastrophic failures in superalloys and thus must be avoided. High processing costs are associated with this need to avoid TCP formation. The emphasis is on size effects and electron factors. Most of the TCP phases can be considered to be electron compounds, but the Laves phases cannot, and it was necessary to consider these separately from the others. A remarkably error-free map was obtained for the occurrence and non-occurrence of Laves phases. In the non-Laves phases, an effective d-band hole count was introduced which may have considerable practical utility in superalloy design. Suggestions of alloy systems in which TCP phases have not yet been reported were given, and doubt was sown concerning the reality of some reported TCP phases.

The above considerations on TCP phases have been extended to the effects of aluminum additions. A new approach has been suggested in terms of assigning to aluminum an "effective" d-band hole count. Aluminum, an important non-transition metal in superalloys, is often added in order to precipitate high volume fractions of gamma prime phase for strength and is believed to play a significant role in the formation of TCP phases. Other predictive schemes give differing guidance to superalloy developers for the effects of aluminum. Semi-empirical models of the sort we are providing for TCP formation have, as one of their most useful aspects, the potential to provide useful input to thermodynamic modeling of multicomponent phase diagrams.

In another collaborative effort with Drs. R. E. Watson and R. M. Sternheiner of the Brookhaven National Laboratory, the trends in the nuclear electric quadrupole hyperfine fields as probed by dilute impurity atoms in transition-metal/transition-metal alloys were examined. Diverse data have been assembled from the literature and some patterns emerge. Such experimentally observed field gradients provide a measure of aspherical chemical bonding effects associated with either charge transfer or with valence charge concentrated along directional lines.

Plasma Arc Coating
Subtask 2 of Task 15445

R.D. Shull, K. J. Bhansali, L. K. Ives, P. A. Boyer

During the last year, the feasibility of incorporating hard carbide particles on the surfaces of light metal substrates was explored. Hard adherent coatings of TiC, WC, and Cr_3C_2 powders (with and without the simultaneous deposition of an aluminum alloy binder) were successfully placed onto titanium substrates by means of the plasma transferred arc (PTA) process. Depending upon the deposition power and the speed of deposition, the hard carbide particle size and distribution was found to be adjustable. The abrasive wear resistance of these coatings was subsequently tested by the Dry Sand Rubber Wheel Test Method. In all cases, the coatings provided increased resistance to wear. The TiC particle deposit placed in a 5456 Al alloy binder provided the best resistance: three times that of D2 tool steel (61 HRC hardness). Work is continuing to optimize the hard particle distribution in these coatings and to study the role of phases formed at the interface in interfacial bonding between the particle and matrix.

Magnetic Particle Inspection Standards

Lydon J. Swartzendruber

This project was initiated by the Specification and Technical Data Branch of the Army Materials and Mechanics Research Center, Watertown, Massachusetts. Military Specification MIL-M-11472, Magnetic-Particle Inspection: Process for Ferromagnetic Materials, is being reviewed for proposed revision or cancellation and replacement by Military Specification MIL-STD-271, Military Specification MIL-I-6868, or American Society for Testing and Materials Recommended Practice E709-80. The contents of these documents have been compared with current state-of-the-art practice in magnetic particle inspection as revealed by industrial practice, available literature, current applicable Military Standards, Aerospace Materials Specifications, and American Society for Testing and Materials documents. A draft version of a revised MIL-M-11472 was prepared. This initial draft was circulated to Department of Defense users. Many valuable comments and suggestions were contained in the responses. The plan of the original document was to provide a standard which incorporated the necessary requirements for Department of Defense use with reference to ASTM E709 for a considerable portion of the detailed requirements. However the comments from a number of the users indicated that this is not a satisfactory procedure, either because the resulting document does not give enough control over the inspection procedure, or because the application of the external document causes too many difficulties in interpretation. Accordingly, a revised version has been prepared which contains the benefit of the comments received and also contains the necessary detailed requirements. This revised version is currently being evaluated by the Department of Defense users.

Magnetic Measurements

Lydon J. Swartzendruber

One of the crucial elements of achieving valid magnetic particle tests is the establishment of correct magnetization levels in the part under test. There are basically three ways to obtain correct magnetization levels:

(1) use of the so-called 'rules of thumb',
(2) use of a Hall probe, paste on defect, etc., and
(3) use of a test piece with known defects.

The first method, rules of thumb, is mainly useful in the field where test pieces and Hall probe instrumentation are unavailable or difficult to use, and for parts with particularly simple geometries such as flat plates or cylinders. The rules of thumb are also useful as a guide to approximating the required current levels. The second method, Hall probes, paste on defects, etc., is useful for both complicated and simple geometries for establishing the current levels required in a one-time or a repetitive test procedure. The third method, use of test pieces with known defects, is probably the best procedure because not only does it insure that the magnetization level is correct, it also proves the other variables in the test method. However, the use of test pieces has a number of drawbacks. First of all, such test pieces are often not available or are difficult to fabricate. It is also difficult to include all possible types and locations of defects of interest. It is therefore often not feasible or economic to apply the test piece method.

Of the three methods, perhaps the most effective is the use of the Hall probe. We have developed both experimental and theoretical experience to show that a field of between 30 and 80 gauss parallel to, and directly above, the surface of the part being tested, ensures a satisfactory test in most cases. The use of paste on defects or similar indicators is not as reliable because such devices lean to the low end of the acceptable range and do not allow a procedure to be changed if the higher fields are found necessary. Their use should therefore be discouraged.

As an example of the problems with the rules of thumb in the current ASTM magnetic particle inspection procedure (E709), consider the one given for overall magnetization. E709 recommends 700 to 900 A/inch on cylindrical parts up to 5 in in diameter, 500 to 700 A/inch between 5 in. and 15 in., and 100 to 300 A/inch for diameters over 15 inches. The jump from a minimum of 500 A/inch at 15 in. to a maximum of 300 A/inch above 15 in. is rather arbitrary. The minimum figure of 100 A/inch would give a surface field of only about 8 gauss, too small to give a valid magnetic particle test for any but the least exacting requirements. The figure cited in military specification MIL-I-6868 is 1000 A/inch for any diameter part. Such a high current is probably only useful for parts of smaller diameters with good surface finish and with a very nearly circular cross section. It is too high for many parts using mild steel and a rough surface finish. Further, if the cross section deviates from circular, free poles will be created, causing interfering indications and large field gradients which can sweep the inspection particles past real defects causing them to be missed in the inspection process.

The consideration of proper part magnetization thus comprises one of the most difficult aspects of creating a valid specification. These factors are currently being considered by ASTM committee E-7 for inclusion in a revised version of the ASTM magnetic particle inspection document.

CORROSION AND PROTECTION OF METALS
Task 15446

The activities of this Task are aimed at combatting the deleterious effects of corrosion, which continue to cause severe economic losses to the Nation and pose serious threats to safety and reliability. Many of the major forms of attack are poorly understood, and thus part of our activities involves basic studies of the underlying mechanisms. In addition, an important part of our efforts is directed to measurement methodology; this involves the development and evaluation of test methods for both laboratory and field use, and the development of SRMs. Data activities represent an increasing part of our program. These consist of the generation of specialized types of new data, e.g. corrosion rates of steel reinforcing bars in concrete, a traditional activity of the Task; and, an important new program, the evaluation and organization of existing data from the literature. The latter began in FY 83 with the establishment of the Corrosion Data Center at NBS, which is being developed in cooperation with the National Association of Corrosion Engineers. The Center is designed to provide industry with rapid access to a central source of reliable, evaluated data which are essential in the selection of materials to combat corrosion.

The mechanistic studies continue to focus on localized corrosion, emphasis being placed on a specific form, namely environmentally-induced cracking. During FY 84, attention centered on stress corrosion cracking (SCC) and hydrogen embrittlement (HE). The former is an ongoing problem which occurs in virtually all engineering alloys and afflicts all segments of private and government endeavor. The environments, usually aqueous, generally cause little damage in the absence of stress, but induce catastrophic failure in stressed components. Current examples include the cracking of stainless steel and Inconel piping in nuclear reactors, caused by exposure to high-purity water. Hydrogen embrittlement is most commonly encountered in steels, particularly in sulfide-bearing media such as those found in sour oil wells, but it also occurs in many other important materials. For example, serious failures have been encountered in titanium alloys used in the Space Shuttle.

Research on the structure and breakdown of passive films, traditionally a major strength at NBS, continued to receive attention in FY 84. These thin oxide films are responsible for the excellent corrosion resistance of materials such as austenitic stainless steel, aluminum and titanium, but unfortunately they can undergo local breakdown in the presence of certain chemical species, leading to the practical problem of pitting. In FY 84, studies of the breakdown of passive films was continued by means of analysis of electrochemical noise, a new and potentially valuable approach.

Our programs were strengthened during the year by the participation of several guest workers: V. H. Desai, The Johns Hopkins University; A. J. Forty, University of Warwick, England; F. Qiu, Fujian Institute of Research on the Structure of Matter, the Peoples Republic of China; and D. K. Tanaka, Technological Research Institute of Sao Paulo, Brazil.

Stress Corrosion Cracking
Subtask 1 of Task 15446

E. N. Pugh, U. Bertocci, V. H. Desai, J. L. Fink, A. J. Forty, M. J. Kaufman, and J. Smit

The path of stress corrosion cracking (SCC) can be either intergranular or transgranular, often in the same alloy-environment system, and service failures are divided approximately equally between the two modes. It has not been established whether the mechanism is the same for the two forms, but our view is that they are basically different. With a few exceptions, the intergranular form is thought to occur by the film-rupture model in which the crack advances by preferential anodic dissolution at the crack-tip where plastic deformation continually ruptures a passive film. Our earlier studies demonstrated that transgranular SCC is basically different, the crack propagating by a series of discontinuous cleavage events, i.e., by brittle mechanical fracture, as shown in figure 1.

In FY 84, we continued to focus on the transgranular form of SCC. An exciting development has been our recognition of the importance of cleavage step formation in the propagation of the transgranular cracks. Such cracks advance on a series of parallel but displaced crystallographic planes, joined by steps which are also crystallographic in nature, figure 2(a). Because of their orientation with respect to the stress axis, the steps are generally not formed by the cleavage process which produces the primary facets but rather by an alternative process. For example, in alpha phase copper-zinc alloys/aqueous ammonia, a system of long term interest to us, our earlier work has shown that primary cleavage occurs on {110} planes and that the faces of the steps consist of two alternating {111} planes which are perpendicular to the {110} facets, figure 2(b). These steps are thought to be produced by highly localized plastic shearing on these {111} slip planes.

The importance of the step formation process in transgranular SCC can be seen in our work on Al-Zn-Mg alloys. By virtue of the high strength which can be produced by precipitation hardening, these alloys are widely used for aerospace applications, but their usefulness is impaired by their susceptibility to intergranular SCC. The transgranular form of cracking is not a practical problem in these alloys, although it can be produced in the laboratory in chloride solutions if large stresses are applied. Transgranular cracking in these FCC alloys again occurs on {110} planes but the steps are produced by cleavage on two secondary {110} planes rather than by {111} shear, despite the unfavorable orientation of these cleavage planes. This difference in behavior is now attributed to the large critical resolved shear stress of these precipitation hardened alloys. Thus the relative immunity of these alloys to transgranular SCC may be due to difficulty in forming the cleavage steps by shear rather than to any intrinsic resistance to the cleavage process. To pursue this possibility, experiments are being conducted on Al-Zn-Mg specimens aged to various strength levels, including the underaged, fully hardened, and overaged conditions.

The magnitude of the minimum potential at the crack tip has been estimated using more realistic boundary conditions than in earlier modeling. Specifically, a wedge shaped crack with bare walls was assumed and the distribution of current and potential calculated using a transmission line approach. The calculations support our previous findings that hydrogen evolution is unlikely at the crack tip, essentially ruling out hydrogen embrittlement as the cause of cracking. An alternative proposal which is attracting considerable attention is that embrittlement results from selective dissolution per se. The specific mechanism by which this process induces cleavage has not been determined and, moreover, the observation that pure copper can be made to undergo transgranular SCC clearly rules out dealloying as a single unified mechanism. The remaining possibility being advocated, that brittle fracture is induced by adsorption of a critical species, cannot be ruled out on the basis of our modeling, but the identity of the species remains obscure.

Hydrogen Embrittlement
Subtask 2 of Task 15446

C. G. Interrante, S. A. Harrison, and S. C. O'Connor

Industrial users of steels must often employ costly strategies to reduce the possibility of the occurrence of hydrogen embrittlement. Knowledge of bulk properties and average stress levels is often not sufficient to predict the damaging effects of hydrogen because local property differences may enhance embrittlement susceptibility. Work in this area at NBS has centered on relating the fundamental parameters controlling hydrogen-assisted crack growth in structural and pressure vessel steels. The objective is to relate the measurable effects of hydrogen, such as crack growth rate for various stress-intensity (K) levels and the threshold value of K for hydrogren-assisted cracking, to the driving force (the fugacity of hydrogen associated with a given metal/environment system) and to the important metallurgical factors, such as hardness and inclusion size, shape, and orientation. These empirical relationships will be useful in predicting conditions under which cracking is to be expected. These relations can also be useful in the development of our understanding of the cracking process. When taken with other information they aid in the development of theoretical models that describe the mechanism of hydrogen embrittlement.

In our program, the effects of hydrogen are assessed with fracture mechanics specimens of steels used commercially in the petrochemical industry, and with severe hydrogen-charging environments containing hydrogen sulfide, a common contaminant found in that industry.

To date these NBS studies have included development of several techniques for: (1) measurement of permeation of hydrogen in steels; (2) removal of iron sulfides from fracture surfaces that have been exposed to aqueous sulfide environments; and (3) an automated real-time system for the study of crack growth rates in aggressive environments. This system uses electric-resistance methods for measurement of crack length. Recently, using this system, conditions that promote crack branch formation in steels tested in high-fugacity environments have been successfully analyzed.

In cooperation with the University of Notre Dame, a method for measurement of the effective fugacity of hydrogen in steels and environments of interest to this program was developed last year. Using this method in FY 84, selected fugacity measurements were completed to complement this overall program and to aid in redirecting the crack growth studies. Some improvements were made this year in the sensitivity of a crack-length measurement system that is used with test specimens, and ways for making further improvements have been identified but not yet implemented.

A new area of research initiated in FY 84 involves the use of acoustic measurements to supplement the other measurements in developing a better understanding of the cracking process and the mechanism of embrittlement. This work is being interfaced with other studies being conducted within the Division in the Nondestructive Characterization Group. Preliminary results are encouraging. The aim is to characterize the cracking process in more than one way and cover the smallest step size possible, so as to gain insight into the nature of the cracking (e.g. its intermittent character: the magnitude of the crack jumps, their location in relation to the crack front and to microstructural features, etc.) In this way, models will be developed that describe the process and mechanism of hydrogen-assisted cracking in steels. In these tests, crack length will be continuously monitored so that real-time estimates can be made of the crack-growth rate and the crack-extension force (the elastic energy made available at the crack front per unit of crack extension). Thus, the acoustic energy detected can be related to the strain energy released.

Finally, both a new computer and a servo-hydraulic test system have been purchased for use in these and other studies of environmental cracking phenomena. The computer is very powerful and has broad capabilities for both data acquisition and analysis that will accelerate the progress of this work. With this computer, data from the electric-resistance measurements will be coordinated with acoustic emission data to analyze the cracking process. Further, after the servo-hydraulic test system is installed and calibrated, it will permit studies to be conducted in a myriad of modes. At present using wedge- or bolt-loaded specimens, only fixed-displacement tests have been possible. Other modes of loading, such as constant K, fatigue, rising load, etc. have advantages that will now be available.

After further development of these laboratory systems is completed, studies will be continued on various alloys, and principally on the 2.25 Cr - 1 Mo steel, using specimens of the double-beam and the compact types and using various partial pressures of H_2S in an aqueous acetic acid environment. These studies of hydrogen embrittlement of steels have been conducted under the guidance of the Subcommittee on Hydrogen Effects of the Pressure Vessel Research Committee (PVRC) of the Welding

Research Council (WRC). Another work (in process) for the PVRC is an interpretive report that will be titled "Effects of Hydrogen on Pressure Vessel Steels," to be published by the WRC.

Studies of Passive Films and Pitting
Subtask 3 of Task 15446

U. Bertocci and F. Qiu

Studies of the breakdown of passive films continued in FY 84 using the electrochemical noise technique. This new method promises to yield further insight into the mechanism of pitting, and also to provide a practical method for monitoring critical components. In FY 84, the fluctuations in the passive current which are observed in iron-chromium alloys before pit initiation have been recorded with very sensitive instrumentation. These fluctuations are being subjected to a detailed statistical analysis to see which class of statistical models fit the data. The analysis has focused on three characteristic properties of these fluctuations, that is, the distribution of the time intervals between current transients, the amplitude of the transients, and the shape of their decay. Although the analysis is not complete, preliminary results indicate that simple renewal processes, which have been postulated by other workers studying the statistics of pitting, does not fit the experimental data.

Corrosion Data for Specific Practical Applications
Subtask 4 of Task 15446

E. Escalante and D. E. Mathews

The objective of this activity is to apply modern electrochemical techniques to the measurement of corrosion rates in the field. In FY 84, we have continued the application of the linear polarization method to the study of three rather diverse practical problems:

(1) The Corrosion of Steel Reinforcing Bars in Concrete: Corrosion damage to concrete bridge decks and overpasses resulting from the use of deicing salts has led to a need for a non-destructive test to measure the corrosion rate of the steel bars *in situ*. This project, sponsored by the Federal Highway Administration (FHWA), was undertaken to address this problem. Our work to date has established that the linear polarization technique is suitable for this application, and a portable microcomputer controlled system to automate the measurements has been designed and assembled. Up to now, the system has been used to measure the corrosion of steel bars in small concrete slabs under controlled conditions, but preparations are now under way to extend these measurements to larger slabs at a FHWA test site. This will be followed by measurements on several nearby bridge decks with a known corrosion history. Eventually it will be possible for nontechnical personnel to operate this system.

(2) The Atmospheric Corrosion of Structural Materials: This project was started in FY 83 as part of a program directed by the Federal Acid Rain Task Force, with funding provided by the National Park Service. In effect, the linear polarization technique is being considered as a means of measuring atmospheric corrosion rates of metals. So far, a small probe has been developed in which one of the three electrodes necessary in the linear polarization method is made of the metal of interest, and measurements have been made in controlled humidity environmental chambers. The results indicate that measurements can be successfully made only when the relative humidity is 100% and the moisture film responsible for the attack is visible; below this humidity, it appears that the electrical resistance of the film is too large for accurate IR compensation to be made. Nevertheless, the technique shows promise, and currently specimens are being exposed on our roof site and monitored in our laboratory.

(3) Corrosion of Steel Piling in Soil: Since 1958, the American Iron and Steel Institute has supported NBS research on the corrosion of steel piling in soil and seawater. Last year, a long-term investigation of the latter was completed, and our efforts are now focused on corrosion in soil, using the linear polarization method to make *in situ* measurements. The experimental work is being carried out largely at a test site at Montreal, Canada, and has been in progress for approximately 14 years. In FY 84, our data from this and other underground sites, as well as our seawater results, were presented at an International Conference, organized by NBS, on the Durability of Steel Piling in Soil and Coastal Marine Environments (NBS, October, 1983). The proceedings of the meeting are now in preparation for publication in FY 85.

Corrosion Data Center
Subtask 5 of Task 15446

G. M. Ugiansky, U. Bertocci, D. E. Clausen, C. F. Derr, E. Escalante, M. Marek, E. N. Pugh, M. J. Rodriguez, and A. C. Van Orden

Corrosion costs to the nation's economy are estimated to be $143 billion per annum (1983 dollars). These costs can be reduced greatly through the application of presently known corrosion control methods and by the implementation of new, improved practices. This can be achieved through the accessibility to designers, engineers, and scientists of evaluated kinetic (rate) and thermodynamic (stability) corrosion data which are not now available. To provide these data, a central facility, the Corrosion Data Center, was established. This Center is the NBS component of a joint program between the National Association of Corrosion Engineers (NACE) and NBS; it is funded in part by the NBS Office of Standard Reference Data. The program is concerned with the collection, evaluation, and effective dissemination of corrosion data, and focuses on the establishment of an evaluated corrosion data base which can be easily computer accessed to provide the user with the required data in any of a number of possible graphical or tabular formats.

Several pilot projects have been initiated in the areas of kinetic and thermodynamic corrosion data. In the kinetic area, the projects include atmospheric corrosion of structural alloys, localized corrosion of stainless steel and other alloys, and uniform corrosion of alloys in aqueous and nonaqueous media. In the thermodynamic area, efforts have been focused on the use of computers for the calculation and display of stability diagrams of the electrochemical potential-pH type known as Pourbaix diagrams.

These pilot projects will be expanded and others will be added as the program continues to expand. The projects are planned in close collaboration with the NACE Steering Committee on the NACE-NBS Corrosion Data Program. An NACE Research Associate at NBS is developing dissemination methods for each project and the NACE committee is developing funding support from industry to support an enlarged corrosion data evaluation effort which will involve experts throughout the corrosion community.

Several projects are in progress on kinetic data:

(1) Atmospheric Corrosion: The project on atmospheric corrosion of structural alloys is funded in part by the National Park Service. In this project, existing data from the literature have been collected and computer filed. These data describe corrosion rates for carbon steel, galvanized steel, weathering steel, zinc, aluminum alloys, and bronze alloys at sixty sites in the United States, including rural, industrial, urban, and seacoast areas. Data on weather, atmospheric pollution, acid rain, for example, for the same time periods as the corrosion exposures have also been computer stored. The corrosion rate data are being correlated with the atmospheric data for display on a map of the United States using computer graphics techniques. These correlations, being studied in cooperation with the University of Washington (St. Louis, MO), will lead to predictability of corrosion rates of metals and alloys at other sites in the United States for which the required atmospheric data are available.

(2) Localized Corrosion: The project on localized corrosion has focused initially on the pitting and crevice corrosion of austenitic stainless steels in aqueous chloride environments. Rate data for pitting and crevice corrosion of 304 and 316 stainless steels have been collected, computer filed, and statistically analyzed. Computer graphics formats for the most effective presentation and dissemination of localized corrosion data are being developed.

The computer files contain data for material variables such as composition of the alloy, pretreatment, and surface finish; environmental data include concentration of chloride, concentration of other species in solution, pH, temperature, and additional information related to the test parameters and the techniques used. Some of the parameters considered for the evaluation of the pitting resistance of the alloys include the breakdown and protection potentials obtained from polarization tests, pit propagation rate, and statistics of pitting. For crevice corrosion, data for crevice corrosion indices and critical temperature for crevice corrosion are included as well as other data from multiple crevice assembly tests and cyclic scan hysteresis tests with artificial crevices.

(3) Uniform Corrosion: Uniform corrosion is of importance to all sectors of the economy, especially the chemical process industries. In these industries, a problem of universal interest is the corrosion of carbon steel by sulfuric acid, and this system was chosen for the pilot project on uniform corrosion. Other systems will be added as the evaluation methodology and dissemination methods are developed. Data on the corrosion of alloys in both aqueous and non-aqueous environments of the type published in the NACE CORROSION DATA SURVEY are also being examined from the point of view of collecting additonal data from the literature and industry files, evaluation, and computer dissemination techniques.

Uniform corrosion data are usually obtained from corrosion weight loss measurements and expressed in terms of rate of penetration as mils per year or millimeters per year. These data are often presented graphically as isocorrosion charts as shown schematically in figure 3. Along with the data that are used to construct these isocorrosion charts, data will also be included so that these diagrams may be displayed for various cuts of a multi-dimension system which includes not only the variables of concentration and temperature, but others such as velocity, concentration of other species in solution, and electrochemical potential.

In the area of thermodynamic corrosion data, efforts have focused on the development and establishment of a centralized computer facility for storage of evaluated thermodynamic data and for the calculation, graphical presentation, and dissemination of stability diagrams utilizing that data. The most useful graphical representation of the thermodynamic behavior of metals exposed to aqueous environments is the Pourbaix diagram which shows regions of stability of the metal (immunity), solid compounds (passivity), and soluble species (corrosion) as a function of electrochemical potential and pH. A Pourbaix diagram produced in the Corrosion Data Center is shown in figure 4. These diagrams can be calculated and graphically displayed to show the effects of: 1) changes in concentrations of the soluble species; 2) the presence of up to four other elements and their soluble species at any concentration; and, 3) changes in temperature up to 300 C.

Further developments in this area will involve detailed studies of Pourbaix diagrams for alloys as well as the development of similar systems for other stability diagrams for metals and alloys such as those used for high temperature gaseous reactions.

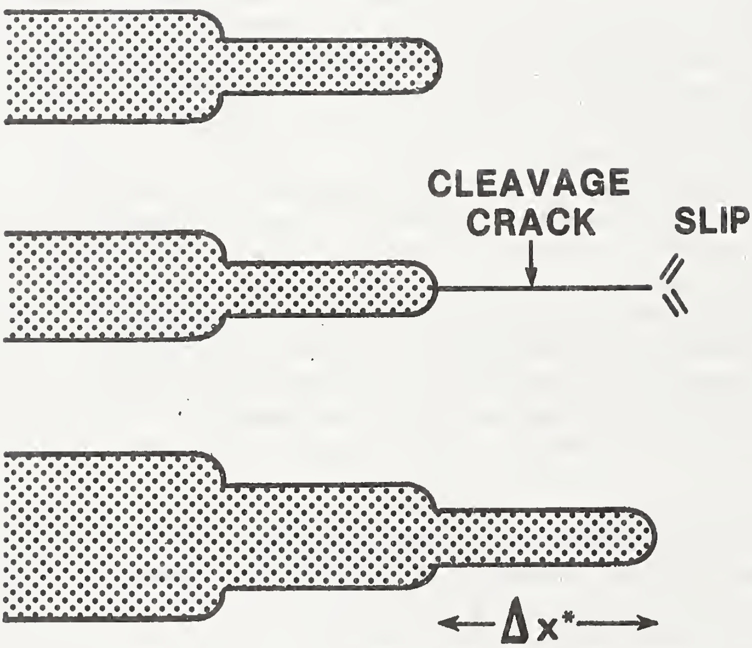

Figure 1. Schematic of our view of the propagation of transgranular stress corrosion cracks, in which the crack advances discontinuously by cycles of cleavage, crack arrest and blunting, and re-initiation. The crack advance distance, Δx^*, is of order 1 μm, and the time interval between successive events varies between fractions of a second to minutes, depending on the system and on the environmental and mechanical conditions.

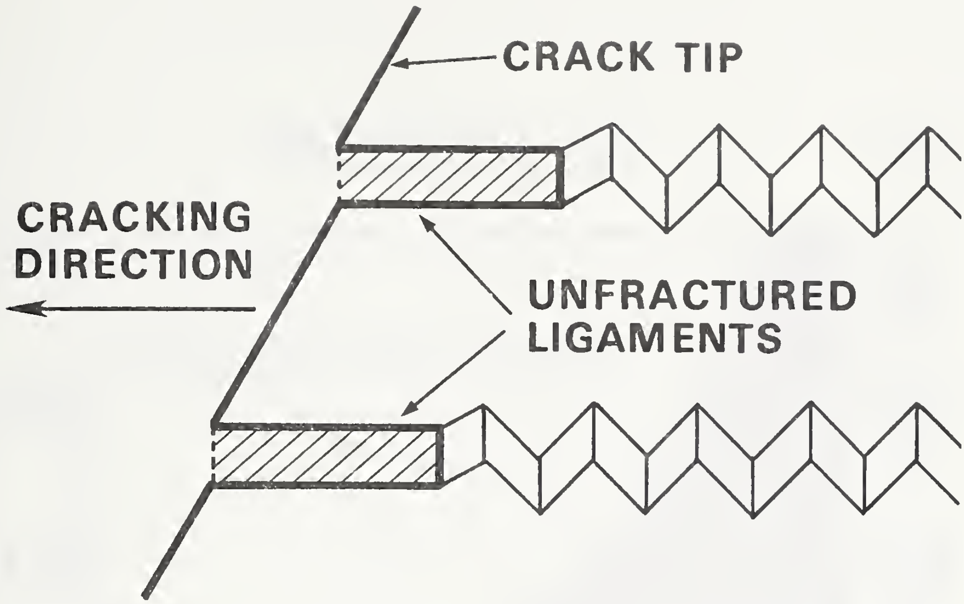

Figure 2(a). Schematic of the fracture surface produced by transgranular SCC, showing parallel primary facets separated by serrated steps, and unfractured ligaments at the crack tip.

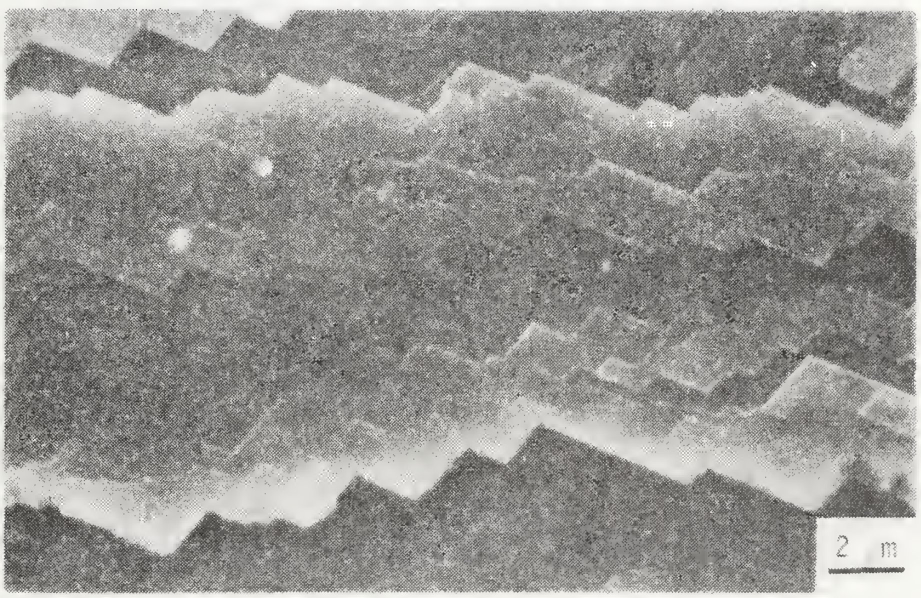

Figure 2(b). Scanning electron micrograph of a transgranular fracture surface in copper-30 zinc/aqueous ammonia, viewed normal to the {110} primary facets.

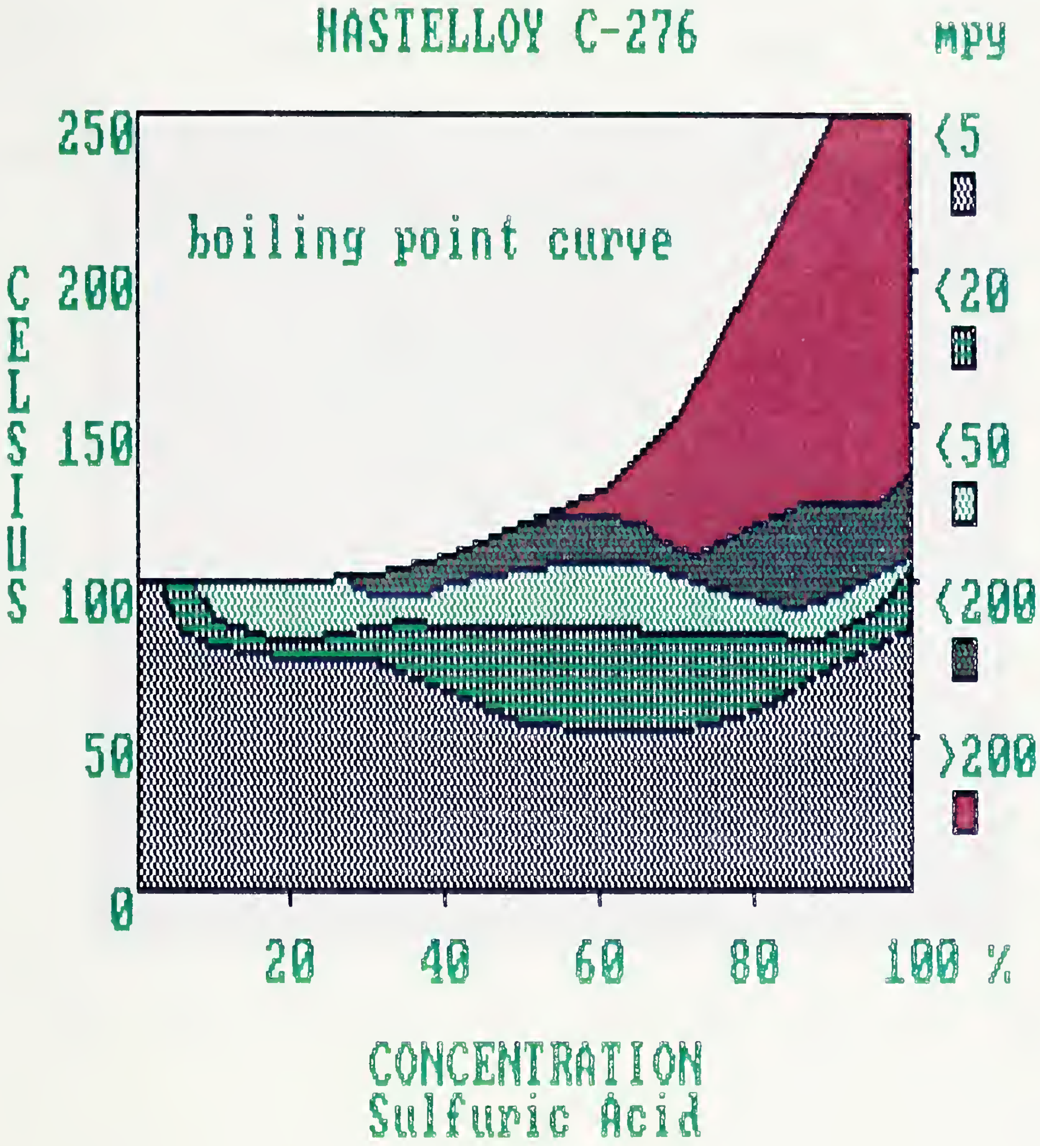

Figure 3. Isocorrosion chart for Hastelloy C-276 in sulfuric acid showing regions of corrosion rate of <5 to >200 mils per year as a function of concentration of sulfuric acid in water and temperature.

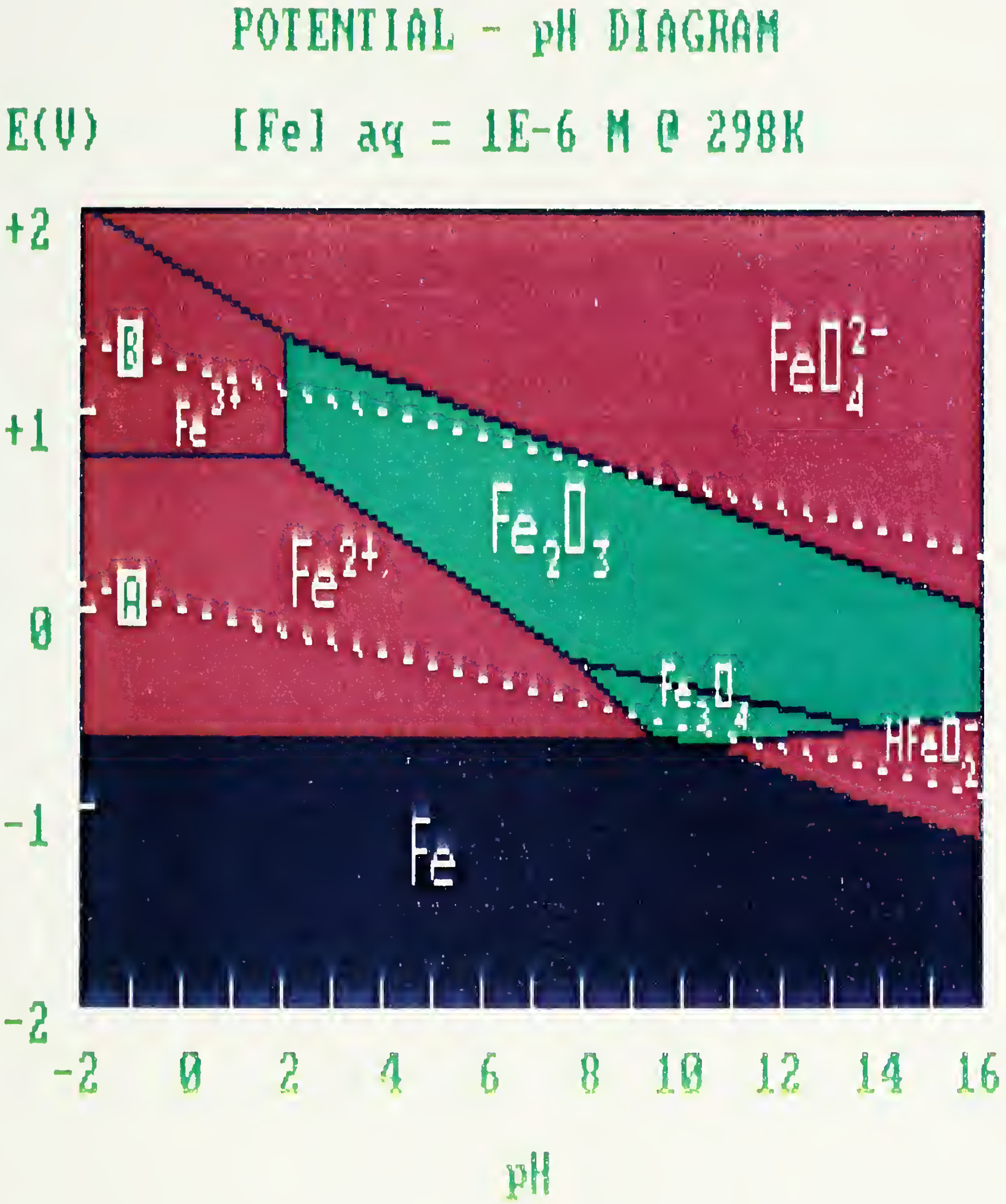

Figure 4. Pourbaix (stability) diagram for the system iron-water at 298K and a concentration of soluble species of 10^{-6} M. The regions of immunity (blue), passivity (green), and corrosion (red) are shown as a function of electrochemical potential expressed as volts versus the standard hydrogen electrode and of pH.

ELECTRODEPOSITION (ELECTROCHEMICAL PROCESSING)
Task: 15447

The electrodeposition group is concerned with measurement and standards connected with electrodeposited coatings. The objectives of the group are: (1) to determine the critical mechanistic, material, and process variables controlling the structure/property relationships of electrodeposited coatings, and to extend methodology to the development of approaches that will result in new wear resistant and corrosion resistant alloys; (2) to produce new Standard Reference Materials (SRM's) which are necessary for the measurement technology used by the coatings industry; and (3) to devise new SRM's requiring electrodeposition for their fabrication, for use in metrology and in non-destructive evaluation processes.

Coatings are very important to industry, for example: (1) coatings help in the conservation of strategic materials. It has been estimated by the National Materials Advisory Board that up to 30% of chromium presently used could be saved if coated low carbon steel substrate were substituted for bulk stainless steels. Many of the properties of a material are only required at the surface, so that incorporation of coatings is an important strategy for the conservation of critical materials. Particularly important among critical materials is chromium, used both for stainless steels and electroplated as a pure element. Research underway in the Electrodeposition Group connected with nickel (cobalt)-chromium alloys and nickel-phosphorus metallic glass alloys has demonstrated that in many applications coated substrates can perform better than bulk stainless steels. (2) Coatings are the most common form of corrosion protection. It has been estimated that the cost of corrosion to the U. S. economy is in the neighborhood of 143 billion dollars. (3) The cost of wear in the U.S. has been estimated at from thirty to fifty billion dollars per year. Electrodeposited coatings play an important role in improving surface wear properties thereby allowing use of base material optimized for mechanical properties and surface coatings optimized for wear.

I. Standards Activities

Microhardness Standards

C. Johnson, D. Kelley, D. Lashmore

Highlights of this year's activities include the availability (through the Office of Standard Reference Materials) of two microhardness standards fabricated by electrodeposition technology. The standards are certified to an accuracy of 5 percent at loads of 25, 50, and 100 g-f on both the Vickers and Knoop scales. The hardness values of the standards are nominally 125 and 600. These standards far exceed the accuracy of available commercial standards. Industry has shown much interest in the standards themselves, to meet contract specifications and traceability to NBS and in the results from the investigation of the metrology of the hardness measurement process. Research efforts have continued with the development of another microhardness standard which will be in the range of 800-1000 for both the Vickers and Knoop scales.

Dye Penetrant Crack Testing

D. Kelley, C. Johnson, D. Lashmore

Production has continued on dye penetrant test blocks. A new test block with a roughened surface is available (through the Office of Standard Reference Materials) as SRM 1851. Further work on the dye penetrant test blocks will be dictated by industry demand.

Coating Thickness Standards

R. Brown, D. Lashmore

Techniques to improve the production efficiency of coating thickness standards were implemented this past year. A new industrial adhesive is now used to put the cards together and to mount the individual samples on the cards. This adhesive eliminates the use of hazardous and time consuming contact cement. A new computer program was written to calculate coating thickness obtained directly from chemical analysis.

Six SRM's with an especially low tolerance (±3%) were made for the Frank J. Koch Company.

New masters (±1%) were made for 1301's (2.25-2.75µm) in order to expand the range of our present masters in this thickness range.

A total of approximately 370 special samples were mailed to nine different companies. Over 200 specials were sent to Frank J. Koch Company. This demand resulted in two new SRM's for next year. Several companies sent a total of twenty-five recalibrations to be done.

All the computer programs for measuring SRM's are currently in use for the Cr/Cu/steel. Since no gold SRM's were made this year, the computer program for these thickness measurements are only completed for use with the x-ray fluorescence and not the Beta Back Scatter method.

Step Test Standard Reference Material

R. Brown, F. Ogburn, D. S. Lashmore

NBS has been requested by the automotive industry to provide standard reference material that can be used to calibrate their corrosion "step test" equipment. In response to their request, the electrodeposition group is providing a "STEP TEST" SRM, which should be available by mid-FY 1985.

The standard is made of a multilayered coating. The layers consist of nickel of a high sulfur content, nickel of a lower sulfur content, and copper. The test is used by electrochemically machining a cylinder through the layer which simultaneously measures both the change in thickness (amount of material removed) and electrochemical potential. The production system is now designed to record the electrochemical information on a digital oscilloscope which serves as a data logger to subsequently transfer the data to a floppy disc for permanent storage. The computer system doing the control also serves to provide graphical output of the data to give to the SRM customer as well as to print the required SRM certificates. A sample graph is shown in figure 1.

II. Research Activities

Ultra-Black Coatings

C. Johnson

Patents on the process and application of the ultra-black coating developed by this group have been licensed by industry. Modifications made by industry have increased the operational range of wavelength for high absorption (95-99%) to 45μm. The coating is presently being used as a baffle coating and as a coating for satellite sun shades and screens. This coating appears to be the only practical coating (black optical) capable of surviving laser threat environment and is being considered for the second generation of the space telescope as well as by several private companies for use as an optical absorbing coating.

Coatings Resistant to Hot Phosphoric Acid

C. Johnson, J. Mullen, D. Lashmore

Under contract with the Department of Energy, an investigation to determine the corrosion performance of a number of different coatings in phosporic acid based fuel cells was completed. Coatings evaluated involved metallic glasses of different compositions and noble metals including lead, silver, ruthenium, and gold. The environment in these fuel cells is pure phosphoric acid at 200 °C. The ultimate purpose of this program was to evaluate coatings that could be used to protect the copper heat exchangers used in this type of fuel cell. The degree of protection of the coatings was evaluated in cooperation with the Corrosion Group, using atomic absorption analysis of the electrolyte for the presence of substrate metal ions after prolonged exposure as shown in Table 1 and in figure 2. Corrosion rates (mm/yr) were determined from weight-loss of samples immersed in concentrated phosphoric acid at 200 °C. These results are also tabulated in Table 1. It was found that electrodeposited silver offered excellent protection in this severe environment. Engelhard Industries has taken our lead and is now plating all of their metallic components that are subject to corrosion, with silver. This is being done as part of their work in phosphoric acid based fuel cells.

Metal Matrix Composites (MMC):

C. Johnson, D. Lashmore

As part of the metals processing effort, preliminary work is underway on the use of electrodeposition technology as a precise and rapid method of applying a uniform "matrix" coating to fibers for use as precursors for metal matrix composites. Electrodeposition techniques are readily adaptable for continuous application of single or multilayer coating systems. It may be desirable to create a multilayer coating system on a fiber for the purpose of minimizing interdiffusion and providing a means of accommodating strains resulting from different coefficients of thermal expansion and for minimizing fatigue cracking. Previous attempts by others to use electrodeposition to coat fibers resulted in poor bonding of the coating to the fiber after compaction by hot pressing. The poor bond resulted from volatilization of water that was absorbed by the fibers during electrodeposition from aqueous electrolytes. A technique is being investigated that incorporates the application of a metallic barrier coating to water, prior to electrodeposition from aqueous electrolytes. Electrodeposits of copper and nickel have been applied to amorphous carbon coated silicon carbide fibers, figures 3a, 3b, 4a, and 4b. Evaluation of these coatings will lead to an investigation of fibers electrodeposited with aluminum, aluminum alloys, and titanium.

Bureau of Engraving and Printing

C. Johnson, J. Mullen, M. Ratzker, D. Lashmore

A program funded by the Bureau of Engraving and Printing was started in late FY 1984. The purpose of this program was to provide information on how to improve current coating technology for engraving plates so that they could be used for much longer time before replacement. This investigation is a joint effort between the tribology group and the electrodeposition group. The former is responsible for the development of an accelerated wear test whose results will serve as a parameter used to optimze the coating deposition parameter. New kinds of particulate composite coatings consisting of diamonds and/or silicon carbide in nickel were also being evaluated in this first phase of the study as well as multilayer coatings designed to distribute interfacial strains over larger volume elements.

Theoretical Modeling

C. Beauchamp, D. Lashmore

A theoretical model based on mass transport and kinetic considerations was developed for alloy deposition. It predicts the concentration profile of ionic species in solution uder pulsed-electrodeposition on a rotating disk electrode and hence the alloy composition. Mass transport of ionic in the bulk of the solution is accounted for through diffusion, migration, and convection considerations. The set of boundary conditions includes kinetic and hydrodynamic limitations.

Diffusion is solved using Fick's law, migration through mobility calculations, and convection using the hydrodynamic equations for the rotating disk electrode. At steady state these equations for the rotating disk also fixes one of the boundary conditions, the other being fixed by the Butler-Volmer equation which describes the reaction at the interface.

A computer program was written for solving the differential equations using a finite-element method.

Experimental aspects includes polarization techniques for determining kinetic parameters required by the Butler-Volmer equation for each of the metals to be deposited. These parameters include such things as rate constants, current efficiency, Tafel slopes, diffusion layer thickness, and diffusion coefficients. Electrolytic cells and electrodes for realizing the tasks described were designed. The applicability of the model is being tested against data collected on copper alloy systems

Automation of Microhardness Testing

D. S. Lashmore, J. Mullen, T. Van Vechten

It has been found that the single most serious error in the certification of hardness standard reference materials is the optical measurement of the indention width. In order to improve the accuracy of these SRM's, an automatic measuring system was designed. This system makes use of a Z80A based microcomputer operating on a S-100 bus to interface with a commercial microhardness testing instrument. The indentation depth into the sample is measured using a capacitance probe reference to the sample. The load was also measured using a small load cell which in the present configuration serves to support the sample.

Because the penetration rate of the indentor is initially very rapid, the data taking rate of the computer had also to be very rapid. This requirement necessitated the use of a machine language controlled A/D board and software written in PASCAL. This system provides not only information on bulk hardness of materials which compares with that obtained from optical measurements but also gives dynamic information on load-displacement as shown in figure 5a, hardness-time as shown in figure 5b, and hardness-displacement, figure 5c after impact. In principle, this data is a microprobe of the mechanical properties and complements the development of a system developed by Polvani of NBS, whose advice enabled rapid development of the hardware.

Future modifications to eliminate the load cell for the sole purpose of measuring standards is now underway and repositioning a new shorter probe holder to help reduce elastic bending occurring in the indentor support beam.

Corrosion Studies in Hank's Solution of Electrodeposited Metallic Glasses

M. Ratzker and D. Lashmore

The purpose of the research is to compare corrosion performance of three electrodeposited alloys with those alloys commonly used in simulated physiological solutions. Three kinds of coatings, nickel-phosphorus (Ni-P), cobalt-phosphorus (Co-P), and cobalt-chromium (Co-Cr), are compared to a titanium alloy (Ti-6Al-4V), 316L stainless steel (SST), and nickel (Ni). Only Ni-P has been evaluated.

The electrolyte was prepared according to Brenner's electrolyte type Ni-H (high phosphorus). Direct current (DC) and Pulse Plating methods were used. Current densities (C.D.) for both methods were varied from 10 Amp/dm^2 to 150 Amp/dm^2. The coatings were on a Rotating Disk using low (100 RPM) and high (3000 RPM) speeds. Some coatings on flat, static specimens were made.

The corrosion environment was 'Hank's' solution. Polarization Resistance and Potentiodynamic Scan were the methods used to compare the corrosion performance of the platings and the bulk alloys. Immersion time before conducting the measurements was 30 minutes for Polarization Resistance and 45 min. for Potentiodynamic Scan.

Polarization Resistance measurements are shown in Table 2. Potentiodynamic Plots for various C.D. are shown in figure 6, for Pulse Plating. Figure 7 shows the data for three alloys (Ti-SST-Ni) compared to Ni-P plating.

The results presented above were taken from one or two samples. For information on the scatter of the data is necessary before an individual measurement can be relied upon. Some tentative conclusions reached: (a) Lower current (deposition current) improves the corrosion performance most probably because the low current results in a high phosphorous deposit. (b) Breakdown of the corrosion current does not occur in deposits produced at low current. (c) Both the direct current and pulsed current samples behave about the same as low deposition current densities. (d) Samples plated on a rotating disk at high speed gave better corrosion performance than samples plated under the same conditions but at low speed. Note that speed of rotation is equivalent to increasing mass transport.

Nickel-phosphorous alloys do not exhibit severe breakdown like 316L or nickel, so that failure by corrosion is likely to be gradual and predictable. At potentials above say 300 MV, the nickel-phosphorous alloy outperforms 316L stainless and nickel and only Ti seems superior.
This study is continuing with electrodeposited Co-Cr, and Co-P alloys.

TABLE 1

Atomic absorption analysis of copper after exposure of various coated copper substrates in phosphoric acid at 200 °C.

CHEMICAL RESISTANCE OF ELECTRODEPOSITED METALS IN 85% H_3PO_4 AT 200 °C

METAL COATING	SOAK TIME HRS	A.A. COPPER ANALYSIS PPM	CORROSION RATE MM/YEAR
SILVER	1704	0.84	0.0045
RUTHENIUM	168	46.80	0.026
SILVER : LEAD	960	3.53	0.057
GOLD : LEAD	456	4.60	0.084
GOLD	744	313.75	0.470
LEAD	504	2.85	0.740
METALLIC GLASS ALLOYS:			
EN (Ni - 9P)	240	38.50	1.69
Ni - 14P	192	19.00	3.10
Ni - 8P (EN Type)	216	29.00	3.98
Ni - 12P	45	4.90	4.85
Ni - 16P	22	4.00	5.04
Ni - 12P - Mo	96	10.96	6.64
Over EN			
Ni - 12P - Mo	72	-----	7.00
Ni - 14P + Saccharin	50	1.80	7.84
Co - 10P	48	18.63	31.46

Table 2: Polarization Resistance Results

Platings Parameter of Alloys	E_{corr} [mV]	I_{corr} [μA]	Rp [SL]	Corrosion Rate [mpy] [x25 μm/yr]
DC, 10 A/dm^2, 2000 RPM	-317	1.54	21140	0.415
DC, 20 A/dm^2, 3000 RPM	-323	1.92	16940	0.517
DC, 50 A/dm^2, 2000 RPM	-411	15.64	2083	4.206
PUL, 10 A/dm^2, 2000 RPM	-336	1.61	20170	0.434
PUL, 20 A/dm^2, 2000 RPM	-340	1.78	18340	0.478
PUL, 50 A/dm^2, 2000 RPM	-385	12.55	2596	3.375
PUL, 75 A/dm^2, 2000 RPM	-369	7.00	4656	1.882
PUL, 20 A/dm^2, 150 RPM	-363	4.88	6679	1.312
PUL, 50 A/dm^2, No Rotating	-390	19.91	1636	5.355
Ti-6AL-4V	+125	0.037	88630	0.025
316 L Stainless Steel	-168	0.020	1651000	0.008
99.999% Ni	-183	0.429	75910	0.182

Pulsing was carried out at 2 msec on, 0.2 msec off times.

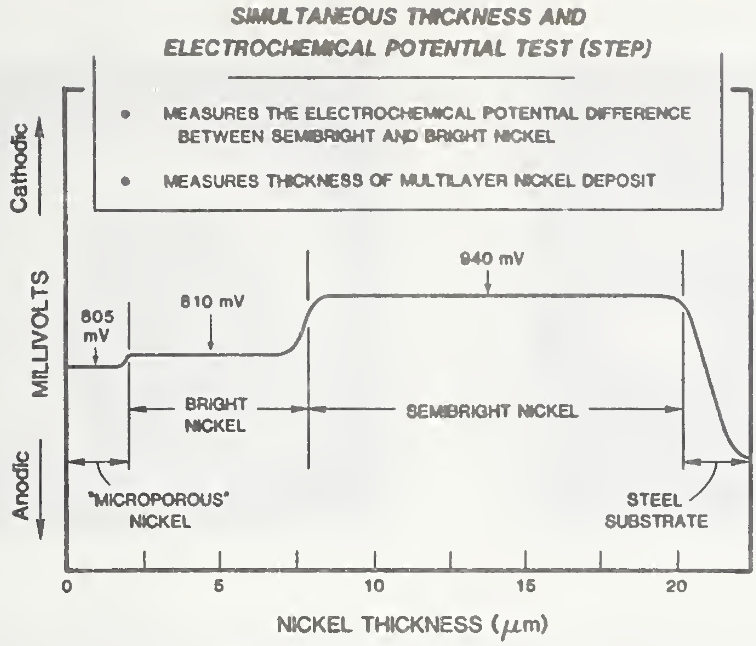

Figure 1. Sample graph of Simultaneous Thickness and Electrochemical Potential Test (STEP).

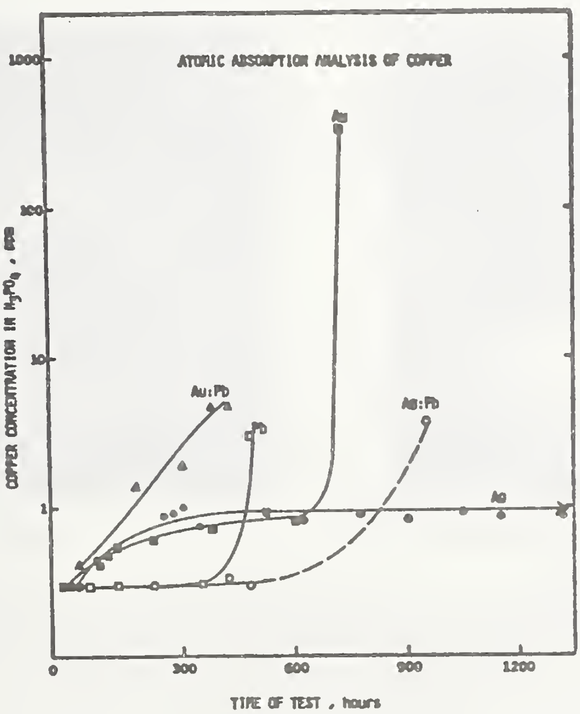

Figure 2. Atomic absorption analysis of copper after exposure of plated copper substrates to hot phosphoric acid for extended time periods.

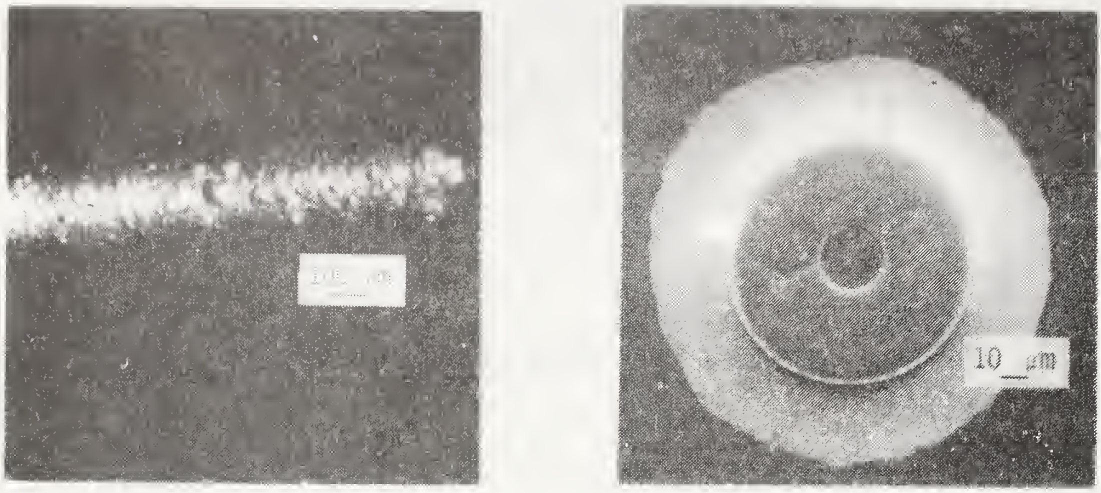

(a) (b)

Figure 3. Electrodeposited copper on an amorphous carbon coated silicon carbide fiber. (a) Surface of copper plated fiber. (b) Section of copper plated fiber.

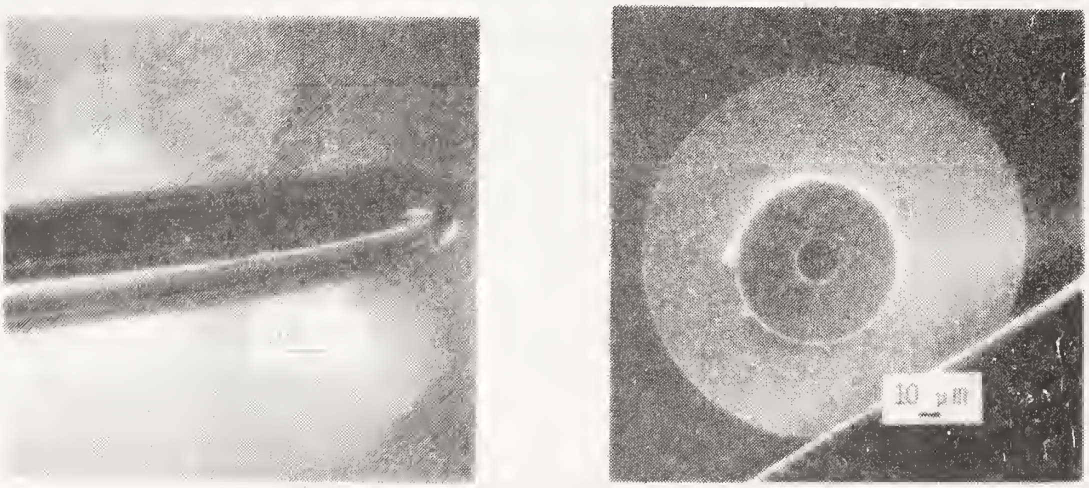

(a) (b)

Figure 4. Electrodeposited bright nickel on an amorphous carbon coated silicon carbide fiber. (a) Surface of nickel plated fiber. (b) Section of nickel plated fiber.

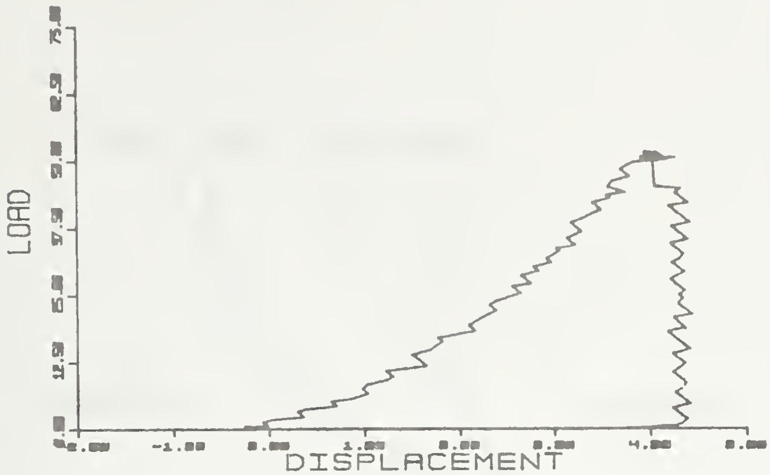

(a)

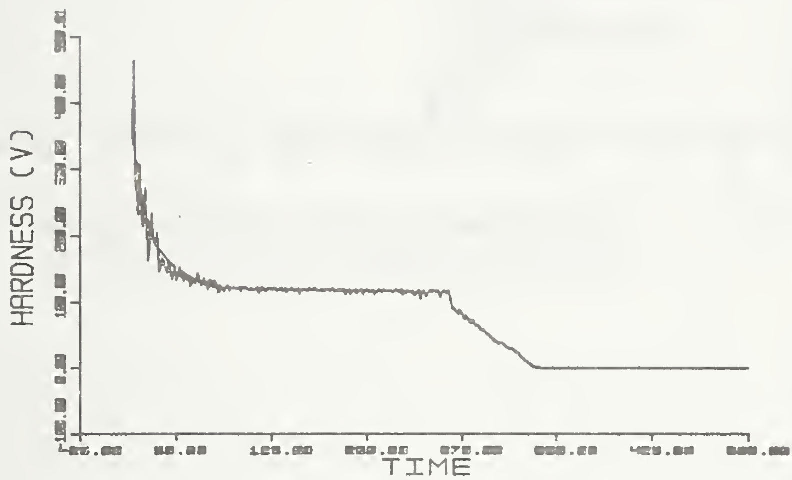

(b)

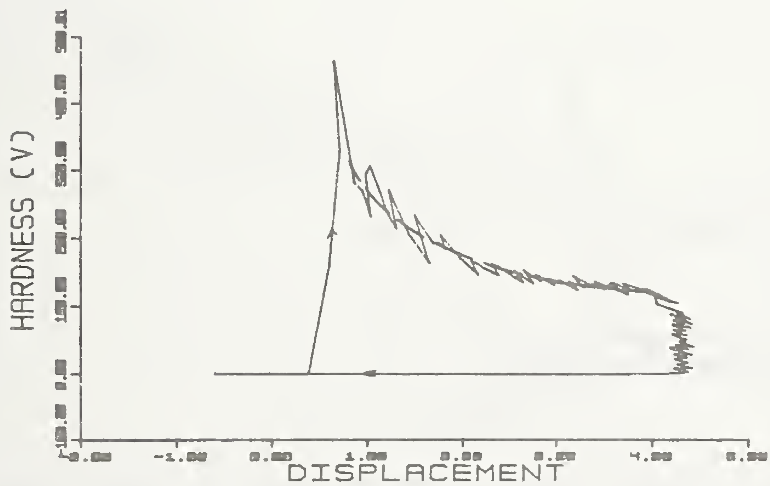

(c)

Figure 5. Graphs of dynamic information obtained from automated microhardness tester. (a) load (g-f) vs displacement (μm), (b) hardness (VHN) vs time, and (c) hardness (VHN) vs displacement (μm).

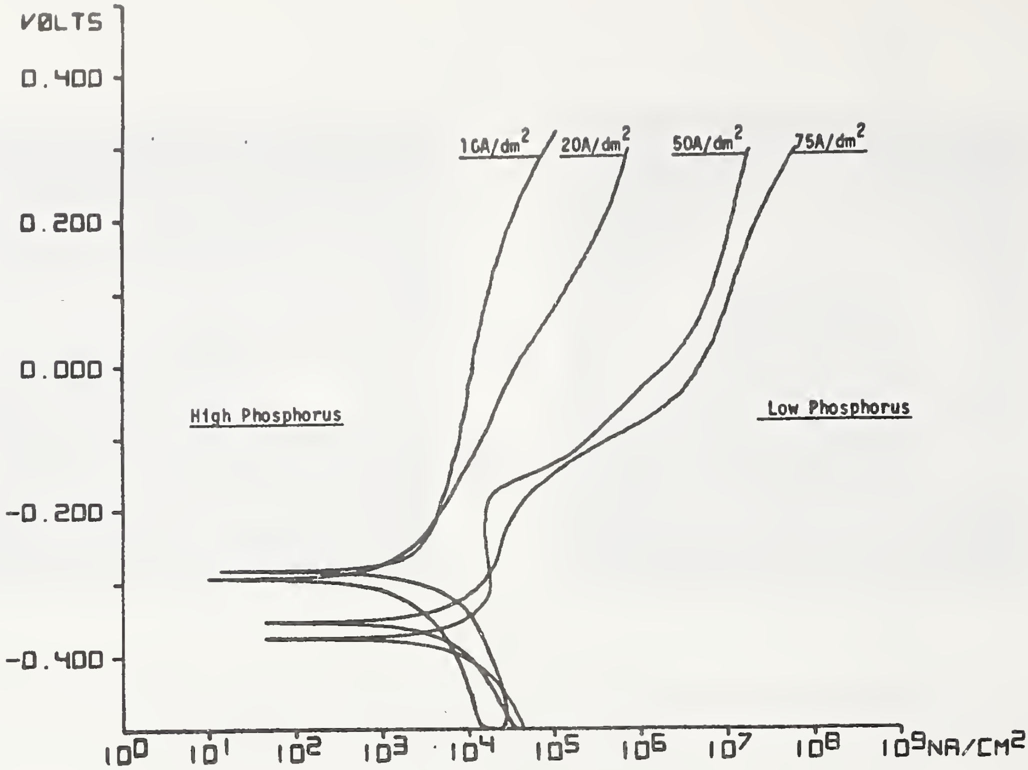

Figure 6. Potentiodynamic plots comparing current densities (phosphorus content) for pulse plating.

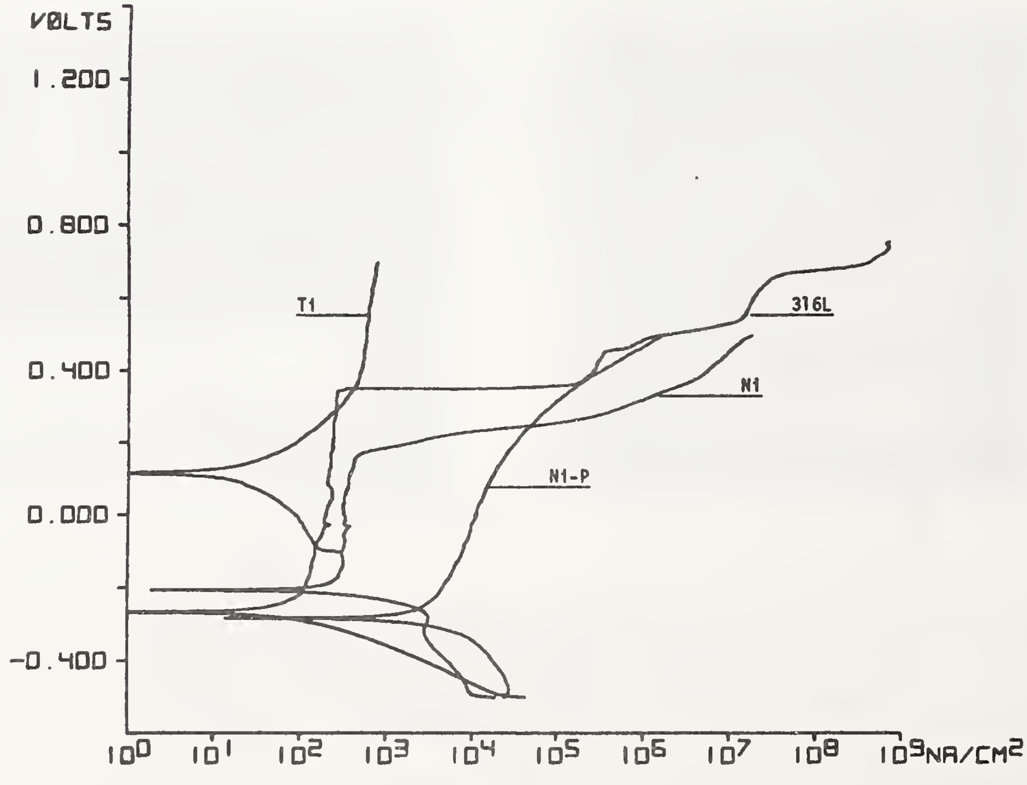

Figure 7. Potentiodynamic plots comparing various alloys, Ti-6Al-4V, 316L SST, and 99.999% Ni to pulse plated Ni-P.

NONDESTRUCTIVE CHARACTERIZATION
Task 15448

For much of our recent past, materials have been prepared by empirically derived methods with only a crude understanding of the complex changes that occurred during their production. As materials have become more advanced and have been required to deliver higher performance, the critical importance of microstructure in controlling properties has become recognized. Theoretical and experimental work has begun to result in a better understanding of the relations between process variables and microstructure. Predictive process models have emerged which can be exploited to design advanced processing methods. Many of the failures of our most advanced systems can now be traced to a failure to ensure a homogeneous distribution of optimal properties through either inadequate microstructure control or a failure to detect defects formed during processing.

Task 15448's primary goal is to develop advanced methods for the measurement of microstructure and properties and the detection of defects during materials processing. These methods must be nondestructive for they are to be applied in situ during the actual processing procedure. The data they supply will enable in-process microstructure characterization. The data can be used as inputs into numerical process models which in turn predict the changes that must be made to process parameters for achievement of optimal quality products. This closed loop feedback control methodology, relying for its recent emergence upon new nondestructive microstructure measurements (sensors) and the advent of microcomputers,artiticial intelligence and high speed image processing promises to revolutionize U.S. materials processing, leading to improvements in both quality and productivity that could restore international competitiveness to our materials industries and their domestic utilizers.

The ability to measure, in situ, changes in microstructure during processing also opens the way to a deeper scientific understanding of the basis of materials behavior. Thus, our research programs are both trying to develop and apply advanced measurement methodologies for process control and to use these techniques to improve our understanding of the basic mechanisms of material transformations.

To achieve these objectives, we have developed extensive expertise in three techniques capable of in situ measurements:

- Ultrasonic imaging
- Acoustic emission
- Eddy currents

In the past year, significant advances in measurement methodology have been made to each technique: their scientific foundations have been further improved and their ranges of usefulness extended.

The research and development activities of Task 15448 have been strongly supportd by the Office of NDE. In addition, Major funding for the coupling of rapid solidification processing and advanced NDE has been provided by the Defense Advanced Research Projects Agency (DARPA). Additional support has also been provided by the Naval Sea Systems Command for studies of acoustic emission during crack growth of low alloy steels.

During FY 84 numerous collaborative interactions have been initiated or extended. Under an agreement with the American Iron and Steel Institute, B. Droney (Bethlehem Steel), J. Toth (L.T.V./Republic Steel), D. Rogers, G. Dykeman, and R. Rudolph (U.S. Steel) have collaborated with the group as Research Associates. Jeffrey Martinez of AISI has also recently joined the cooperative program providing much needed technical assistance. The fruitful collaboration with Johns Hopkins University has continued with Prof. Moshe Rosen continuing his Guest Worker appointment. Cooperatively working with several group members, graduate students of Prof. Rosen's (J. Smith, T. Hsieh and B. Elkind) have also each made valuable contributions to our programs. Dr. Moshe Gvishi has spent a sabbatical from Israel (one year) with our group and has pioneered the application of nondestructive techniques to the *in situ* characterization of transformations in shape-memory alloys.

Throughout FY 84, very close collaboration has occurred with other groups in the Center for Materials Science. In particular, one of us served as the principal editor of an extensive review documenting NDE activities in the CMS and was heavily involved in developing a strategy for NDE research in CMS during the next five years. A second group member is collaborating with The Fracture and Deformation Division by carrying out acoustic emission monitoring of crack arrest in pressure vessel steels.

One member of the group is editor of the journal "Ultrasonic Imaging" and was Chairman of the 1984 "Symposium on Ultrasonic Imaging and Tissue Characterization". A second group member was General Co-Chairman of the "Sixth International Conference on NDE in the Nuclear Industry" and Organizer of a recent ASM sponsored conference on "In-Process Nondestructive Characterization and Process Control" held at the 1984 ASM Metals Congress in Detroit.

Acoustic Emission Imaging
Subtask 1 of Task 15448

S. J. Norton and M. Linzer

During the past year, we have investigated theoretically two approaches to the reconstruction of two-dimensional random source images from measurements of the emitted radiation recorded over multiple transducer arrays. In the first approach, a closed-form analytical inversion formula was derived for the special case in which the transducers are equally spaced around the circumference of a circle enclosing the source region. We have shown that the existence of a closed-form solution requires the assumption of a spatially-incoherent source (i.e., where the radiation emitted from separate points in the source is statistically uncorrelated). Sources that can be modeled as random and spatially incoherent are common in nature. Thermal or black-body sources are good examples in the optical regime. In ultrasonics, acoustic emission sources arising from dislocations, microcracking or material transformations (e.g. martensitic transformations) sometimes satisfy these conditions.

As a first step in obtaining a closed form solution to the inverse source problem, the emitted radiation is recorded over all points on the circumference of a circle enclosing the source region. These recorded signals are then cross-correlated pair-wise. If the source is statistically-stationary and spatially incoherent, this cross-correlation operation may be shown to reduce to an integral equation that arises in the two-dimensional inverse-scattering problem. This particular equation can be solved in closed form for a circular recording geometry. The three-dimensional generalization of this exact solution (in which the receiving array is spherical, rather than circular) is also presented. A paper describing the above inverse source solutions was recently accepted for publication by the Journal of the Acoustical Society of America.

In the past year, we have also carried out a theoretical analysis of a backprojection algorithm for reconstructing source intensity distributions. In this method, far-field approximations are made in deriving the source reconstruction formula. This approach is computationally more efficient and less restrictive with respect to the source characteristics than the above exact solution. Moreover, the method, in principle, may be implemented with an array of any shape, unlike the exact solution for which a circular array is necessary. In the backprojection approach, the emitted radiation is recorded at multiple transducer locations and correlated pair-wise, optimally filtered, and then backprojected into image space. The filtering and backprojection operations are essentially similar to those employed in image reconstruction algorithms in medical x-ray tomography. If a large number of transducer elements are used, this approach may make it practical, for the first time, to image acoustic emission source distributions and to detect acoustic emission signals below the random electronic noise of the receiving system. A paper describing these results is in preparation.

<u>Acoustic Emission in Metallurgy</u>
Subtask 2 of Task 15448

R. B. Clough, M. Gvishi, M. Rosen, J. A. Simmons, C. Turner and H. N. G. Wadley

During the past year work has progressed on the measurement of acoustic emission in rapid solidification processing (RSP), phase transformations and on the vector calibration of AE transducers.

RAPID SOLIDIFICATION PROCESSING

Acoustic emission can be used to monitor rapid solidification to detect flaw production as well as to provide fundamental knowledge of RSP phenomena. Our current AE studies of RSP represent a new type of acoustic emission measurement developed for in situ monitoring of such materials processing. Previously we have reported the characteristics of such measurements and some preliminary results.[1] We have now completed the bulk of the measurements for pure aluminum and Al-4.5% Cu.[2,3]

The acoustic emission results for Al and Al-4.5% Cu are shown in Figs. 1 and 2, separated into heating and cooling phases. A particularly significant result is the systematic dependence of the acoustic emission on the condition of the substrate. This indicates that plastic deformation and/or microfracture of the substrate controls the AE, both in the solid and solid/liquid regions.

Much less is known about emission mechanisms during melting and solidification. The liquid-solid interface itself moves too slowly to produce the high frequency signals observed. Possible explanations may be the collapse of the compressive center on melting, which is accompanied by annihilation of the associated internal stress fields, or rapid creep relaxation of the surrounding material. This high frequency emission effect grows quite rapidly above the melting transition. During solidification, no cracks are observed in the pure Al, so that emission there is caused entirely by dislocation processes. In the alloy which is peak hardened, large intergranular cracks remain upon solidification. These are much less pronounced in the softer, underaged alloy material. The number of cracks decreases with melt depth. These important observations suggest that fracture during surface modification can be minimized by (a softening) heat treatment prior to surface modification.

LASER DRILLING

Another area of application of acoustic emission technology to RSP is that of laser drilling. Because of its speed, controllability and the capability of penetrating tough or exceptionally hard materials, laser drilling is a rapidly growing manufacturing method. However, beam power spikes and intervening disintegration products can disrupt or diminish energy transmission at the hole site, resulting in variable hole depth. To improve this situation, a method was developed for in situ acoustic emission monitoring of the specimen during drilling.[4] In laser drilling, acoustic emission can result, e.g., from the thermally-induced stresses in the heated zone ahead of the advancing hole, or from the stresses which accompany the expulsion of vapor and liquid from the hole.

The physical basis of the measurement is a new type of acoustic emission method developed here which permits quantitative results to be obtained from near net shape components in industrial manufacture. The method monitors acoustic emission energy. To quantify the measurement, a new procedure called "scalar calibration" was developed. Here the system is calibrated with a stress wave source of known energy (a pulsed infrared laser). The energy of the unknown event is determined by comparison with this calibration.

There is a considerable amount of scatter in the depth of laser drilled holes as predicted by the laser energy density. However, there is an improvement of about 9% (in the statistical residuals) by monitoring the acoustic emission energy as opposed to laser pulse energy. This is presumably because in situ acoustic emission monitoring detects only the acoustic effects resulting from the energy which is transmitted to the specimen, i.e., that effective for hole drilling. When combined with additional information, namely the laser energy, there is a significantly improved accuracy in hole depth determination. The residuals have decreased by 25% as compared to those from laser energy alone. It appears feasible for industrial application, and a patent is being pursued by the DoC.[5] This work was carried out in cooperation with R. J. Schaefer of the Metallurgical Processing Group.

MARTENSITIC TRANSFORMATIONS

Work has been carried out on the acoustic emission associated with the martensitic transformation.[6] The majority of phase transformations occur at a rate controlled by diffusion. There are, however, important classes of transformations for which atomic diffusion is not rate controlling. These include the martensitic transformations, twinning and deformation in which the change of crystal structure is accomodated by a so-called "diffusionless" shear transformation; diffusion, if it occurs, is over the range of a lattice parameter. The velocity at which the transformation propagates varies enormously from one alloy to the next, but velocities of 30% of the shear wave speed have been reported. Acoustic emission is a commonly observed by product of these types of transformation.

The thermoelastic martensitic phase transformation of the shape-memory alloy NiTi (CsCl <--> monoclinic martensite) was studied as a function of temperature by means of both acoustic emission and electrical resistivity methods. AE measurements were made of accumulative events, amplitudes, risetimes and event duration. Both AE and resistivity were recorded dynamically during the heating and cooling semicycles in the temperature range between -196°C and +190°C.

These data enabled determination of the critical temperatures and the kinetic parameters of the martensitic phase change. The critical points were found to be: M_s=0°C, M_f=103°C, A_s=85°C and A_f=150°C. Acoustic emission at low threshold levels was found to be an extremely sensitive indicator of the martensitic transformation in this alloy, substantially better than electrical resistivity; and the critical points were more prominently detected and better defined by AE than by resistivity measurements. AE also demonstrated the existence of both athermal and isothermal martensite for this alloy.

A quantitative description of the nature of AE signals associated with martensitic transformations and deformation twinning has also been developed.[7,8] Starting from a 4-dimensional formulation for elastodynamics in which the time components of the extended stress are the negative momentum terms and the time components of the distortion are the velocity terms, the representation was given for wave propagation and scattering. This representation was obtained by direct generalization of the projection operator formalism previously developed for static inclusions. An approximate solution for this problem was obtained for wavelengths large in comparison to the size of the transformed region and by eliminating reverberation effects. Using a six dimensional vector terminology (such as the Voight convention) where vectors are symmetric 3 x 3 matrices, the effective stress drop associated to the transformation was shown to be:

$$\underline{\Delta\sigma}(t) = [\underline{\underline{I}} + \Delta\underline{\underline{C}}\ \underline{\underline{D}}]^{-1}\ [(\underline{\underline{C}} + \Delta\underline{\underline{C}})\ \underline{\beta}^{*} \ - \ \underline{\underline{C}}\ \ \underline{\beta})]\, V_{\Omega}(t) \quad .$$

Here the matrix $[I + \Delta C\ \overline{D}]^{-1}$ gives the feedback correction associated with the inhomogeneity effect, the term $(C + \Delta C)\ \beta^{*}$ gives the stress drop associated with the transformation strain and $-\Delta C\ \beta^{\circ}$ gives the interaction of the elastic pre-stress with the inhomogeneity. The entire expression is seen to be proportional to the volume of the transformed region. This model shows that the acoustic emission signal contains quantitative information about six properties of such phase transformations:

1. Volume of the transformed region
2. Dilatational strain in the transformed region.
3. Shear/rotational strain of the transformed region.
4. Habit plane for disc-like martensitic tranformations.
5. Internal stresses in the region of the transformation.
6. Duration of the transformation.

Detailed expressions were given for spherical and disklike inclusions.

VECTOR CALIBRATION

The theory for vector transducer calibration was developed for acoustic emission transducers.[9] This theory takes into account the finite size of the transducer by expanding the motion modes of the transducer face in a user selected orthogonal expansion. The calibration is then given in terms of three simultaneous convolution equations:

$$v_j(t) = \sum_{i=1}^{3} \; {}_i(t) * G_i(t) * s_j(t)$$

where G gives the vector response of the sample at the transducer, s describes the signal source and Δ gives the vector impulse response for calibrating the transducer. The solution of these equations is then reduced to a single one-dimensional deconvolution problem for each of the motion modes of the transducer face.

A simpler technique for vector calibration was also developed which makes use of the fact that an elastic plate produces no vertical response from a horizontal force applied transversely to the source/-transducer axis. This technique separates the three simultaneous convolution equations so that deconvolution can be done one component at a time. An initial apparatus was constructed for applying these methods, but a small vertical component was found from the ostensibly horizontal force. A new apparatus is under construction to remove this problem.

[1] R. B. Clough, H. N. G. Wadley and R. Mehrabian, "Experimental Studies of the Dynamics of Rapid Solidification Using Acoustic Emission" in "Rapid Solidification Processing--Principles and Technologies III", R. Mehrabian, ed., pp. 403-415, NBS, 1983.

[2] R. B. Clough, H. N. G. Wadley and R. Mehrabian, "Heat Flow-Acoustic Emission-Microstructure Correlations in Rapid Solidification of Aluminum Alloys", in 2nd Intl. Conf. on "Application of Lasers in Materials Processing", E. Metzbower, ed., ASM, 1984.

[3] R. B. Clough, H. N. G. Wadley and R. Mehrabian, "In Situ Studies of High Intensity Electron Beam Interactions with Aluminum", to be published in Met. Trans.

[4] R. B. Clough, H. N. G. Wadley and R. Schaefer, "Acoustic Emission Monitoring of Laser Drilling", to be published in Materials Evaluation.

[5] R. B. Clough and H. N. G. Wadley, "Acoustic Emission Monitoring of Laser Drilling", patent pending.

[6] M. Gvishi, M. Rosen and H. N. G. Wadley, "Nondestructive Characterization of the Martensitic Phase Transformation in NiTi by Means of Acoustic Emission", to be published in the proceedings of the Conference: Reviews of Progress in Quantitative NDE, July 8-13, 1984.

[7] J. A. Simmons and H. N. G. Wadley, "Theory of Acoustic Emission from Inhomogeneous Inclusions", pp. 51-60 AMD -Vol 62 on "Wave Propagation in Homogeneous Media and Ultrasonic Nondestructive Evaluation", published by ASME, June, 1984.

[8] J. A. Simmons and H. N. G. Wadley, "Theory of Acoustic Emission from Phase Transformations", NBS Journal of Research, pp. 55-64, vol. 89,1984.

[9] J. A. Simmons and H. N. G. Wadley, "Vector Transducer Calibration", in "Review of Progress in Quantitative Nondestructive Evaluation", D. O. Thompson and D. E. Chimenti, eds., Vol. 3B, pp. 699-706, Plenum Publ., 1984.

Eddy Current Conductivity in Materials
Subtask 3 of Task 15448

A. H. Kahn and K. Long

The objective of this project is to provide theoretical research for developing electromagnetic methods of NDE for determining depth profiles of electrical conductivity. The importance of this objective lies in that the principal method used for producing wear-resistant surfaces for crankshafts, bearings, and gear wheels is by surface microstructure modification. Accompanying this modification are variations in electrical conductivity and magnetic permeability. Eddy current methods are currently used in manufacturing processes, mostly by calibration of measuring equipment against selectively treated production samples. The goal of this project is to apply modern inversion techniques to multi-frequency eddy current data in order to perform a quantitative reconstruction of the conductivity profile of the test material.

The principle of the process of inversion is based on the following concepts: at a given frequency, the electromagnetic surface impedance of the test material is determined by a complex average of the conductivity beneath the surface to a distance of approximately one skin-depth. By varying the frequency, the skin depth is varied and different depths are sampled. Then from general methods of electromagnetic theory a reconstruction of the conductivity profile is possible.

Several methods of inversion of electromagnetic data in geological applications have been discussed by Parker (ref.1) and Parker and Whaler (ref.2). Professor Parker has made his computational algorithms available and this has helped greatly in the present work. These, and other inversion methods, were critically discussed with Dr. John Simmons.

The model which has shown the most favorable results operates by treating the sample material as a set of thin shells with conductances and spacings considered as unknowns to be determined from the data. The conductance of each shell may be visualized as equivalent to an integrated conductivity over the space adjacent to the shell. This has been applied to the case of a uniformly stratified slab, the exciting current being supplied by a uniform current sheet. This could be looked upon as equivalent to an axially symmetric cylindrical sample in a solenoid, in the limit of large radius.

As an example, consider a set of shells of conductances S_i and separations h_i. The admittance, $Y(\omega)$ is given by the continued fraction representation (ref.1),

$$i\omega\mu_0 Y(\omega) = h_0 + \cfrac{1}{i\omega\mu\tau_1 + \cfrac{1}{h_1 + \cfrac{1}{i\omega\mu_0\tau_2 + \cdots,}}}$$

where μ_0 is the permeability of free space and is the angular frequency. The continued fraction terminates for a finite number of shells. The admittance is then a rational function of the frequency and the decomposition into the continued fraction is accomplished by successive division operations. The inversion parameters $\{h_i, {}_i\}$ are then obtained by inspection. To perform this process, Y must be measured at a sufficiently large number of frequencies to allow approximation of $Y(\omega)$ as a ratio of two polynomials in ω. This inversion method is commonly used in electrical circuit synthesis (ref.3).

As a preliminary test of this inversion technique we have considered two examples of input data. The first is the case of a semi-infinite slab of uniform material. The second case corresponds to the same bulk material, but with an added surface layer having a conductivity equal to half the bulk value. For demonstration purposes, the bulk conductivity is taken as that of aluminum and the surface layer is given a thickness of 1.0 mm. For these two cases the forward calculation of the admittance is easily computed; 26 values of admittance over a range of four decades of frequency were used as input data for each model. The results for the uniform slab are shown in Fig. 3 and for the stepped slab in Fig. 4. The bold lines in the figures show the positions of the shells. Figs. 3 and 4 show the profiles obtained if each conductive shell is considered to be uniformly spread over its associated spacing. The input conductivities are shown in Figs. 3 and 4 as dotted lines.

These results show a coarse reproduction of the input conductivity. The method is now under examination to determine its sensitivity to number of data points and frequency range of the data points. The method is also being extended to the case of cylindrical geometry. Further work is also being performed on the determination of the analytic form of $Y(\omega)$ from the input data.

[1] R. L. Parker, Journal of Geophysical Research 85, 4421 (1980).

[2] R. L. Parker and K. A. Whaler, Journal of Geophysical Research 86, 9574 (1981).

[3] G. C. Temes and J. W. LaPatra, Introduction to Circuit Synthesis and Design (McGraw-Hill, New York 1977). See pp. 61-69.

Ultrasonics in Metallurgy
Subtask 4 of Task 15448

Bernard Droney, Brett Elkind, Timothy Hsieh, Melvin Linzer, Floyd Mauer, Stephen Norton, Moshe Rosen, Kurt Sandstrom, John Smith, Jim Toth, Christian Turner, Dave Rogers and Haydn Wadley

In FY84, significant advances have been made in developing techniques for obtaining temperature-velocity data and for generating accurate temperature profiles in hot steel.

VELOCITY-TEMPERATURE MEASUREMENTS

Accurate values of longitudinal wave velocities as a function of temperature are needed in order to convert data obtained by time-of-flight tomography into temperature profiles in hot steel bodies. Standard reference data will be required for each new material, and a method is being sought that will give an accuracy of better than 1 part in 10^3 on a routine basis.

A method using quartz buffer rods to couple two ultrasonic transducers to a specimen in a furnace was applied to 304 stainless steel at temperatures up to 1045°C. The maximum error was estimated to be about 20 ms^{-1} corresponding to an error of 30°C in temperature. This error is about three times greater than is permitted by our design requirements, and other methods are being evaluated. Most of the difficulties experienced with this first method could be traced to the couplant at the interfaces between the buffer rods and the specimen. These interfaces were subjected to temperatures from ambient to 1000 C, and no single couplant could be found that would cover the entire range without burning, caking, evaporating, or eroding the mating surfaces.

A new method is being evaluated which eliminates the hot couplant problem by using a laser beam to excite the ultrasonic wave directly in the specimen, and by using a one-piece, stepped rod to provide both a test section and buffering rod. The laser pulse can be applied to either the outer end of the test section or to the step where it joins the buffering section. The difference in time-of-flight gives the time-of-flight in the test section, which must be at a uniform temperature. Tests have shown that the outer end of the rod can be kept at a temperature below 100 C, which will not damage the transducer. The signal transmitted by the rod is more than adequate even at the highest temperature, and the noise level is not excessive. A new platimum-wound furnace with a reflective heat shield has been built to insure uniform heating and is undergoing tests. An example of the velocity-temperature relation for 304 stainless steel obtained by this method is shown in Fig. 5.

TEMPERATURE TOMOGRAPHY

Cylindrical Geometry

In preparation for further tests of ultrasonic tomography applied to temperature profiling in cylindrical specimens, a rotary table has been set up and equipped with jigs for mounting and adjusting transducers. Tests have been conducted which indicate that the chord length can be computed with sufficient accuracy from table rotation if the test cylinder is carefully centered and the angle is determined to 0.1°. The tests show that it is necessary to allow for the diameter of the laser beam (1 mm) and the tip of the transducer (1 mm) in computing the chord length.

Using laser excitation, ultrasound was transmitted through a 6-inch diameter 304 stainless steel cylinder at room temperature, and time-of-flight measurements were made at 11 angles. The cylinder was then heated by induction coil to about 400 °C and, after a few minutes of cooling, time-of-flight measurements were made at 4 angles. An iterative least-squares reconstruction algorithm was applied to the two sets of measurements yielding the temperature profiles shown in figure 6. The dots indicate the temperature measured at the center of the cylinder by an embedded thermocouple. The agreement between the measured temperatures and the calculated temperature profiles are well within experimental error.

Square Geometry

1. Theoretical

We have extended our analysis of the tomographic reconstruction of temperature in a cylindrical geometry to bodies of rectangular cross section. Heat flow analysis demonstrates that under certain conditions (that are often approximated in practice) the two-dimensional temperature distribution $T(x,y)$ that exists on a cross-section with a square boundary factors into the product of two one-dimensional solutions, i.e., $T(x,y)=f(x)f(y)$. (The following results can also be generalized to rectangular cross sections.) This is an important simplification, since it implies that a single set of ultrasonic time-of-flight measurements over parallel paths (i.e., one "projection") is sufficient to recover the unknown function $f(x)$, and hence $T(x,y)$. This should be contrasted with the far more difficult problem of reconstructing an arbitrary function $T(x,y)$, in which case hundreds of projections measured at small angular increments over 180 degrees are required to tomographically recover $T(x,y)$. Computer heat flow modeling and simulated reconstructions have shown that the assumption of factorability of the two-dimensional temperature distribution significantly simplifies the experimental complexity and computational burden of the temperature tomography problem.

2. Experimental

A computer-controlled instrument is being designed to image the temperature distribution in a square geometry. A steel bar with a 6 inch by 6 inch cross section will be used as the initial sample, with the objective of reconstructing the temperature within a 16 by 16 grid. A laser will serve as the ultrasonic source and a PZT transducer with a conical buffer rod and high temperature couplant will be employed as the receiver. Accurate distance measurement will be obtained by means of LVDTs affixed to the receiver probes.

A test rig is now being constructed that will be used to evaluate the components and algorithms that will be incorporated in the computer-controlled instrument. A specimen six inches square and 15 inches high is being prepared for temperature profiling based on multiple paths intersecting both obliquely and at right angles. This specimen will be fitted with thermocouples in wells to provide an actual temperature profile for comparison with the results of time-of-flight tomography.

High Temperature EMATS

The experimental program to date has concentrated upon the use of laser generated ultrasound and piezoelectric detection. Because of the high temperatures encountered and the rough surface texture, noncontact detection schemes are considered to be highly advantageous. Electromagnetic acoustic transducers (EMATS) capable of operating ∿800 °F have been obtained and are being evaluated as noncontact devices for measuring ultrasonic TOF in hot steel and aluminum. Initial results indicate sufficient sensitivity to detect laser generated ultrasonic pulses. Further efforts are currently underway to establish operating parameters for thermal mapping applications.

RELAXATION PHENOMENA IN GLASSY ALLOYS

The study of relaxation phenomena in glassy alloys was preceded by a theoretical and experimental treatment of the application of guided ultrasonic waves for the determination of the elastic moduli of melt-spun ribbons. The significant achievement of this research task was the determination of all the elastic moduli in thin ribbons, namely Young's and shear moduli, adiabatic compressibility, Poisson's ratio and the Debye temperature. This was made possible by successfully launching Lamb and shear horizontal waves in melt-spun ribbons that enabled determination of the transverse wave velocity in amorphous ribbons.

Isothermal annealing heat treatments below the glass transition temperature resulted in significant changes in the elastic moduli that can be correlated with structural and compositional relaxation processes occurring in the glassy state. Work is in progress to establish the kinetics of these phenomena and to identify the apparent mechanisms responsible for the behavior.

PHASE STABILITY IN EXTENDED SOLID SOLUTIONS OF RAPIDLY SOLIDIFIED ALUMINUM TRANSITION METAL ALLOYS

Laser generated-piezoelectrically detected ultrasonic waves are being used to characterize the stability of supercooled aluminum-transition metal alloys against thermal decomposition into equilibrium phases. In addition to ultrasonic characterization of the ribbons, x-ray, electrical resistivity and metallographic techniques are being employed. The isothermal decomposition kinetics were determined for Al-Mn alloys over a wide composition range. An unexpected dip in the elastic properties for the low alloy concentration was revealed. The behavior of the eleastic properties were corroborated by x-rays and electrical resistivity measurements. A similar behavior was observed in Al-Cr alloys prepared by rapid solidification. Work is in progress on a wide spectrum of alloy additions and compositions in order to systematically investigate the decomposition kinetics and the mechanism of thermal stability of extended solid solutions of this class of alloys. It is of interest as to what extent do these d-electron alloying additions affect the phase stability. The ultrasonic techniques employed in this research work were found feasible for dynamic, real time, monitoring of properties during processing.

CHARACTERIZATION OF MICROSTRUCTURALLY MODIFIED LAYERS BY MEANS OF RAYLEIGH SURFACE WAVES

This research is concerned with nondestructive characterization and gauging of microstructurally modified surface layers produced by means of electron-beam irradiation. Laser and piezoelectrically generated Rayleigh surface waves, at different frequencies, were used to probe the properties and thickness of modified surface layers on bulk samples of PdCuSi and different grades of steel. The depth of penetration of the Rayleigh waves was determined by their frequency. The magnitude of the Rayleigh wave velocity changes significantly when the depth of penetration exceeded the thickness of the modified surface layer. In addition to nondestructively gauging the layer thickness, we are attempting to determine the elastic moduli of both layer and substrate.

DYNAMIC CHARACTERIZATION OF THE PRECIPITATION HARDENING PROCESS IN ALUMINUM-COPPER ALLOYS BY MEANS OF ULTRASONIC RESONANCE

A noncontact electromagnetic resonance technique was used to study the precipitation hardening process in aluminum alloys due to formation of Guinier-Preston zones. The fundamental resonance of the bar samples was determined over a temperature range, between the ambient and

100°C, while the samples were subjected to aging heat treatment. The variation of the resonant frequency, and the elastic moduli, as a function of aging time correlated well with the change in the mechanical properties during aging. Work is in progress to determine the variation of the shear modulus during aging, thereby enabling calculation of the complete set of elastic properties. In addition, the changes of internal friction during the precipitation hardening process will be measured. From the variation of the elastic moduli as a function of aging time and temperature the kinetic parameters of the process can be established.

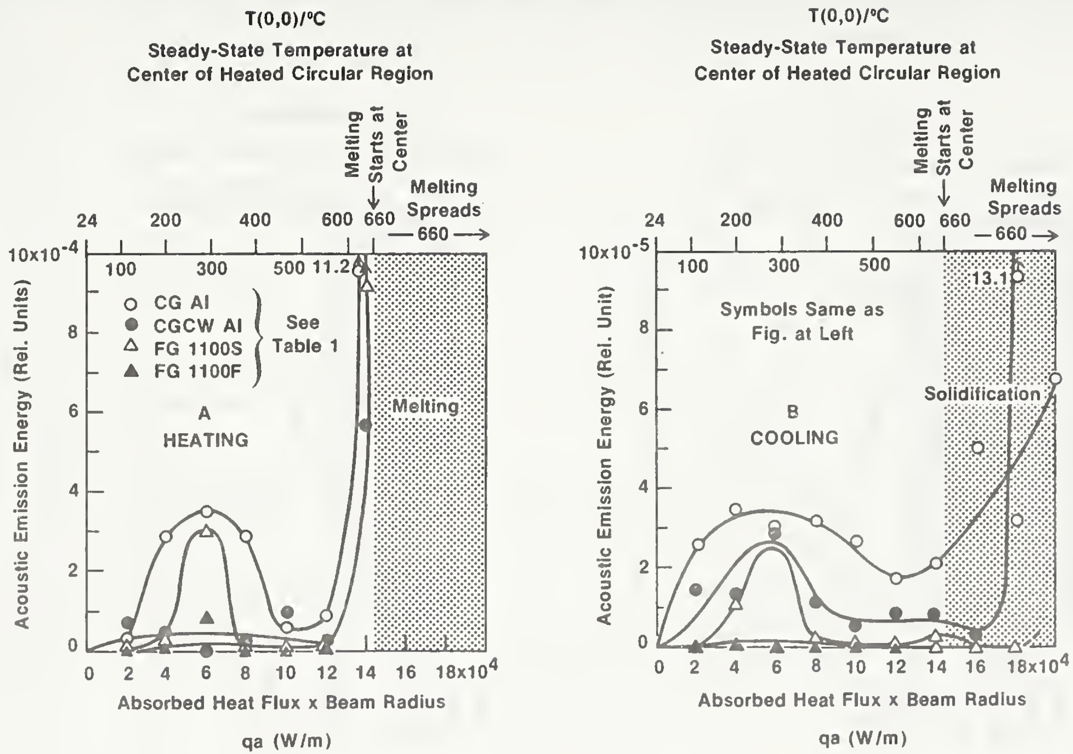

Figure 1. AE energy generated during surface heating and cooling in pure Al. FG represents fine grain and CG represents coarse grain (see Table 1). Data points an average of 4 for coarse grained Al and 2 for fine grained Al. Standard deviation is ±22% on cooling.

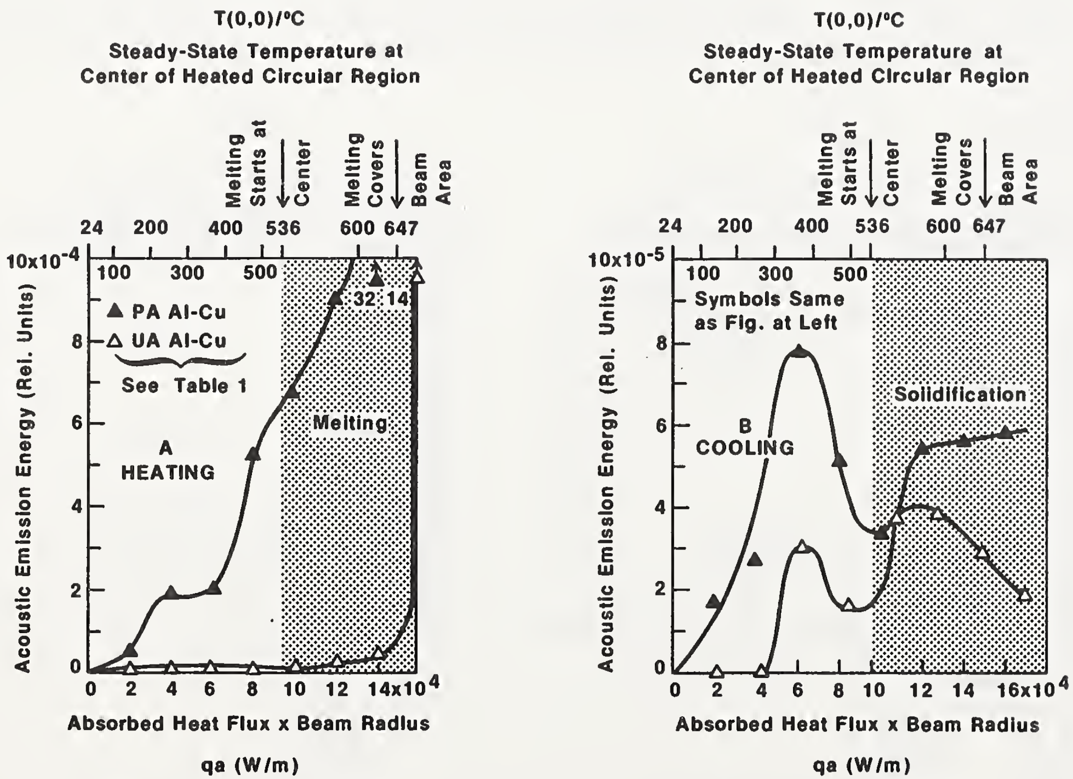

Figure 2. AE energy generated during surface heating and cooling at given qa level in solution-hardened Al–4.5 wt% Cu alloy (see Table 1). Data points an average of 4. Standard deviation is ±43% on cooling.

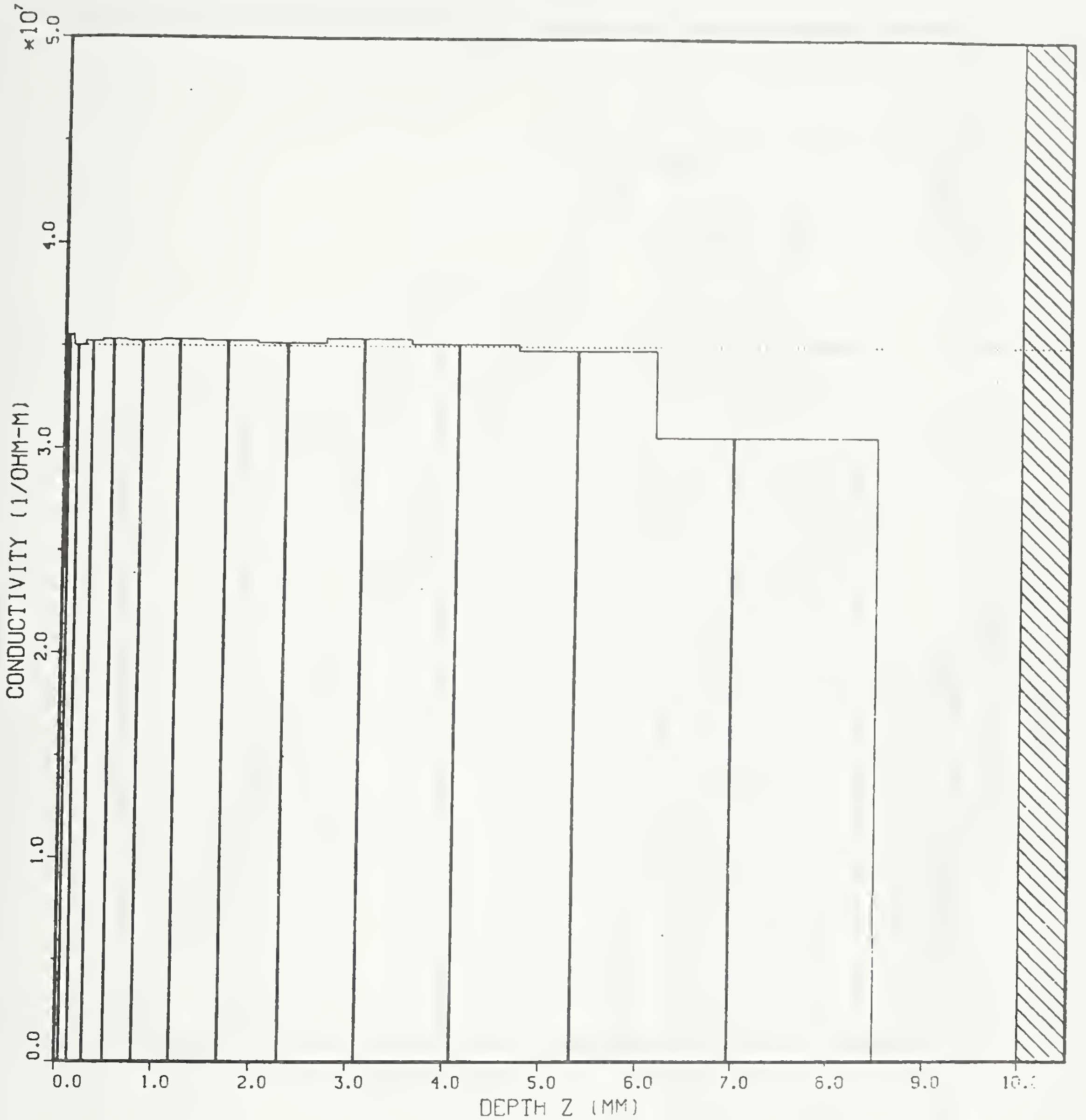

Figure 3. Plot of conductivity vs depth for the uniform slab case, based on uniformly distributing the conductance of each shell over its associated spacing. The input conductivity profile is indicated by the dotted line.

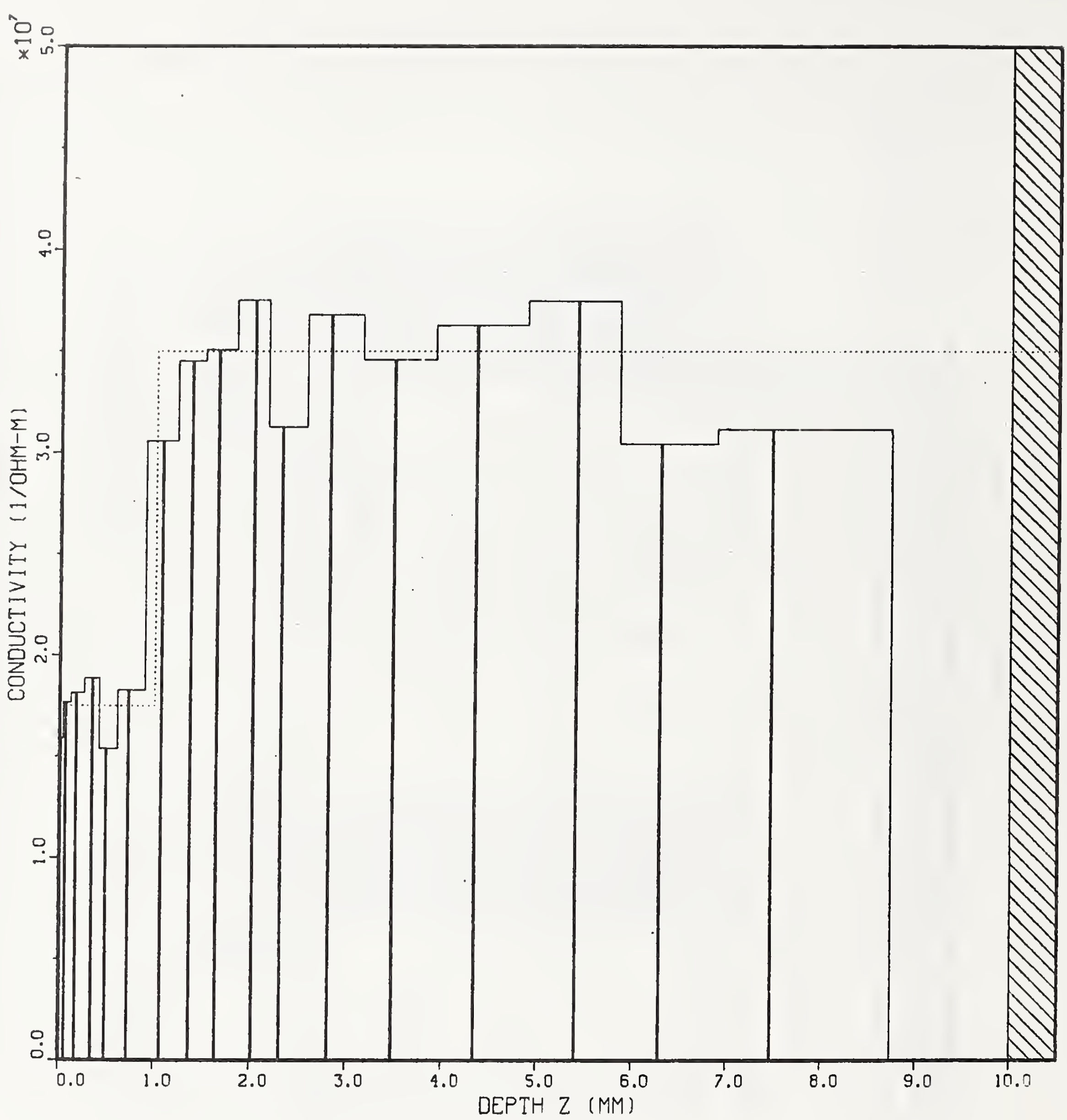

Figure 4. Plot of conductivity vs depth for the stepped conductivity case, based on uniformly distributing the conductance of each shell over its associated spacing. The input conductivity profile is indicated by the dotted line.

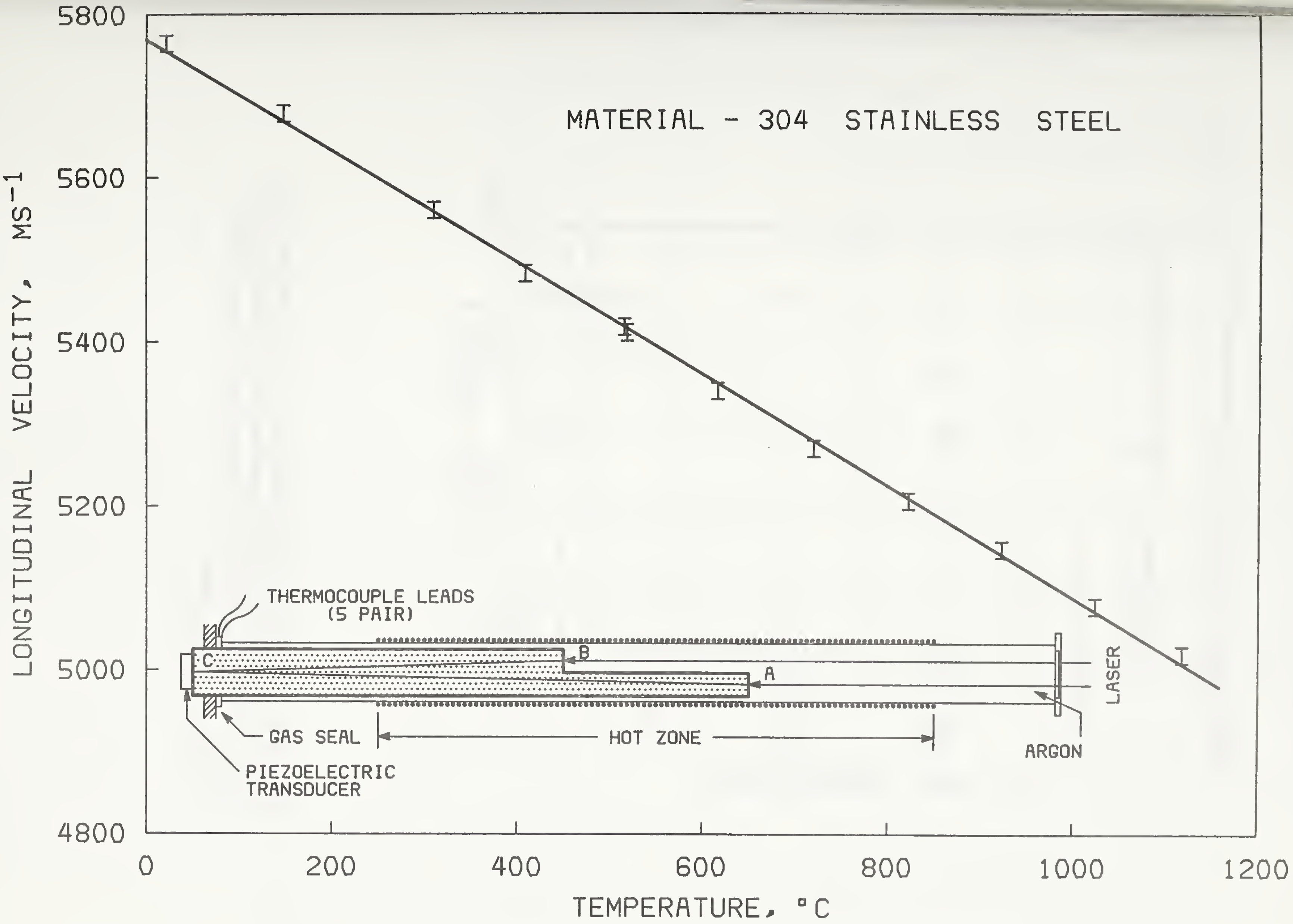

Figure 5. Calibration data for the velocity of a longitudinal wave as a function of temperature in steel. The specimen (inset) is a 24-inch long bar 2 inches in diameter notched at one end so that a laser beam can be focused at A or B to generate an ultrasonic wave. The arrival of the wave at C is detected with a piezoelectric transducer, giving the time-of-flight for path AC or BC. The difference is the time-of-flight for the 8-inch section that is at a uniform temperature in the hot zone and is used to compute the velocity.

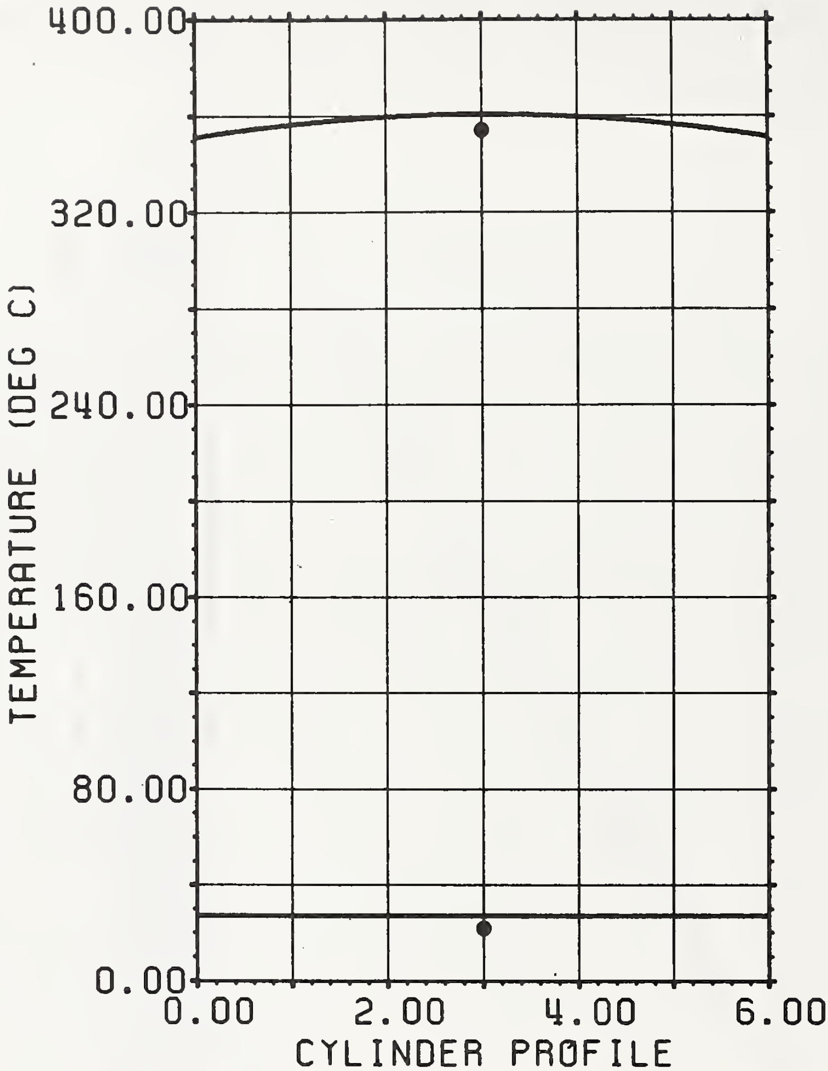

Figure 6. Ultrasonically measured radial temperature profile through a 6 inch diameter bar of 304 stainless steel. The black dots are thermocouple measurements of center temperature.

Corrosion of Electrodeposited Coatings in Hot Phosphoric Acid Environments
Electrochemical Society Meeting
Washington, DC
C. E. Johnson
October 1983

Corrosion Performance of Electrodeposited Metallic Glasses
Electrochemical Society Meeting
Washington, DC
D. S. Lashmore
October 1983

Reconstructing Internal Temperature Distributions from Ultrasonic Time-of-Flight Tomography and Dimensional Resonance Measurements
1983 IEEE Ultrasonics Symposium
Atlanta, GA
S. J. Norton, L. R. Testardi, and H. N. G. Wadley
October 1983

Ultrasonic Measurement of Solid/Liquid Interface Position during Solidification and Melting of Iron and Steel
American Society for Metals Fall Meeting
Philadelphia, PA
R. L. Parker
October 1983

Wear and Related Materials Degredation
Symposium on Industrial Materials Science
Oregon Graduate Center
Beaverton, OR
A. W. Ruff
October 1983

Convection-Induced Distortion of a Solid-Liquid Interface
TMS-AIME Fall Meeting
Philadelphia, PA
R. J. Schaefer
October 1983

Fluid Flow Effects in Electron Beam Surface Melting
TMS-AIME Fall Meeting
Philadelphia, PA
R. J. Schaefer
October 1983

Phase Equilibria in Gas Containing Metal-Metal Systems
American Society for Metals--AIME Fall Meeting
Philadelphia, PA
R. D. Shull
October 1983

Nondestructive Characterization of Rapidly Solidified Al-Mn Alloys
by Ultrasonic and Electrical Resistivity Methods
TMS/AIME Annual Meeting
Philadelphia, PA
J. J. Smith, M. Rosen, and H. N. G. Wadley
October 1983

ASM/NBS Alloy Phase Diagram Program
Oak Ridge National Laboratory
Oak Ridge, TN
K. J. Bhansali
November 1983

First Impressions May be Misleading with Micro-Indentation
Hardness Testing
Central Ohio Metallographic Society
Columbus, OH
P. J. Blau
November 1983

Phase Transitions of Solid Surfaces
Physics Department
Ohio State University
J. W. Cahn
November 1983

Advanced Materials Research at NBS
National Bureau of Standards
Gaithersburg, MD
D. S. Lashmore
November 1983

Rapid Solidification Microstructures and Precipitation of
Al-Mn Alloys
Materials Research Society Annual Meeting
Boston, MA
R. J. Schaefer
November 1983

The NACE-NBS Corrosion Data Program
LaQue Center for Corrosion Technology
Wrightsville Beach, NC
G. M. Ugiansky
November 1983

Corrosion Response of the Interface Tissue to 316L Stainless Steel,
Titanium Based Alloys and Cobalt Based Alloys
American Acadademy of Implant Prosthodontics
Chicago, IL
A. C. Van Orden
November 1983

Mechanisms of Microstructure Formation During Rapid Solidification
Center for the Joining of Materials
Carnegie-Mellon University
Pittsburgh, PA
W. J. Boettinger
December 1983

Metastable Phase Diagrams and Multicomponent Alloy Solidification
Alcoa Technical Center
Alcoa Center, PA
W. J. Boettinger
December 1983

NBS Crossed Cylinder Wear Testing
ASTM Workshop on Crossed Cylinder Wear Test Standard
Bal Harbor, FL
A. W. Ruff
December 1983

The Stochastic Nature of Ostwald Ripening Phenomena
Department of Metallurgical Engineering
Michigan Technological University
Houghton, MI
P. W. Voorhees
December 1983

New Insights into Ostwald Ripening Phenomena
Division of Applied Sciences
Harvard University
Cambridge, MA
P. W. Voorhees
January 1984

Metastable Features of Phase Diagrams
AIME Annual Meeting
Los Angeles, CA
W. J. Boettinger
February 1984

The Development of an Atmospheric Corrosion Probe
Meeting of National Acid Precipitation Assessment Program
Burlington, VT
E. Escalante
February 1984

Report on the Compilation of Existing Atmospheric Corrosion Data
Meeting of National Acid Precipitation Assessment Program
Burlington, VT
E. Escalante
February 1984

Rapid Solidification Research at NBS
COMAT Rapid Solidification Technology Meeting
Alexandria, VA
J. R. Manning
February 1984

Coarsening in Metallurgical Systems
Metallurgy Division
Naval Research Laboratories
Washington, DC
P. W. Voorhees
February 1984

Solute Segregation Following Rapid Solidification
Department of Metallurgical Engineering and Metals Science
Carnegie-Mellon University
Pittsburgh, PA
P. W. Voorhees
February 1984

Passivity and Pitting
Meeting of American Physical Society
Detroit, MI
U. Bertocci
March 1984

ASM/NBS Alloy Phase Diagram Program
ASM Washington Local Chapter
Bethesda, MD
K. J. Bhansali
March 1984

Metallurgy-based Approaches to Studying Fundamental Friction
and Wear Processes
Lehigh University
Bethlehem, PA
P. J. Blau
March 1984

Diffusion-Induced Grain Boundary Migration
Harvard University
Cambridge, MA
D. B. Butrymowicz
March 1984

Convection and Interface Instability During Alloy Solidification
Centre d'Etudes Nucleaires de Grenoble
Grenoble, France
S. R. Coriell
March 1984

Convection and Interface Instability During Alloy Solidification
Workshop on Solidification and Fluid Dynamics in the Earth's and the Space Laboratory
Aachen, Germany
S. R. Coriell
March 1984

Measuring the Rate of Corrosion of Reinforcing Steel in Concrete
Federally Coordinated Program on Bridge Maintenance and Corrosion Protection
McLean, VA
E. Escalante
March 1984

Thermal Charging and the Problem of Disbonding of Austenitic Cladding
WESTEC '84 Symposium on Fracture and Failure Analysis
Los Angeles, CA
C. G. Interrante
March 1984

Terminology for an Emerging ASTM Committee on Hydrogen Embrittlement
Meeting of ASTM Sub-Committee F-7.04 on Hydrogen Embrittlement Testing
Indian Wells, CA
C. G. Interrante
March 1984

Ni(II) Binding to Blood Serum Albumin
International Association for Dental Research
Dallas, TX
G. J. Mattamal
March 1984

Dimensional Instability of Metals
Institute for Materials Science Seminar
University of Connecticut, CT
R. S. Polvani
March 1984

Activities in ONR Tribology Program
DOD Lubrication Coordinating Meeting
Naval Research Laboratory
Washington, DC
A. W. Ruff
March 1984

Patterns in the Occurrence of the Brittle Topologically Close-Packed Phases: Al
The Metallurgical Society Topical Meeting on High Temperature Alloys: Theory and Design
Bethesda, MD
L. H. Bennett
April 1984

The Mystery of Alloys
George Mason University
Fairfax, VA
L. H. Bennett
April 1984

Resonance Methods
ASM Short Course on Modern Techniques of Microstructure
and Surface Analysis
Gaithersburg, MD
L. H. Bennett
April 1984

Analysis of Random Current Transients for the Study of
Localized Corrosion
National Association of Corrosion Engineers, Corrosion '84
New Orleans, LA
U. Bertocci
April 1984

Database Development Under the ASM/NBS Program on Alloy
Phase Diagrams
29th National SAMPE Symposium
Reno, NV
K. J. Bhansali
April 1984

New Challenges to the Understanding of the Liquid to Solid
Transformations in Metals and Alloys
American Physical Society
Washington, DC
W. J. Boettinger
April 1984

Thermosolutal Convection During Alloy Solidification
American Physical Society
Washington, DC
S. R. Coriell
April 1984

Corrosion Fatigue Behavior of Porous Coated Ti-6Al-4V Implant Materials
Second World Congress on Biomaterials
Washington, DC
A. C. Fraker
April 1984

TEM and STEM Applications
ASM Course on Modern Techniques of Microstructural and Surface
Analysis
Gaithersburg, MD
L. K. Ives
April 1984

Application of Synchrotron Radiation to Materials Science
at NBS--Topography and EXAFS
Lawrence Berkeley Laboratory
San Francisco, CA
M. Kuriyama
April 1984

X-ray Scattering and Other Synchrotron Techniques
American Society for Metals, Washington, DC Chapter
Gaithersburg, MD
M. Kuriyama
April 1984

Use of EXAFS to Study Passivity
National Association of Corrosion Engineers
New Orleans, LA
G. G. Long
April 1984

Kinetics of the Ni(II) Reaction with Human Serum Albumin
Second World Congress on Biomaterials
Washington, DC
G. J. Mattamal
April 1984

Progress Towards Understanding the Stress Corrosion Problem
National Association of Corrosion Engineers, Corrosion 84
New Orleans, LA
E. N. Pugh
April 1984

Microstructures of Supercooled Sub-Micrometer Aluminum-Copper
Alloy Powder
ASTM Symposium on Rapidly Solidified Powder Aluminum Alloys
Philadelphia, PA
S. D. Ridder
April 1984

Deconvolution and New Methods in One-Sided Time Series
Parts I, II, and III
Scientific Computing Division Series on New Computing Methods
NBS, Gaithersburg, MD
J. A. Simmons
April 1984

SEM Electron Channeling
ASM Course on Modern Techniques of Microstructural and Surface Analysis
Gaithersburg, MD
A. W. Ruff
April 1984

Effects of Porous Coatings on the Corrosion Behavior of
Co-Cr-Mo Material
Second World Congress on Biomaterials
Washington, DC
A. C. Van Orden
April 1984

Electrochemical Noise Studies of Passive Films
Electrochemistry Center Seminar
Case Western Reserve University
Cleveland, OH
U. Bertocci
May 1984

New Singularities in Surfaces
51st Statistical Mechanics Meeting
Rutgers University
J. W. Cahn
May 1984

Corrosion of Metals Underground
29th Annual Appalachian Underground Corrosion Short Course
West Virginia University
Morgantown, WV
E. Escalante
May 1984

X-ray Absorption Studies of the Roles of Cr and H in the Structure
of Oxide Films on Fe
International Congress on Metallic Corrosion
Toronto, Canada
G. G. Long
June 1984

Chemical and Electrochemical Aspects of SCC of Alpha Brass in
Aqueous Ammonia
9th International Congress on Metallic Corrosion
Toronto, Ontario, Canada
E. N. Pugh
June 1984

Wear Studies of Dual Phase Steel (Poster Session)
Gordon Research Conference on Tribology
New London, NH
A. W. Ruff
June 1984

Remarks on Slurry Erosion Testing (Panel)
ASTM Symposium on Slurry Erosion
Denver, CO
A. W. Ruff
June 1984

Acoustic Emission from Inhomogeneous Inclusions
AMD/ASME Symposium on Wave Propagation in Inhomogeneous Media
and Ultrasonic NDE
San Antonio, TX
J. A. Simmons and H. N. G. Wadley
June 1984

The NACE-NBS Corrosion Data Program
8th International Congress on Metallic Corrosion
Toronto, Canada
G. M. Ugiansky
June 1984

NMR and EXAFS of Ni-P Alloys
Gordon Research Conference on Physical Metallurgy
Andover, NH
L. H. Bennett
July 1984

Alloy Phase Diagram Database Development
Alcoa Technical Center
Alcoa Center, PA
K. J. Bhansali
July 1984

Differentiation Between Dominant Metal Wear Mechanisms by
Discrimination in Measurements of Subsurface Microstructural Features
The Technical Coordination Program (international cooperative program)
Machinery Health Monitoring Action Group
Gaithersburg, MD
P. J. Blau
July 1984

Applications of Microindentation in Tribology Research
ASTM/Int. Metallog. Soc. Symposium on Microindentation Hardness
Philadelphia, PA
P. J. Blau
July 1984

Mechanisms of Microstructure Formation During Rapid Solidification
Department of Metallurgical Engineering
Michigan Technological University
Houghton, MI
W. J. Boettinger
July 1984

Acoustic Emission Studies of Dislocation Motion and Microfracture
in Rapid Solidification in Al and Al-4.5% Cu
Review of Progress in Quantitative NDE
La Jolla, CA
R. B. Clough and H. N. G. Wadley
July 1984

The Martensitic Phase Transformation in TiNi Studied by Acoustic Emission
Review of Progress in Quantitative NDE
La Jolla, CA
M. Givishi, M. Rosen, and H. N. G. Wadley
July 1984

Fabrication of Microhardness Standard Reference Material
Microindentation Hardness Testing Symposium and Workshop
Philadelphia, PA
D. R. Kelley
July 1984

Sensor Needs for Materials Processing
Review of Progress in Quantitative NDE
La Jolla, CA
R. Mehrabian and H. N. G. Wadley
July 1984

Determination of Inhomogeneities of Elastic Modulus and Density Using Acoustic Dimensional Resonance
Review of Progress in Quantitative NDE
La Jolla, CA
L. R. Testardi, S. J. Norton, and T. Hsieh
July 1984

Modification of Material Surfaces by Directed Energy Sources
Department of Energy Meeting on Novel Methods of Materials Synthesis
Boulder, CO
R. J. Schaefer
August 1984

Electrochemical Noise Studies
Materials Science Seminar
Johns Hopkins University
Baltimore, MD
U. Bertocci
September 1984

Microanalytical Observation of the Diffusion Zone Created during Diffusion-Induced Grain Boundary Migration
American Society for Metals Fall Meeting
Detroit, MI
D. B. Butrymowicz
September 1984

Interaction of Composition and Stress
Institute for Theoretical Physics
University of California
J. W. Cahn
September 1984

Acoustic Emission Monitoring of Laser Drilling
In-Process Nondestructive Microstructure Characterization and
Process Control Symposium
ASM Metals Congress
Detroit, MI
R. B. Clough, H. N. G. Wadley, and R. J. Schaefer
September 1984

Microsegregation during Directional Solidification
Symposium on Fundamentals of Alloy Solidification Applied
to Industrial Processes
NASA Lewis Research Center
Cleveland, OH
S. R. Coriell
September 1984

The Influence of Thermal Processing on Fatigue Crack Initiation and
Propagation of Ti-4.5 Al-5 Mo-1.5Cr
Fifth International Conference on Titanium
Munich, Germany
A. C. Fraker
September 1984

Alloy Formation: DIGM, DIR, and Liquid Phase Sintering
American Society for Metals Fall Meeting
Detroit, MI
C. A. Handwerker
September 1984

In-Situ X-ray Topography of Solidification and Grain Growth
TMS-AIME Fall Meeting
Detroit, MI
M. Kuriyama
September 1984

Synchrotron Radiation Topography
12th Annual Materials Science Conference
Argonne National Laboratory
Chicago, IL
M. Kuriyama
September 1984

Sensors for Advanced Materials Processing
In-Process Nondestructive Microstructure Characterization and
Process Control Symposium
ASM Metals Congress
Detroit, MI
R. Mehrabian and H. N. G. Wadley
September 1984

Biaxial Microcreep of Berylium
JOWOG 22-Berylium Subwog Meeting AWRE
Aldermaston, Berkshire, United Kingdom
R. S. Polvani
September 1984

Controlled Rapid Solidification by Electron Beam Surface Melting
American Society for Metals Fall Meeting
Detroit, MI
R. J. Schaefer
September 1984

Nondestructive Characterization of Rapid Solidification Processes
ASM Metals Congress
Detroit, MI
J. J. Smith, L.-C. Fiaut, M. Rosen, and H. N. G. Wadley
September 1984

Seminars for Staff and Guests

The Sources of Defects in InP/InGaAsP Light Emitters
S. Mahajan
Carnegie-Mellon University
October 1983

Influence of Noble Metal Additions on the HE Susceptibility of
AISI 4130 Steel
B. E. Wilde
U.S. Steel Corp.
October 1983

Review of Processes for the Deposition of Chromium-Nickel Alloys
C. Chisholm
Paisley College of Technology, Scotland
October 1983

Intergranular Corrosion: Chemical and Structural Effects
M. Froment
University of Paris, France
October 1983

Adhesion Testing
J. W. Dini
Lawrence Livermore National Laboratory
October 1983

Metal Matrix Composites
R. Arsenault
University of Maryland
November 1983

Effects of Magnetic Fields on Electrolysis and on Electrodeposition of Metals
J. Dash
Portland State University
November 1983

Interdiffusion Studies in Metallic Glasses using Compositionally Modulated Thin Films
A. L. Greer
Harvard University
November 1983

Properties of Ultra-Thin Single Crystal Films of Iron
James J. Krebs
Naval Research Laboratory
November 1983

Fluid Flow in Weld Pools
L. A. Bertram
Sandia National Laboratories
February 1984

Electrodeposition of Alloys for Electronics Industry
J. Cl. Puippe
Werner Flühmann Ag, Switzerland
February 1984

Paper Abrasivity
R. G. Bayer
International Business Machines Corp.
March 1984

Point Defects in GaAs: Bulk and Surface Acoustic Wave Studies
M. Brophy
University of Illinois
March 1984

Nanoindentation Hardness Testing
W. C. Oliver
East Hartford, CT
March 1984

Pattern Formation during Directional Solidification
Gregory Dee
University of California
April 1984

An Overview of the Wear Research Project at John Deere
P. A. Swanson
Deere & Company Technical Center
April 1984

The Behavior of Precious Metal Electrodeposits as Oxygen Evolution Electrocatalysts in Acid Solutions
G. Fisher
International Nickel Corporation
April 1984

Nondestructive Characterization and Evaluation of Metal Matrix Composites via EMAT Scanning
H. M. Frost
EHV-Weidmann Industries
May 1984

Multi-Frequency Eddy Current Measurement of Depth of Case Hardening in Automotive Parts
C. H. Stephan
Ford Motor Company
May 1984

Thermodynamics: A Unifying Approach to Materials Science
T. I. Barry
Division of Materials Applications, National Physical Laboratory
June 1984

Grain Boundary Segregation Temper Embrittlement in 2-1/4 Cr-1 Mo Steels
G. Gage
Atomic Energy Research Establishment, England
July 1984

Electron Microscopy of Aluminum Matrix Composites
S. R. Nutt
Arizona State University
August 1984

The NRL Program in Metal Matrix Composites
C. Sanday
Naval Research Laboratory
August 1984

Properties and Potentialities of Artificial Modulated Materials
J. Hilliard
Northwestern University
August 1984

Geometrical and Thermodynamical Aspects of Short Range Order in Alloys
D. Gratias
University of Paris, France
September 1984

Electrochemistry in Non-Aqueous Solvents
Unconventional Mechanisms of Conductivity in Non-Aqueous and Mixed Solvents
E. Gileadi
University of Tel Aviv, Israel
September 1984

Technical and Professional Committee Participation and Leadership

American Association for Crystal Growth
S. R. Coriell and R. L. Parker, Executive Committee

American Association for the Advancement of Science
G. G. Long, M. Kuriyama, and G. M. Ugiansky, Members

American Chemical Society
G. J. Mattamal, Member

American Electroplaters Society
C. E. Johnson and D. S. Lashmore, Members

Alloy Deposition Committee
D. S. Lashmore, Member

Alloy Deposition Handbook
D. S. Lashmore, Editor

American Institute of Metallurgical Engineers
Alloy Phases Committee of the Metallurgical Society
L. H. Bennett and K. J. Bhansali, Members

Corrosion and Environmental Effects Committee of the Metallurgical Society
E. N. Pugh, Member

Solidification Committee of the Metallurgical Society
R. J. Schaefer, Chairman
W. J. Boettinger, S. R. Coriell, S. C. Hardy, J. R. Manning, and S. D. Ridder, Members

American Society of Lubrication Engineers
Wear Committee
K. J. Bhansali and L. K. Ives, Members

American Society of Mechanical Engineers
Ad Hoc Working Group on Acoustic Emission, Section 5
J. A. Simmons, Member

NDE for Process Control Committee
H. N. G. Wadley, Chairman

Research Committee on Lubrication (Hardfacing and Coatings)
K. J. Bhansali, Member

Tribology Division, Executive Committee
A. W. Ruff

American Society of Mechanical Engineers/American Society for Metals
Wear of Materials Conference Steering Committee
A. W. Ruff, Member and 1985 Vice-Chairman

American Society for Metals
Atomic Transport Committee
J. R. Manning, Member

Bulletin of Alloy Phase Diagrams
L. H. Bennett, Editor
D. J. Kahan and M. E. Read, Associate Editors
R. V. Drew, Editorial Assistant

Education Committee
C. G. Interrante, Member

Electronic Materials Committee
L. R. Testardi, Member

Metals Information Committee
J. S. Sims, Member

Nondestructive Testing Committee
H. N. G. Wadley, Member

Process Modeling Committee
J. R. Manning, Member
Reliability Analysis and Metal Processing Committee
M. Rosen, Member

International Council for the ASM/NBS Program for Alloy Phase Diagrams
L. H. Bennett and K. J. Bhansali, Members

Washington, DC Chapter
P. J. Blau, Treasurer, Executive Committee
A. C. Van Orden, Year Chairperson, Executive Committee
A. C. Fraker, Member
C. G. Interrante, Awards Committee, Member

American Society for Testing and Materials
A1: Steel, Stainless Steel, Related Alloys; Castings
R. L. Parker, Member

B2: Nonferrous Metals and Alloys
S. D. Ridder, Member

B5: Copper and Copper Alloys
M. E. Read and L. J. Swartzendruber, Members

B7: Light Metals and Alloys; Aluminum Alloy Ingots and Castings
W. J. Boettinger and R. D. Shull, Members

B8: Electrodeposited Coatings
C. E. Johnson and D. S. Lashmore, Members

B08: Metallic and Inorganic Coatings
C. G. Interrante, C. E. Johnson, and D. S. Lashmore, Members

B08.01: Terminology, Editing Public Relations and Metrication
WG.05: D. S. Lashmore, Metrication Chairman

B08.02: Substrate Preparation
C. G. Interrante and D. S. Lashmore, Members

B08.03: Decorative Copper, Nickel, Chromium, and
Nickel-Chromium Coatings
WG: Electrodeposited and Electroless Black
Coatings for Solar Use
D. S. Lashmore, Member

B08.04: Zinc and Cadmium Coatings
D. S. Lashmore Member

B08.05: Coatings of Tin, Lead, and Their Alloys
D. S. Lashmore, Member

B08.06: Chemical Conversion Coatings
D. S. Lashmore, Subcommittee Chairman

B07.07.09: Conversion Coatings on Aluminum
D. S. Lashmore, Chairman

B08.10.03: General Test Methods for Microhardness
C. E. Johnson, Liaison to E04

B9: Metal Powders and Metal Powder Products
J. R. Manning, Member

D32: Catalysts
A. J. McAlister, Member

E04: Metallography
P. J. Blau and L. J. Swartzendruber, Members

E04: Task Group on Microhardness Testing
P. J. Blau, Member

E04.03: Phase Diagrams Subcommittee
P. J. Blau, Member

E7: Nondestructive Testing
L. H. Bennett and L. J. Swartzendruber, Members

E7.04: Acoustic Emission
J. A. Simmons and R. B. Clough, Members

Joint Task Group on Acoustic Emission; System Calibration
J. A. Simmons, Chairman

E9: Fatigue
J. A. Simmons, Member

Task Group 3 on Residual Stress of Effect in Fatigue
J. A. Simmons, Member

E9.03: Fatigue of Composite Materials
J. A. Simmons, Member

E10: Nuclear Technology Applications
C. G. Interrante, Member

E10.02: Nuclear Materials, Components and Environmental Effects
C. G. Interrante, Member

E24: Fracture Testing
J. H. Smith, Member
C. G. Interrante, Member of Executive Committee

E24.05: Terminology for Fracture Testing
C. G. Interrante, Chairman

E38: Resource Recovery
J. G. Early, Member-at-Large, and Member of Executive Committee

E38.02: Ferrous Metals Resource Recovery
J. G. Early, Chairman

E42: Surface Analysis
G. G. Long, A. J. McAlister, L. H. Bennett, and L. J. Swartzendruber, Members

F4: Medical and Surgical Materials and Devices
A. C. Fraker and A. W. Ruff, Members

F4/G1: Joint Section on Corrosion of Implants
A. C. Fraker, Co-Chairperson

F7.04: Hydrogen Embrittlement Testing
C. G. Interrante, Chairman, Task Group on Terminology

G01: Corrosion of Metals
U. Bertocci, C. G. Interrante, E. N. Pugh and
G. M. Ugiansky, Members

G01.06: Stress Corrosion Cracking and Corrosion Fatigue
C. G. Interrante, E. N. Pugh and G. M. Ugiansky, Members

G01.10: Corrosion in Soils
E. Escalante, Member

G01.10: Task Group on Electrochemical Polarization
Techniques for Measurement of Corrosion Rates in Soils
E. Escalante, Member

G01.11: Electrochemical Measurements in Corrosion Testing
U. Bertocci, Member

G01.99: Standing Committee on Liaison
E. N. Pugh, Chairman

G2: Erosion and Wear
A. W. Ruff, Executive Committee (Past Chairman)
K. J. Bhansali, P. J. Blau and L. K. Ives, Members

G2.2: Solid Particle Erosion
A. W. Ruff, Task Group Leader
K. J. Bhansali, Member

G2.3: Wear
K. J. Bhansali, P. J. Blau, L. K. Ives and
A. W. Ruff, Members

G2.91: Terminology and Definitions
P. J. Blau, Chairman
L. K. Ives, Member

G2.95: Honors and Awards
L. K. Ives, Chairman

ASTM Standing Committee on Terminology
C. G. Interrante, Technical Committee Representative
P. J. Blau, Member

ASTM Coordinating Group on Terminology for Environmental Efforts
C. G. Interrante, Convener

ASTM Coordinating Group on Terminology for Tribology
P. J. Blau, Chairman

Applied Mechanics Review
R. B. Clough, Member, Review Staff

Army Research Office
Materials Research Evaluation Committee
L. R. Testardi, Member

Case Western Reserve University, Materials Research Laboratory, NSF Visiting Committee
E. N. Pugh, Member

Department of Commerce Space Commercialization Committee
L. R. Testardi, Member

Drexel University
Materials Science Department Evaluation Committee
L. R. Testardi, Member

Electrochemical Society
D. S. Lashmore, Member and Secretary-Treasurer

Editorial Committee
U. Bertocci, Member

Electrodeposition Division
D. S. Lashmore, Secretary-Treasurer

Federation of Materials Societies
U. Bertocci, S. R. Coriell and G. M. Ugiansky, Trustees

Awards Committee
G. M. Ugiansky, Chairman

Institute of Metal Finishing
D. S. Lashmore, Member

International Association for Dental Research
G. J. Mattamal, Member

International Institute of Welding
Commission XV--Fundamentals of Design and Fabrication for Welding
J. H. Smith, Member

International Journal of Crystal Growth
R. L. Parker, Deputy Principal Editor, Editorial Board

International Journal of Diffusion and Defect Data
D. B. Butrymowicz, Advisory Board Member

International Powder Metallurgy Society (Planseeberichte
fur Pulvermetallurgie, Austria)
J. G. Early, Member

International Society of Electrochemistry
Corrosion Division
U. Bertocci, Co-Chairman

International Standards Organization
TC107: Metallic and Other Non-organic Coatings
D. S. Lashmore, Delegate

1: Terminology
D. S. Lashmore, Delegate

2: Methods of Inspection and Coordination
of Test Methods
D. S. Lashmore, Delegate

3: Electrodeposited Coatings and Related Finishes
D. S. Lashmore, Delegate

7: Corrosion Tests
D. S. Lashmore, Delegate

TC156: Corrosion of Metals
G. M. Ugiansky, Delegate

2: Stress Corrosion
G. M. Ugiansky, Delegate

TC164: Medical Testing

1. Terminology
C. G. Interrante, Delegate

Maryland Institute of Metals
W. J. Boettinger, Executive Board Member

Materials Science and Engineering
L. H. Bennett, Associate Editor

Mechanical Failures Prevention Group
Committee on Mechanisms of Failure
J. G. Early, Chairman

National Academy of Science--National Research Council
Committee on Line Spectra of the Elements
J. S. Sims, Member

National Aeronautics and Space Administration, Fluid Flow Working Group
    S. R. Coriell, Member

Committee on Fuel Cell Materials Technology in Vehicular Propulsion
    U. Bertocci, Liaison Representative

National Association of Corrosion Engineers
    G. M. Ugiansky, Director, ex officio, Board of Directors

    Government Affairs Committee
    G. M. Ugiansky, Chairman

    Research Committee
    E. N. Pugh, Member

    Standing Committee on Technology Assessment
    J. L. Mullen, Member

        T10: Underground Corrosion Control
            E. Escalante, Member

Office of Energy-Related Inventions
    J. G. Early, Reviewer of Invention Disclosures

Read Research Conferences
    Organizing Committee
    D. S. Lashmore, Member

Society of Automotive Engineers
    Committee on Automotive Trim
    D. S. Lashmore, Invited Member

Society of Automotive Engineers/American Society of Testing and Materials Unified Numbering System for Metals and Alloys
    L. H. Bennett, NBS Representative

Society for Biomaterials Standards
    A. C. Fraker, Chairperson, Representative

Society for Experimental Stress Analysis
    Residual Stress Committee
    C. J. Bechtoldt, Member

The Metals Properties Council, Inc.
    Task Group on Corrosion Fatigue Testing
    E. N. Pugh, Member

U.S. Civil Service Examiners for Metallurgist
    Interagency Board
    J. G. Early, Chairman

U.S. Department of Transportation
Technical Hazardous Liquids Pipeline Safety Standards Committee
J. H. Smith, Member

Versailles Advanced Materials and Standards
Subcommittee on Wear
A. W. Ruff, Co-Chairman

Welding Research Council
Committee on Hardfacing and Wear
K. J. Bhansali, Member

Pressure Vessel Research Committee
C. G. Interrante, Member

PVRC Subcommittee on Hydrogen Effects
C. G. Interrante, Member

Publications

Bhansali, K. J. Hardfacing and wear, Chapter in Metals Handbook, Vol. 6. Metals Park, OH: American Society for Metals; 1983. 769.

Butrymowicz, D. B.; Piccone, T. J.; Manning, J. R.; Newbury, D. E. Color metallography of diffusion-induced grain boundary migration in Cu-Zn and Cu-As alloys. Metallography 16: 349; 1983.

Cahn, J. W.; Murray, J. L. Comment on "A new critical point in the vicinity of the freezing temperature of K_2C_s." Phys. Rev. Let. 51: 1493; 1983.

Clough, R. B.; Wadley, H. N. G. Wadley; Mehrabian, R. Heat flow-acoustic emission-microstructure correlations in rapid surface solidification, in Lasers in materials processing, E. A. Metzbower, ed. Metals Park, OH: Amer. Soc. Metals; 1983.

Coriell, S. R., Boisvert, R. F.; Mickalonis, J. I.; Glicksman, M. E. Morphological and convective instabilities during solidification. Adv. Space Res. 3: 95; 1983.

Icluda, N.; Sato, T.; Linzer, M. Imaging the nonlinear ultrasonic parameter of a medium. Ultrasonic Imaging 5: 295; 1983.

Kruger, J.; Long, G. G.; Kuriyama, M.; Goldman, A. I. Structural studies of passive films using surface EXAFS, in Passivity of metals and semiconductors. M. Froment, ed. Amsterdam, New York, NY: Elsevier; 1983. 163.

Long, G. G.; Kruger, J.; Kuriyama, M. Ex-situ and in-situ samples and chambers for the study of passive films using surface EXAFS, in Passivity of metals and semiconductors. M. Froment, ed. Amsterdam, New York, NY: Elsevier; 1983. 139.

Long, G. G.; Kruger, J.; Black, D. R.; Kuriyama, M. Structure of passive films on iron using a new surface-EXAFS technique. J. Interfacial and Electroanal. Chem. 150: 603; 1983.

Long, G. G.; Kruger, J.; Black, D. R.; Kuriyama, M. EXAFS study of the passive film on iron. J. Electrochem. Soc. 130: 240; 1983.

McAlister, A. J.; Kahan, D. J. The Al-Sn system. Bull. of Alloy Phase Diagrams 4: 410; 1983.

Mebar, Y.; Shechtman, D. On the adibatic shear of Ti-6Al-4V ballistic targets. Matl. Sci. and Eng. 58: 181; 1983.

Murray, J. L. The Ti-Ag (titanium-silver) system. Bull. of Alloy Phase Diagrams 4(2): 178; 1983.

Murray, J. L. The Al-Ga (aluminum-gallium) system. Bull. of Alloy Phase Diagrams 4(2): 183; 1983.

Murray, J. L. The aluminum-indium system. Bull. of Alloy Phase Diagrams 4(3): 271; 1983.

Murray, J. L. The titanium-gold system. Bull. of Alloy Phase Diagrams 4(3): 278; 1983.

Murray, J. L. The titanium-cadmium system. Bull. of Alloy Phase Diagrams 4(4): 399; 1983.

Murray, J. L. The aluminum-sodium system. Bull. of Alloy Phase Diagrams 4(4): 407; 1983.

Murray, J. L. Titanium binary alloy phase diagram compilation. Letter report to Office of Naval Research, December 1983.

Norton, S. J. Generation of separate density and compressibility images in tissue. Ultrasonic Imaging 5(3): 240; 1983.

Perepezko, J. H.; Boettinger, W. J. Use of metastable phase diagrams in rapid solidification, in alloy phase diagrams. Bennett, L. H.; Massalski, T. B.; Giessen, B. C., eds. Proceedings of Materials Research Society symp. 19. New York, NY: Elsevier North Hollard Publishing Co.; 1983. 223.

Polvani, R. S.; Ruff, A. W.; Strutt, P. R. A mechanism for metalloid strengthening of Udimet 700. J. Materials Science Letters 3: 287; 1983.

Scruby, C. B.; Rusbridge, K.; Wadley, H. N. G. Origin of acoustic emission in aged Al-Zn-Mg alloys: Part I, The basic ternary alloy. Mat. Sci. and Eng. 59: 151; 1983.

Shechtman, D.; Swartzendruber, L. J. Metastable phases in rapidly solidified aluminum-rich Al-Fe alloys. Bennett, L. H.; Massalski, T. B.; Giessen, B. C., eds. Proceedings of the Materials Research Society; 1982 November; Boston, MA, in Alloy Phase Diagrams, Vol. 19. New York, NY: North Holland; 1983. 265.

Shull, R. D. Phase diagram sample preparation. Bull. of Alloy Phase Diagrams 4(1): 5; 1983.

Swartzendruber, L. J. The Fe-Ru (iron-ruthenium) system. Bull. of Alloy Phase Diagrams 4(2): 155; 1983.

Swartzendruber, L. J. The Fe-Os system. Bull. of Alloy Phase Diagrams 4(4): 396; 1983.

Wadley, H. N. G.; Mehrabian, R. Acoustic emission for in-process monitoring and microstructure control, in Nondestructive methods for material property determination. C. O. Ruud and R. Green, eds. New York, NY: Plenum Press; 1983.

Wadley, H. N. G.; Norton, S. J.; Biancaniello, F. S.; Mehrabian, R. Ultrasonic measurement of internal temperature distribution, in Proceedings of the 1983 American Society for Metals symposium on NDE application and materials processing; 1983 October 3-4; Philadelphia, PA.

Wadley, H. N. G.; Rusbridge, K.; Scruby, C. Origin of acoustic emission in Al-Zn-Mg alloys: Part II, The Cu containing quarternary alloys. Mat. Sci. and Eng. 59: 169; 1983.

Wadley, H. N. G.; Scruby, C. B. Elastic wave radiation from cleavage crack extension. Int. J. Fracture 111; 1983.

Watson, R. E.; Bennett, L. H. Disorderly crystal structures in transition metal rich-metalloid alloys: Implications for glass formation. Scr. Metall. 17: 827; 1983.

Watson, R. E.; Bennett, L. H.; Goodman, D. A. A d-band bonding theory of the relative solubilities of transition metal alloys. Acta. Metall. 31: 1285; 1983.

Watson, R. E.; Bennett, L. H. The thermodynamic and physical modeling of alloy phase diagrams. J. Mater. Educ. 5: 635; 1983.

Beggs, D. V.; Hahn, M. T.; Pugh, E. N. Recent observation on the propagation of stress-corrosion cracks and their relevance to proposed mechanisms of SCC, in Hydrogen embrittlement and stress corrosion cracking. R. Gibala and R. F. Hehemann, eds. Metals Park, OH: American Society for Metals; 1984. 181.

Bertocci, U.; Mullen, J. L.; Ye, X-Y. Electrochemical noise measurements for the study of localized corrosion and passivity breakdown, in Passivity of metals and semiconductors. M. Froment, ed. Amsterdam: Elsevier Science Publishers; 1984. 229.

Bertocci, U.; Pugh, E. N. Chemical and electrochemical aspects of SCC of alpha-brass in aqueous ammonia. Proceedings of the International congress on metallic corrosion, Vol. 1. Ottawa, Canada: National Research Council of Canada; 1984. 144.

Bertocci, U.; Thomas, F. I.; Pugh, E. N. Stress corrosion cracking of brass in aqueous ammonia in the absence of detectable anodic dissolution. Corrosion 40: 439; 1984.

Bertocci, U.; Ye, X-Y. An examination of current fluctuations during pit initiation in Fe-Cr alloys. J. Electrochemical Soc. 131: 1011; 1984.

Blau, P. J. Effect of heat treatment and electron beam surface melting on the friction and wear behavior of a Cu-12wt% Al alloy. Wear 94: 1; 1984.

Blau, P. J. The effect of flat-on-ring sample alignment on sliding friction break-in curves for aluminum bronze on 52100 steel. Wear 94: 201, 1984.

Blau, P. J. Investigation of the nature of micro-indentation hardness gradients below sliding contacts in five copper alloys worn against 52100 steel. J. of Materials Science 19: 1957, 1984.

Boettinger, W. J.; Coriell, S. R.; Sekerka, R. F. Mechanisms of segregation-free solidification. Mat. Sci. & Eng. 65: 27; 1984.

Boettinger, W. J.; Schaefer, R. J.; Biancaniello, F. S.; Shechtman, D. The effect of solidification velocity on the microstructure of Ag-Cu alloys. Met. Trans. 15A: 55; 1984.

Bond, T. L.; Yeske, R. A.; Pugh, E. N. Studies of stress-corrosion crack growth in Al-Zn-Mg alloys using the double torsion method, in Environment-sensitive fracture: evaluation and comparison of test methods, ASTM STP 821. S. W. Dean, E. N. Pugh, and G. M. Ugiansky, eds. Philadelphia, PA: American Society for Testing and Materials; 1984. 128.

Butrymowicz, D. B.; Newbury, D. E.; Turnbull, D.; Cahn, J. W. Diffusion-induced grain boundary migration in the Ag-Au system. Scripta Met. 18: 1005; 1984.

Coriell, S. R.; McFadden, G. B.; Boisvert, R. F.; Glicksman, M. E.; Fang, Q. T. Coupled convective instabilities at crystal-melt interfaces. J. Crystal Growth 66: 514; 1984.

Early, J. G.; Hime, H. L. An evaluation method for comparing domestic and foreign materials specifications. J. Testing and Evaluation 12(3): 125; 1984.

DeWit, R.; Interrante, C. Application of an elastic-plastic model to the use of small specimen strength ratio for measuring fracture toughness. Eng. Fracture Mech. 19(6): 1151; 1984.

Early, J. G. Recycling ferrous metals, Chapter on ferrous metals in Recycling, fuel and resource recovery: economic and environmental factors. M. Grayson, ed. New York, NY: John Wiley and Sons; 1984. 124.

Early, J. G.; Harne, D. E. Metallographic analysis and mechanical characterization of API 5LX-70 weldments. Fitness-for-service criteria for pipeline girth-weld quality. Welding Research Council Bulletin No. 296; 1984. 64.

Eitzen, D. G.; Wadley, H. N. G. Acoustic emission: Establishing the fundamentals. J. Res. Nat. Bur. Stand. (U.S.). 89(1): 75; 1984 January-February.

Glicksman, M. E.; Voorhees, P. W. Ostwald ripening and relaxation in dendritic structures. Met. Trans. 15: 995; 1984.

Interrante, C. Standard terminology related to fracture testing, ANSI/ASTM E616-82E1, in Annual book of ASTM standards 03.01. Philadelphia, PA: American Society for Testing and Materials; 1984.

Interrante, C. G.; Low, S. R.; Early, J. G.; Dancer, D. Observations of the April 8, 1979 railroad accident at Crestview, Florida. Nat. Bur. Stand. (U.S.) NBSIR 84-2858; 1984 April.

Ives, L. K.; Peterson, M. B. Solid lubrication of steel by SbSbS4. Shives, T. R.; Peterson, M. B., eds. Proceedings of 37th meeting of the mechanical failure prevention group: mechanical properties, performance, and failure modes of coatings; 1983 May 10-12; Gaithersburg, MD. Nat. Bur. Stand. (U.S.); New York, NY: Cambridge University Press; 1984. 208-219.

Johnson, C. E.; Mullen, J.; Lashmore, D. S. Corrosion tests of electrodeposited coatings resistant to boiling phosphoric acid, in Proceedings of the 37th meeting of the mechanical failure prevention group; 1983 May 10-12; Gaithersburg, MD. Nat. Bur. Stand. (U.S.); New York, NY: Cambridge University Press; 1984. 124-133.

Kahn, A. H. Impedance of a coil in the vicinity of a crack, in Review of progress in quantitative nondestructive evaluation, Vol. 3A. New York, NY: Plenum Press; 1984. 579.

Kahn, A. H. Impedance of a coil in the vicinity of a crack. J. Res. Nat. Bur. Stand. (U.S.). 89(1): 47; 1984 January-February.

Kelley, D.; Johnson, C. E.; Lashmore, D. S. Electroformed microhardness standards, Shives, T. R., Peterson, M. B., eds. Proceedings of the 37th meeting of the mechanical failure prevention group; 1983 May 10-12; Gaithersburg, MD. Nat. Bur. Stand. (U.S.); New York, NY: Cambridge University Press; 1984. 55-58.

Lashmore, D. S.; Weisshaus, I. Pulsed electrodeposition of nickel-chromium alloys, Shives, T. R., Peterson, M. B., eds. Proceedings of the 37th meeting of the mechanical failure prevention group; 1983 May 10-12; Gaithersburg, MD. Nat. Bur. Stand. (U.S.); New York, NY: Cambridge University Press; 1984. 39-48.

Lashmore, D. S. Pulsed electrodeposition of nickel chromium alloys, Proceedings of Interfinish '84; 1984 October 21-26; Jerusalem, Israel. Jerusalem, Israel: Interfinish; 1984.

McAlister, A. J. The Al-Pb system. Bull. of Alloy Phase Diagrams. 5: 69; 1984.

McAlister, A. J. The Al-Bi system. Bull. of Alloy Phase Diagrams. 5: 247; 1984.

McFadden, G. B.; Coriell, S. R.; Boisvert, R. F.; Glicksman, M. E. Asymmetric instabilities in buoyancy-driven flow in a tall vertical annulus. Phys. Fluids 27: 1359; 1984.

McHenry, H. H.; Cheng, Y. W.; Dewit, R.; King, R. B.; Read, D. T.; Early, J. G. Development of allowable flaw-size curves. Fitness-for-service criteria for pipeline girth-weld quality. Welding Research Council Bulletin No. 296; 1984.

Murray, J. L. Calculation of stable and metastable equilibrium diagrams of the Ag-Cu and Cd-Zn systems. Met. Trans. A. 15A: 261; 1984.

Murray, J. L.; McAlister, A. J. The Al-Si system. Bull. of Alloy Phase Diagrams 5: 74; 1984.

Norton, S. J.; Testardi, L. R.; Wadley, H. N. G. Reconstructing internal temperature distributions from ultrasonic time-of-flight tomography and dimensional resonance measurements. J. Res. Nat. Bur. Stand. (U.S.). 89(1): 65-74; 1984 January-February.

Parker, R. L. Ultrasonic measurement of solid/liquid interface position during solidification and melting of iron and steel, in Nondestructive evaluation: applications in materials processing. O. Buck and S. Wolf, eds. Metals Park, OH: Amer. Soc. Metals; 1984.

Peterson, M. B.; Ruff, A. W. A strategy for section of tribological coatings, Shives, T. R., Peterson, M. B., eds. Proceedings of 37th meeting of the mechanical failure prevention group: mechanical properties, performance, and failure modes of coatings; 1983 May 10-12; Gaithersburg, MD. Nat. Bur. Stand. (U.S.); New York, NY: Cambridge University Press; 1984. 137.

Rondelli, G.; Kruger, J.; Ritter, J. J.; Bertocci, U. A study of the film on austenitic stainless steel at the passive-transpassive transition, in Passivity of metals and semiconductors. M. Froment, ed. Amsterdam: Elsevier Science Publishers; 1984. 619.

Ruff, A. W. Wear and related materials degredation, chapter 10 in Industrial materials science and engineering. L. E. Murr, ed. New York, NY: M. Dekker; 1984. 299-351.

Shawker, T. H., Linzer, M.; Hubbard, V. S. Chronic pancreatitis: The diagnostic significance of pancreatic size and echo amplitude. J. Ultrasound in Medicine 3: 261; 1984.

Shechtman, D.; Kattamis, T. Z.; Biancaniello, F. S.; Boettinger, W. J. The microstructure of rapidly solidified NiAl-Cr quasibinary eutectic. Acta Met. 32: 749, 1984.

Shull, R. D.; Boyer, P. A.; Ives, L. K. and Bhansali, K. J. Plasma arc carbide coatings on titanium, in Plasma processing and synthesis of materials, Vol. 30. Proceedings of Mat. Res. Soc. Symp. Szekely, J.; Apelian, D., eds. New York, NY: Elsevier Scientific Publishing Co.; 1984. 297-301.

Simmons, J. A.; Wadley, H. N. G. Vector transducer calibration, in The review of progress in quantitative nondestructive evaluation, Vol. 3B, D. O. Thompson and D. E. Chimenti, eds. New York, NY: Plenum Press; 1984. 699-706.

Simmons, J. A.; Wadley, H. N. G. Theory of acoustic emission from phase transformations. J. Res. Nat. Bur. Stand. (U.S.). 89(1): 55-64; 1984 January-February.

Simmons, J. A.; Wadley, H. N. G. Theory of acoustic emission from inhomogeneous inclusions, in Homogeneous media and ultrasonic nondestructive evaluation, Vol. 62, G. C. Johnson, ed. ASME AMD; 1984. 51-59.

Slattery, P. W.; Smit, J.; Pugh, E. N. Use of a load-pulsing technique to determine stress-corrosion crack velocity, in Environment-sensitive fracture: evaluation and comparison of test methods, ASTM STP 821. S. W. Dean, E. N. Pugh, and G. M. Ugiansky, eds. Philadelphia, PA: American Society for Testing and Materials; 1984. 399.

Spal, R. Collimation of x-rays with cylindrically bent, asymmetrically cut crystals. Nucl. Instr. and Meth. 222: 193; 1984.

Spal, R.; Dobbyn, R. C.; Burdette, H. E.; Long, G. G.; Boettinger, W. J.; Kuriyama, M. NBS materials science beamlines at NSLS. Nuclear Instr. and Methods in Phys. Res. 222: 189; 1984.

Swartzendruber, L. J. The Fe-Ir system. Bull. of Alloy Phase Diagrams 5(1): 48; 1984.

Takagi, S.; Chow, L. C.; Brown, W. E.; Dobbyn, R. C.; Kuriyama, M. Parallel beam microradiography of dental hard tissue using synchrotron radiation and x-ray image magnification. Nuclear Instr. and Methods 222: 256; 1984.

Testardi, L. R.; Norton, S. J.; Hsieh, T. Determination of inhomogeneities of elastic modulus and density for one dimensional structures using acoustic dimensional resonance. J. Appl. Phys. 56: 2681; 1984.

Wadley, H. N. G.; Simmons, J. A.; Turner, C. Predictive modeling of quantitative acoustic emission waveforms, in The review of progress in quantitative nondestructive evaluation, Vol. 3B. D. O. Thompson and D. E. Chimenti, eds. New York, NY: Plenum Press; 1984. 683-697.

Watson, R. E.; Bennett, L. H. Transition metal alloy formation. The occurrence of topologically close packed phases. Acta Metall. 32: 477; 1984.

Watson, R. E.; Bennett, L. H. Model predictions of volume contractions in transition-metal alloys and implications for Laves phase formation. Acta Metall. 32: 491; 1984.

Balko, B.; Bucci, E.; Berger, R. L.; Swartzendruber, L. J.; Montemarano, J. X. Iron electronic structure in oxyhemoglobin and carboxy peptidase digested derivatives. J. Biochem. Biophys. Methods; in press.

Bendersky, L. A.; Boettinger, W. J. Cellular microsegregation in rapidly solidified Ag-15 wt% Cu alloys. Proceedings of the fifth international conference on rapidly quenched metals; in press.

Bendersky, L. A.; Schaefer, R. J.; Biancaniello, F. S.; Shechtman, D. Rapidly solidified Al-Cr alloys: Structure and decomposition behavior. Met. Trans.; in press.

Bennett, L. H.; Long, G. G.; Kuriyama, M.; Goldman, A. I. Local atomic structure in transition metal/metalloid glasses: Ni-P, in Structure and bonding in noncrystalline solids. G. E. Walrafen, ed.; in press.

Bennett, L. H.; McAlister, A. J. Vegard's law. Encyclopedia of Materials Science and Engineering; in press.

Bennett, L. H. Mossbauer techniques. Encyclopedia of Materials Science and Engineering; in press.

Bennett, L. H.; Watson, R. E. Patterns in the occurrence of the brittle topologically close-packed phases: Al, in High temperature alloys: theory and design. J. O. Stiegler, ed. Warrendale, PA: The Metall. Soc., AIME; in press.

Bertocci, U. Modeling of crack chemistry in the alpha brass-ammonia system. Gangloff, R. P., ed. Proceedings of TMS-AIME Symposium on localized crack chemistry and mechanics in environment sensitive cracking; 1983 October; Philadelphia, PA; in press.

Bertocci, U. Electrochemical principles of corrosion, in Encyclopedia of materials science and engineering. New York, NY: Pergamon Press; in press.

Bhansali, K. J.; Redmiles, D. F.; Murray, J. L.; Sims, J. S. Database development under the ASM/NBS program on alloy phase diagrams, in Proceedings of the 29th National SAMPE Symp.; 1984 April 3-5; in press.

Blau, P. J. Relationship between scratch and Knoop micro-indentation hardness and implications for abrasion of metals. Microstructural Science 12; in press.

Blau, P. J. Applications of microindentations in tribology research, in Microindentation hardness testing and applications. Blau, P. J. and Lawn, B. R., eds. Philadelphia, PA: ASTM Special Tech. Pub.; in press.

Blau, P. J.; Shives, T. R. Progress in micro-indentation hardness testing methods: Applications and interpretation of data. Metal Progress; in press.

Boettinger, W. J.; Shechtman, D.; Kattamis, T. Z.; Schaefer, R. J. The effect of rapid solidification velocity on microstructure and phase solubility extension in NiAl-Cr quasibinary eutectic. Steel, S.; Warlimont, H.; eds. Proceedings of the fifth international conference on rapidly quenched metals; 1984 April; in press.

Bomberger, H. B.; Meyn, D. A.; Fraker, A. C. Environmental effects on titanium and its alloys. Proceedings of the fifth international conference on titanium, 1984 September; in press.

Butrymowicz, D. B.; Newbury, D. E.; Piccone, T. J. Diffusion-induced grain boundary migration in the Cu-As system. Acta Met.; in press.

Butrymowicz, D. B.; Newbury, D. E. Microanalytical observation of the diffusion zone created during diffusion-induced grain boundary migration, in Interface migration and control of microstructure. Rath, B. B.; Pande, C. S., eds. Metals Park, OH: American Society for Metals; in press.

Dirnfeld, S. F.; Shechtman, D.; Mironi, J. Microstructure and mechanical properties of unidirectionally solidified Ni-Sn eutectic alloys. Mat. Sci. and Eng.; in press.

Dobbyn, R. C.; Yoo, K. C. Observations of dislocation images in surface reflection by synchrotron radiation topography. Applications of x-ray methods to materials science, U.S.-France Cooperative Science Seminar, S. Weissman, ed. New York, NY: Plenum Press; in press.

Escalante, E. Soil corrosion, in Encyclopedia of materials science and engineering. New York, NY: Pergamon Press; in press.

Escalante, E. Corrosion studies in municipal solid waste-fired and coal-fired boiler systems, Proceedings of the research review on the characterization of municipal solid waste; 1984 October; in press.

Escalante, E. Corrosion of materials used in steam generating boiler systems. Nat. Bur. Stand. (U.S.) NBSIR; in press.

Escalante, E. Measurement of corrosion rates of underground steel piles at Turcot Yard, Montreal, Canada, in Proceedings of the conference on the durability of steel piling in soil and coastal marine environments. Houston, TX: National Association of Corrosion Engineers; in press.

Escalante, E. The durability of steel piles in a natural sea water environment, in Proceedings of the conference on the durability of steel piling in soil and coastal marine environments. Houston, TX: National Association of Corrosion Engineers; in press.

Forty, A. J.; Danko; G.; Farabaugh, E. N.; Long, G. G. An EXELFS study of the short range order in films of various non-stoichiometric disordered silicon oxides; in press.

Gilmore, C. M.; Imam, M. A.; Fraker, A. C.; Yang, S. H.; Van Orden, A. C. The influence of thermal processing on fatigue crack initiation and propagation of Ti-4.5Al-5Mo-1.5Cr. Proceedings of the fifth international conference on titanium; 1984 September; Munich, Germany; in press.

Gvishi, M.; Rosen, M.; Wadley, H. N. G. Acoustic emission characterization of martensitic phase transformations in NiTi, in The review of progress in quantitative nondestructive evaluation, Vol. 4; in press.

Goldman, A. I.; Long, G. G.; Bennett, L. H.; Lashmore, D. S.; Kuriyama, M. Observations of two structurally distinct states in glassy Ni-P using EXAFS. Phys. Rev. Letters; in press.

Hahn, H.; Lare, P. J.; Rowe, R. H.; Fraker, A. C.; Ordway, F. Structure and mechanical properties of porous titanium alloy coatings applied by plasma arc. ASTM Special Technical Publication 859, 1984; in press.

Handwerker, C. A.; Butrymowicz, D. B.; Cahn, J. W. Alloy formation: DIGM, DIR, and liquid phase sintering. Proceedings of symposium on atomic transport in concentrated alloys and intermetallic compounds; Metals Park, OH: American Society for Metals; in press.

Handwerker, C. A.; Morris, P. A.; Coble, R. L.; Gabbe, D. R.; Howard, R. Characterization of low α-particle emitting ceramics. Proceedings of electronic components conference; 1984 May; New Orleans, LA; in press.

Hardy, S. C. Surface tension of liquid silicon. J. Crystal Growth; in press.

Interrante, C. G.; Low, S. R.; Brady, C. H.; Hicho, G. E. Metallurgical observations of 21 plate materials taken from seven tank cars involved in the April 18, 1979 railroad accident at Crestview, Florida. Nat. Bur. Stand. (U.S.) NBSIR; in press.

Ives, L. K. An extraction replica method for the study of surface films. Am. Soc. of Lubrication Eng.; in press.

Johnson, C. E.; Lashmore, D. S.; Mullen, J. Evaluation of electrodeposited protective coatings for use in phosphoric acid based fuel cells. Nat. Bur. Stand. (U.S.) NBSIR; in press.

Kaufman, M. J.; Fraser, H. L. Microstructural analysis of rapid solidification and undercooling in the Al-Ge system. Kear, B. H.; Giessen, B. C., eds. Proceedings of the MRS symposium on rapidly solidified metastable materials, Vol. 28; in press.

Kaufman, M. J.; Fraser, H. L. Importance of undercooling in the formation of non-equilibrium structures in the Al-Ge alloy system. Int. J. Rapid Solidification; in press.

Kaufman, M. J.; Fraser, H. L. Characterization of metastable crystalline phases in the Al-Ge alloy system. Acta. Met.; in press.

Kaufman, M. J.; Pearson, D. D.; Fraser, H. L. The use of convergent beam electron diffraction to determine local lattice distortions in Ni-base superalloys. Phil. Mag.; in press.

Kelley, D.; Johnson, C. E.; Lashmore, D. S. Fabrication and certification of electroformed microhardness standards, in Proceedings of International Metallurgical Society/American Society for Testing and Materials 17; 1984 July 15-18; Philadelphia, PA. Philadelphia, PA: ASTM STP; in press.

Kuriyama, M.; Boettinger, W. J. Asymmetric crystal topography with x-ray image magnification. Applications of x-ray methods to materials science, U.S.-France Cooperative Science Seminar, S. Weissman, ed. New York, NY: Plenum Press; in press.

Kuriyama, M.; Long, G. G. Extinction theory in x-ray topography. Applications of x-ray topography to materials science, U.S.-France Cooperative Science Seminar, S. Weissman, ed. New York, NY: Plenum Press; in press.

Lashmore, D. S. Electrodeposition on aluminum. Invited paper in Plating and Surface Finishing. 71(12); in press.

Lichter, B. D.; Cassagne, T. B.; Flanagan, W. F.; Pugh, E. N. Metallographic studies of transgranular stress corrosion cracking in copper-gold alloys. Microstructural Science; in press.

Long, G. G.; Kruger, J.; Kuriyama, M.; Black, D. R.; Farabaugh, E. N.; Sanders, D. M.; Goldman, A. I. EXAFS and near-edge study of the effect of Cr and H on the passive film on iron. J. Appl. Phys.; in press.

Long, G. G.; Revisz, A. G.; Kuriyama, M. X-ray absorption study of tantatum oxide films on silicon. J. Noncrystalline Matls.; in press.

McAlister, A. J.; Murray, J. L. The Al-Gc system. Bull. of Alloy Phase Diagrams; in press.

McAlister, A. J. The Al-Sb system. Bull. of Alloy Phase Diagrams; in press.

McAlister, A. J. The Al-As system. Bull. of Alloy Phase Diagrams; in press.

Mehrabian, R.; Wadley, H. N. G. Sensor needs for materials processing, in The review of progress in quantitative nondestructive evaluation, Vol. 4. New York, NY: Plenum Press; in press.

Murray, J. L. The titanium-zinc system. Bull. of Alloy Phase Diagrams 5(1); in press.

Murray, J. L. The aluminum-copper system. Internatl. Metals. Rev.; in press.

Murray, J. L.; Bhansali, K. J. Phase diagrams, in Encyclopedia of Science and Technology. New York, NY: McGraw Hill; in press.

Murray, J. L. Titanium binary alloy phase diagram compilation. Letter report to Office of Naval Research, September 1984; in press.

Nayeb-Hashemi, A. A.; Clark, J. B.; Swartzendruber, L. J. The Fe-Mg system. Bull. of Alloy Phase Diagrams; in press.

Norton, S. J. Iterative reconstruction techniques: Convergence as a function of spatial frequency. J. Opt. Soc. Amer.; in press.

Norton, S. J.; Linzer, M. Reconstructing a spatially-incoherent random source in the near field: Exact inversion formulas for circular and spherical arrays. J. Acoust. Soc. Amer.; in press.

Norton, S. J.; Wadley, H. N. G. Tomographic reconstruction of internal temperature, in The review of progress in quantitative nondestructive evaluation, Vol. 4. New York, NY: Plenum Press; in press.

Okamoto, H.; Massalski, T. B.; Swartzendruber, L. J.; Beck, P. A. The Au-Fe system. Bull. of Alloy Phase Diagrams; in press.

Polvani, R. S. Effects of silicon-vacancy clusters on the creep of NiAl, J. Res. Nat. Bur. Stand. (U.S.); in press.

Polvani, R. S.; Reeve, C. P.; Veale, R. C. An optical test method for measuring biaxial deformations. J. Testing and Evaluation (ASTM); in press.

Pugh, E. N. Stress-corrosion cracking, in Encyclopedia of materials science and engineering. Bever, M., ed. New York, NY: Pergamon Press; in press.

Pugh, E. N. Metallurgical aspects of corrosion, in Encyclopedia of materials science and engineering. Bever, M., ed. New York, NY: Pergamon Press; in press.

Pugh, E. N. Progress towards understanding the stress corrosion problem. Corrosion; in press.

Ridder, S. D.; Shechtman, D. Microstructure of supercooled sub-micrometer aluminum-copper alloy powder, in Rapidly solidified powder aluminum alloys. Philadelphia, PA: American Society for Testing and Materials; in press.

Rosen, M.; Klinker, H. Effect of hydrostatic pressure on the elastic properties of the rare earth-iron Laves phase compounds: equation of state and Grueneisen parameters. J. Phys. Chem. Solids; in press.

Rosen, M.; Ives, L.; Ridder, S. D.; Biancaniello, F. S.; Horowitz, E.; Mehrabian, R. Correlation between ultrasonic and hardness measurements in aged 2024 aluminum alloy. J. Matls. Sci.; in press.

Schaefer, R. J.; Shechtman, D.; Biancaniello, F. S. Rapid solidification microstructures and precipitation in Al-Mn alloys. Proceedings of Materials Research Society Symposium; 1983 November; Philadelphia, PA; in press.

Shechtman, D.; Blech, I. The microstructure of rapidly solidified Al_6M_n. J. Appl. Phys.; in press.

Shechtman, D.; Schaefer, R. J.; Biancaniello, F. S. Precipitation in rapidly solidified Al-Mn alloys. Met. Trans.; in press.

Shull, R. D.; Singhal, S. P.; Mozer, B.; Maeland, A. Phase decomposition in Cu-Ti metallic glass, in Rapidly solidified metastable materials. B. H. Kear; B. C. Giessen, eds. New York, NY: Elsevier Science Publishing Co.; in press.

Shull, R. D.; McAlister, A. J.; Reno, R. C. Phase equilibria in the titanium-aluminum system, in Titanium '84 science and technology. New York, NY: North Holland Publishing Co.; in press.

Simmons, J. A. New methods for deconvolution and signature analysis of causal and transient time series. IEEE Trans. ASSP; in press.

Rosen, M.; Klinker, H. Effect of hydrostatic pressure on the elastic properties of the rare earth-iron Laves phase compounds: Equation of state and Grueneisen parameters. J. Phys. Chem. Solids; in press.

Simmons, J. A. The role of theory in identifying crack growth modes of reactor steels using acoustic emission. Jones, R. H., ed. Proceedings of the workshop on observation and identification of crack growth modes in reactor steels using acoustic emission; in press.

Singhal, S. P.; Biancaniello, F. S.; Alperin, H. A.; Herman, H. Small-angle neutron scattering study of phase decomposition in the Ni-rich side of the Ni-$NiAl_3$ miscibility gap. Acta Met.; in press.

Swartzendruber, L. J. The Ag-Fe system. Bull. of Alloy Phase Diagrams; in press.

Swartzendruber, L. J. The Fe-Rh system. Bull. of Alloy Phase Diagrams; in press.

Testardi, L. R.; Norton, S. J.; Hsieh, T. Determination of inhomogeneities of elastic modulus and density using acoustic dimensional resonance, in The review of progress in quantitative nondestructive evaluation, Vol. 4. New York, NY: Plenum Press; in press.

Van Orden, A. C. Corrosive response of the interface tissue to 316L stainless steel, titanium based alloys and cobalt based alloys. Proceedings Am. Acad. of implant prosthodontics, 1983 November; Chicago, IL; in press.

Voorhees, P. W.; Glicksman, M. E. Ostwald ripening in two-phase mixtures--Part I. Theoretical development. Acta Met.; in press.

Voorhees, P. W.; Glicksman, M. E. Ostwald ripening in two-phase mixtures--Part II. Computer simulations. Acta Met.; in press.

Voorhees, P. W. Influence of anisotropic surface energy on grain boundary groove morphology. J. Crystal Growth; in press.

Watson, R. E.; Bennett, L. H. Optimized predictions for heats of formation of transition-metal alloys II. CALPHAD; in press.

Watson, R. E.; Sternheimer, R. M.; Bennett, L. H. Trends in the electric quadrupole fields at dilute impurity sites in transition metal-transition metal alloys. Phys. Rev.; in press.

Watson, R. E.; Bennett, L. H. Physical modelling of transition metal alloying: the roles that different levels of theory play, in High temperature alloys: theory and design. J. O. Stiegler, ed. Warrendale, PA: The Metall. Soc., AIME; in press.

Special Reports

Early, J. G.; Harne, D. E. Metallographic analysis and mechanical characterization of API SLX-70 weldments. Fitness-for-service criteria for pipeline girth-weld quality. Nat. Bur. Stand. (U.S.) NBSIR 83-1695; 1983.

Fraker, A. C.; Ruff, A. W.; Bundy, K. J. Metallurgical studies of interface bondings of implant alloys, to the Food and Drug Administration, November 1983.

Ives, L. K.; Boyer, P. A.; Ruff, A. W. Evaluation of a modified Timken test for the characterization of motor oils. Becker, D. A., ed. Proceedings of measurements and standards for recycled oil--IV. 1983; Gaithersburg, MD; Nat. Bur. Stand. (U.S.) Spec. Publ. 674.

McHenry, H. I.; Cheng, Y. W.; Dewit, R.; Early, J. G.; King, R. B.; Read, D. T. Development of allowable flaw size curves. Fitness-for-service criteria for pipeline girth weld quality. Nat. Bur. Stand. (U.S.) NBSIR 83-1695; 1983.

Mehrabian, R.; McKinley, J. D.; Steiner, B. W.; Bhansali, K. J. Technical aspects of critical materials use by the steel industry. Nat. Bur. Stand. (U.S.) NBSIR 83-2679-1; 1983.

Wadley, H. N. G.; Biancaniello, F. S.; Clough, R. B.; Cohen, M. I.; Ridder, S. D.; Rosen, M.; Schaefer, R. J.; Simmons, J. A.; Smith, J. NDE and RSP: Research on coupling two emerging technologies, Technical R&D status report to Defense Advanced Research Projects Agency, Department of Defense; September 1, 1982, to December 31, 1983.

Early, J. G. Mechanical properties of a leaded, resulfurized, rephosphorized steel in various thermo/mechanical conditions. Nat. Bur. Stand. (U.S.) NBSIR 84-2839; 1984.

Interrante, C. G.; Low, S. R.; Early, J. G. Observations of the April 8, 1979 railroad accident at Crestview, Florida. Nat. Bur. Stand. (U.S.) NBSIR 84-2858; 1984.

Manning, J. R. NBS: Materials measurements. Nat. Bur. Stand. (U.S.) NBSIR 84-2882; 1984.

Smith, J. H.; Mallen, A. W. (DOT). Evaluation of exemption application 9165N for high strength seamless steel cylinders. Memorandum Report; 1984.

Ives, L. K.; Boyer, P. A.; Peterson, M. B. Effect of $SbSbS_4$ on wear by greases containing abrasive particles, Nat. Bur. Stand. (U.S.) NBSIR; in press.

Kreider, K. G.; Semancik, S.; Olson, C. Advanced thin film thermocoupler. Nat. Bur. Stand. (U.S.) NBSIR; 1984; in press.

Ruff, A. W.; Blau, P. J. Microscopic aspects of wear, report to Office of Naval Research. Nat. Bur. Stand. (U.S.) NBSIR; 1984; in press.

Smith, J. H. Evaluation of metallic wood-burning stove chimney. Nat. Bur. Stand. (U.S.) NBSIR; 1984; in press.

Smith, J. H.; Berger, H. (Industrial Quality, Inc). Evaluation of nondestructive evaluation methods for hoop wrapped cylinders. Nat. Bur. Stand. (U.S.) NBSIR; 1984; in press.

Books

Dean, S. W.; Pugh, E. N.; Ugiansky, G. M., eds. Environment-sensitive fracture: Evaluation and comparison of test methods, ASTM STP 821. Philadelphia, PA: American Society for Testing and Materials; 1984.

Fraker, A. C.; Griffin, C. D. Corrosion and degradation of implant materials II, ASTM STP 859. Philadelphia, PA: Americal Society for Testing and Materials; 1984.

Interrante, C. G. ASTM Committee on Terminology Member Handbook. Philadelphia, PA: American Society for Testing and Materials; 1984.

Early, J. G. ed. Failure mechanisms in high performance materials. Proceedings of the 39th meeting of the mechanical failure prevention group; 1984 May 1-3; Gaithersburg, MD. New York, NY: Cambridge University Press; in press.

Wadley, H. N. G., ed. NDE in the nuclear industry. Proceedings of the sixth international conference. Metals Park, OH: American Society for Metals; in press.

Conferences and Workshops Sponsored

Fall Meeting of the Metallurgical Society, AIME
Session on Representation of Phase Diagrams
L. H. Bennett
October 1983

The Durability of Steel Piling in Soil and Coastal Marine Environments
Sponsored by NBS, NACE, AISI, ASTM
E. Escalante
October 1983

Medical Device Data Base
Co-sponsored by AMA, ASTM, ECRI, FDA and NIH
A. C. Fraker, Organizer
October 1983

Sixth International Conference on NDE in the Nuclear Industry
H. N. G. Wadley, Co-General Chairperson
November-December 1983

Modern Techniques of Microstructural and Surface Analyses (Course)
Sponsored by NBS, NRL, and Washington Chapter of ASM
C. G. Interrante, Coordinator and Member of Organizing Committee
April 1984

Second World Congress on Biomaterials
A. C. Fraker, Organizer
April-May 1984

Mechanical Failures Prevention Group Symposium
Failure Mechanisms in High Performance Materials
Sponsored by NBS, ONR, and AMMRC
J. G. Early, Chairperson
May 1984

Navy Tribology Fundamentals Workshop
Office of Naval Research
A. W. Ruff, Organizer
July 1984

Gordon Research Conference on Corrosion
G. M. Ugiansky, Session Chairperson
July 1984

Review of Progress in Quantitative NDE
Acoustic Emission Session
H. N. G. Wadley, Chairperson and Organizer
July 1984

Panel Study on Novel Methods for Materials Synthesis
Sponsored by U.S. Department of Energy
L. R. Testardi, Co-Chairperson
August 1984

Gordon Conference on NDE
Session on Acoustic Techniques Related to Measurement of Stress
H. N. G. Wadley, Chairperson
August 1984

In Process Nondestructive Microstructure Characterization and
Process Control
H. N. G. Wadley, Organizer
September 1984

Annual Meeting of the Materials Research Society
Symposium on Alloy Phase Diagrams
L. H. Bennett
November 1984

Tribology Workshop
Industrial Research Institute
A. W. Ruff, Organizing Committee
January 1985

NBS-AGA Conference, Composite Reinforced Metal
National Bureau of Standards
John H. Smith, Organizer
January 1985

Wear of Materials International Conference
American Society of Mechanical Engineers
A. W. Ruff, Chairman
April 1985

Consulting and Advisory Services

Advisory Committee of the Center for the Joining of Materials
Carnegie-Mellon University
S. R. Coriell

Interagency Strategic Material Stockpile Advisory Group
J. G. Early

Nuclear Regulatory Commission Evaluation Panel
J. G. Early

Department of Justice
Technical Assistance--Litigation of U.S.A. vs. Westinghouse
Electric Corp.
E. Escalante, E. N. Pugh, and G. M. Ugiansky

Department of Navy
Office of Naval Research, Naval Air Systems, Naval Sea Systems
A. W. Ruff

Department of Energy Advisory Committee on Novel Methods of
Materials Synthesis
R. J. Schaefer

Occupational Safety and Health Administration
Metallurgical Consultant on Union Oil Refinery Explosion
R. D. Shull

Department of Transportation
Office of Hazardous Materials Regulations
J. H. Smith

Department of Energy
Evaluation of Processes for Direct Casting of Steel
J. H. Smith

Department of Justice
Technical Assistance in Trial on Failure of Oil Pipeline
J. H. Smith

Department of Transportation
Technical Pipeline Safety Standards Committee
J. H. Smith

External Recognition

J. G. Early
ASTM Award of Merit
October 1983

C. G. Interrante
The ASTM Standards Department Certificate of Appreciation for Editorial Excellence
November 1983

A. W. Ruff
ASTM Award of Appreciation
December 1983

A. C. Fraker
ASTM M.O.S.E.S. Award
May 1984

E. N. Pugh
Willis Rodney Whitney Award
National Association of Corrosion Engineers
April 1984

E. N. Pugh
Fellow, American Society for Metals
September 1984

A. W. Ruff
American Society for Metals (Washington, DC)
George Kimball Burgess Award
May 1984

A. W. Ruff
ASTM-G2 Committee Certificate of Appreciation
May 1984

New SRMs

SRM 1851 - Dye Penetrant Crack Block with a Dull Surface
D. R. Kelley, D. S. Lashmore, and C. E. Johnson; 1983

(Number not yet assigned) - 1000 KHN, Microhardness Standard Reference Material
D. R. Kelley, C. E. Johnson, and D. S. Lashmore; 1984

Patents

Process and Bath for Electroplating Nickel-Chromium Alloys
D. S. Lashmore
U.S. Patent 4,461,680
July 24, 1984

Acoustic Emission Monitoring of Laser Drilled Hole Depth
R. B. Clough and H. N. G. Wadley
Approved for patenting
1984

Electrodeposition Process for Cobalt-Phosphorus and Nickel-Phosphorus Alloys
C. E. Johnson
Disclosure filed
1984

An Optical Method for Measuring Biaxial Deformations
R. S. Polvani
Disclosure filed
1984

Industrial Interactions

Industrial Research Associates

D. E. Clausen, National Association of Corrosion Engineers
G. M. Ugiansky, Sponsor
Responsible for the development of methods for computer dissemination of corrosion data (both tabular and graphical) for the collaborative NACE-NBS Corrosion Data Program.

B. E. Droney, Bethlehem Steel Corporation
H. N. G. Wadley, Sponsor
Responsible for ultrasonic techniques for measuring temperature and pipe/porosity in hot steel bodies for the AISI/NBS program.

J. Martinez, American Iron and Steel Institute
H. N. G. Wadley, Sponsor
Responsible for technical assistance in measurement of temperature distribution and pipe/porosity in hot steel bodies for AISI/NBS program.

J. Toth, Republic/LTV
H. N. G. Wadley, Sponsor
Development of noncontact high temperature transducers (EMATS and lasers) for the AISI/NBS program.

C. D. Rogers, U.S. Steel Corporation
H. N. G. Wadley, Sponsor
Automated data processing requirements of AISI/NBS program detection program.

R. G. Rudolph, Bethlehem Steel Corporation
H. N. G. Wadley, Sponsor
Dimensional resonance temperature profiling in slab geometries for the AISI/NBS program.

G. Dykeman, U.S. Steel Corporation
H. N. G. Wadley, Sponsor
Dimensional metrology of hot steel bodies for the AISI/NBS program.

J. S. Sims, American Society for Metals
K. J. Bhansali, Sponsor
Responsible for the development and operation of a computer database management system for graphics and text for the ASM/NBS Alloy Phase Diagram Program.

R. Forsen, American Society for Metals
K. J. Bhansali, Sponsor
Responsible for the development and operation of graphic data input techniques for the ASM/NBS Alloy Phase Diagram Program.

Industrial Guest Workers

M. A. Imam, George Washington University and Geotech Corp.
A. C. Fraker, Sponsor
Study of the microstructure of quenched specimens of titanium alloys.

P. I. Poulose, George Washington University
A. C. Fraker, Sponsor
Collaboration regarding microstructures and mechanical behavior of titanium alloys.

P. Sung, Center for Devices and Radiological Health, Food and Drug Administration
A. C. Fraker, Sponsor
Participation in implant metal research projects.

Archival Technical Papers Co-authored with Industrial Employees

Database Development under the ASM/NBS Program on Alloy Phase Diagrams, K. J. Bhansali, D. F. Redmiles, J. L. Murray, and J. Sims, Proceedings of SAMPE Symposium, Reno, NV; February 1984.

Phase Decomposition in Cu-Ti Metallic Glass, R. D. Shull, S. P. Singhal, B. Mozer, and A. Maeland (Allied Corporation, Morristown, NJ), in Rapidly Solidified Metastable Materials, B. H. Kear and B. D. Giessen, eds. New York, NY: Elsevier Science Publishing Co.; in press.

Formal Industrial Visits to NBS and from NBS

Allied Corporation/October 19, 1983
Consulted with NBS scientists concerning rapid solidification.

Carpenter Technology/October 27, 1983
Obtained assistance from NBS Metals Processing Laboratory on liquid phase sintering of refractory metals.

Indian Institute of Metals/October 1983
Visited NBS Alloy Phase Diagram Data Center.

General Electric Co. P.I.C./October 1983
Visited NBS Alloy Phase Diagram Data Center.

American Society for Metals/October 1983, March 1984
Visited NBS Alloy Phase Diagram Data Center.

Mobil Solar/November 23, 1983
Discussed laser cutting and cracking of metals.

International Copper Research Association/December 14, 1983
Discussed NBS evaluations of diffusion in copper alloys.

Alcoa Technical Center/December 16, 1983
Visited by W. J. Boettinger to discuss NBS work on rapid solidification of aluminum alloys.

SPM Corporation/January 12, 1984
Prepared research samples by using melt-spinning facilities in NBS Metals Processing Laboratory.

Hughes Aircraft/January 12, 1984
Discussed rapid solidification.

Alcoa Technical Center/January 23, 1984
Visited NBS Metals Processing Laboratory and discussed rapid solidification problems.

General Research Committee of American Iron and Steel Institute/January 1984
Visited AISI/NBS Sensor Program laboratories.

General Electric Company/February 14, 1984
Discussed cooperative activities on rapidly solidified alloy.

Martin Marietta Laboratories/February 17, 1984
Discussed cooperative work on powder processing.

Akashi/Leco Corporation/February 10, 1984
Discussed possible modifications to microhardness test machine to alleviate impact loading at low levels.

Texas Instruments/March 22, 1984
Visited surface modification facility in NBS Metals Processing Laboratory.

American Society for Metals/March 1984
Visited NBS Alloy Phase Diagram Data Center.

Deere & Company/May 16, 1984
Consulted with NBS scientists concerning interpretation of Deere & Co. experiments on cast iron performed under microgravity conditions.

Richards Medical Company/June 14, and August 7, 1984
Prepared rapidly solidified alloys for possible medical implant applications using facilities in NBS Metals Processing Laboratory.

IBM Corporation/June 11, 1984
Visited NBS Metallurgy laboratories and data centers.

Alcoa Technical Center/June 25, 1984
Visited by C. G. Interrante, M. J. Kaufman, and E. N. Pugh to discuss cooperative programs on the stress corrosion cracking of Al alloys.

Alcoa Technical Center/August 1984
Visited NBS Metallurgy laboratories and data centers.

Leco Corporation/August 29, 1984
Received overview on modification of microhardness test machines (static) to dynamic microhardness testing.

Wilson Corporation/September 27, 1984
Received overview on modification of microhardness test machines (static) to dynamic microhardness testing.

W. Canning & Company/September 17, 1984
Interested in licensing our patent on Ni-Cr alloy deposition.

Cooperative Programs

American Iron and Steel Institute (William Dennis)
Conduct research and development for sensors to measure temperature distributions and pipe/porosity in hot steel bodies.
H. N. G. Wadley

University of Notre Dame, Notre Dame, IN (Prof. G. Sargent)
Fugacity measurements of steels in sulfide environments
C. G. Interrante

Vanderbilt University, Nashville, TN (Prof. B. D. Lichter)
SCC of copper alloys
E. N. Pugh

Wyle Laboratories (Ralph MacDonald) and Lehigh University, Bethlehem, PA (Prof. D. Updike)
Joint project on the stress analysis of intermodel cargo tank
J. H. Smith

Wyle Laboratories (R. Quinne)
Joint project on tensile ductility of cylinders
J. H. Smith

Industrial Quality, Inc. (H. Berger), and Detek, Inc. (A. Julien)
Joint project on development of eddy current techniques for inspection of composite cylinders
J. H. Smith

Microalloying International (Dr. M. Grey)
Application of ductility parameter to pipeline fracture
J. H. Smith

Artech Corporation, Falls Church, VA
Joint project on arc plasma spraying
A. C. Fraker

3-M Corporation, Minneapolis, MN
Joint project on fatigue of cobalt alloys
A. C. Fraker

Howmedica, Inc., Rutherford, NJ
Joint project on pitting/crevice corrosion of cobalt alloys
A. C. Fraker

Depuy, Inc., Warsaw, IN
Joint project on corrosion fatigue of porous cobalt alloys
A. C. Fraker

C. S. Draper Laboratory, Inc., Cambridge, MA
Support and interaction to determine the microcreep of two developmental grades of beryllium
R. S. Polvani

Data Programs with Substantial Industrial Support and/or Guidance

(1) ASM-NBS Alloy Phase Diagram Program

The ASM-NBS International Program for Alloy Phase Diagrams involves critical evaluation, publication, and computerization of phase diagram and ancillary data. ASM has raised nearly $4 million in support of the data program. Several industrial laboratories have been designated "prototype users" of the on-line computer database to aid in the design of the searching capabilities. Funding for the program has been solicited by ASM and provided by foundations, industry, government, and individual contributors. Support is provided for all elements of the program.

(2) NACE-NBS Corrosion Data Program

Agreement between the National Association of Corrosion Engineers (NACE) and NBS resulted in the placement of a full-time Research Associate at NBS to work on dissemination methods for the NACE-NBS Corrosion Data Program. The central focus of this program is the establishment of an evaluated corrosion database which can be easily computer accessed to provide the user with the required data in any of a number of possible graphical or tabular formats. Data projects have been initiated in the areas of kinetic and thermodynamic corrosion data. In the kinetic area, the projects include atmospheric corrosion, localized corrosion, and uniform corrosion. In the thermodynamic area, efforts have been focused on stability diagrams of the electrochemical potential-pH type known as Pourbaix diagrams.

Other Significant Formal Interactions

Participated in Westinghouse Electric Corp. Panel Meeting on Steam Generator J-Tube Wall Thinning, Pittsburg, PA, February 1984.
E. N. Pugh

Idaho National Engineering Laboratory, Idaho Falls, ID, Evaluation of direct casting metals for steel.
J. H. Smith

American Die Casting Institute, Cleveland, OH, Participation in quarterly meetings to advise, coordinate research on wear and erosion.
A. W. Ruff

Industrial Research Institute, planning committee work for Tribology Conference in January 1985.
A. W. Ruff

APPENDIX

U.S. Department of Commerce
National Bureau of Standards

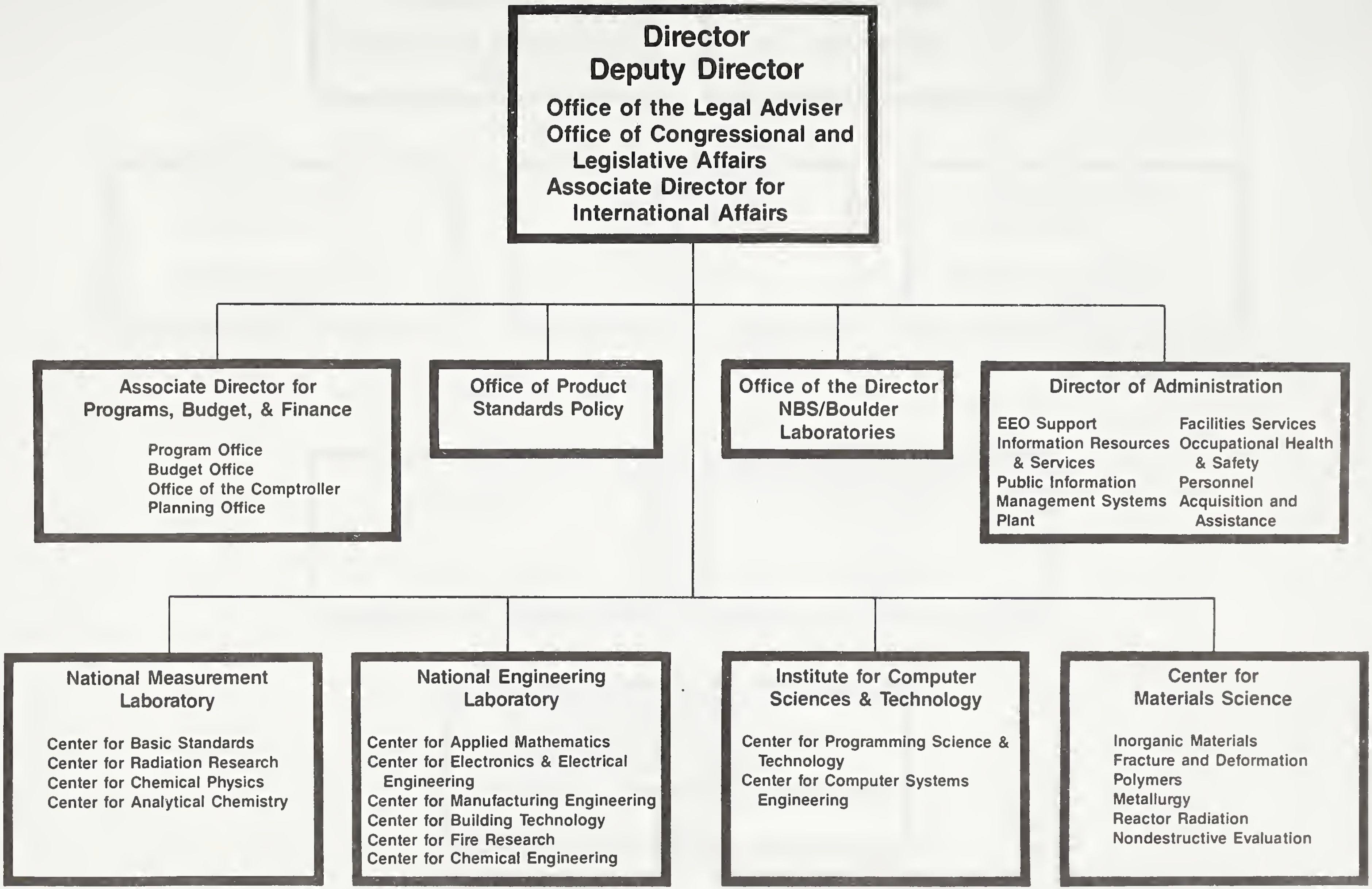

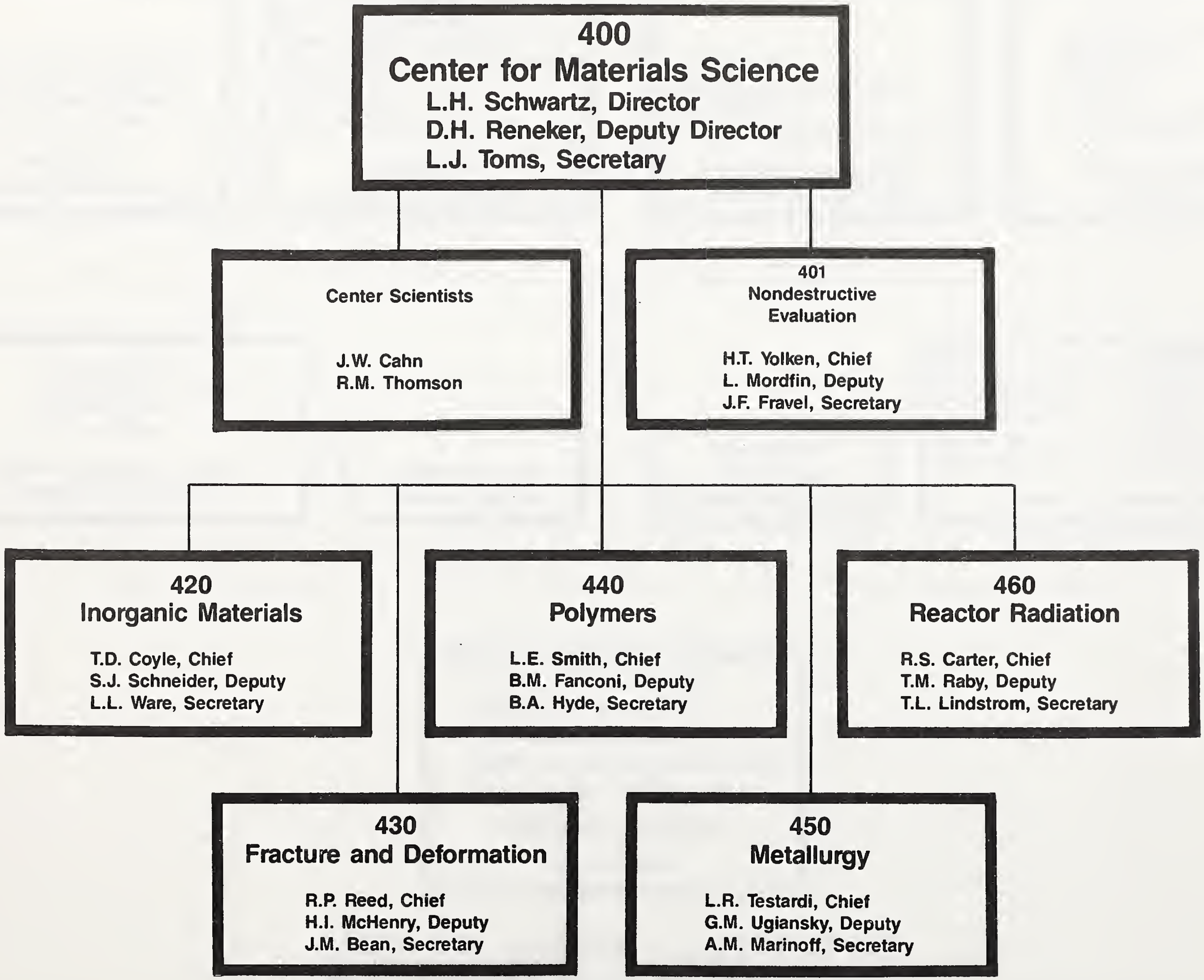
400
Center for Materials Science
L.H. Schwartz, Director
D.H. Reneker, Deputy Director
L.J. Toms, Secretary
Center Scientists
J.W. Cahn
R.M. Thomson
401
Nondestructive Evaluation
H.T. Yolken, Chief
L. Mordfin, Deputy
J.F. Fravel, Secretary
420
Inorganic Materials
T.D. Coyle, Chief
S.J. Schneider, Deputy
L.L. Ware, Secretary
440
Polymers
L.E. Smith, Chief
B.M. Fanconi, Deputy
B.A. Hyde, Secretary
460
Reactor Radiation
R.S. Carter, Chief
T.M. Raby, Deputy
T.L. Lindstrom, Secretary
430
Fracture and Deformation
R.P. Reed, Chief
H.I. McHenry, Deputy
J.M. Bean, Secretary
450
Metallurgy
L.R. Testardi, Chief
G.M. Ugiansky, Deputy
A.M. Marinoff, Secretary

NBS-114A (REV. 2-80)

U.S. DEPT. OF COMM. BIBLIOGRAPHIC DATA SHEET (See instructions)	1. PUBLICATION OR REPORT NO.	2. Performing Organ. Report No.	3. Publication Date
	NBSIR-84-2995		January 1985

4. TITLE AND SUBTITLE

Metallurgy Division Technical Activities 1984

5. AUTHOR(S) L. R. Testardi, G. M. Ugiansky, M. Kuriyama, J. R. Manning, A. W. Ruff, K. J. Bhansali, E. N. Pugh, D. S. Lashmore, H. N. G. Wadley

6. PERFORMING ORGANIZATION *(If joint or other than NBS, see instructions)*

NATIONAL BUREAU OF STANDARDS
DEPARTMENT OF COMMERCE
~~WASHINGTON, D.C. 20234~~
Gaithersburg, MD 20899

7. Contract/Grant No.

8. Type of Report & Period Covered

9. SPONSORING ORGANIZATION NAME AND COMPLETE ADDRESS *(Street, City, State, ZIP)*

10. SUPPLEMENTARY NOTES

☐ Document describes a computer program; SF-185, FIPS Software Summary, is attached.

11. ABSTRACT *(A 200-word or less factual summary of most significant information. If document includes a significant bibliography or literature survey, mention it here)*

This report summarizes the 1984 activities of the Metallurgy Division of the National Bureau of Standards. The research centers upon the structure-processing-properties relations of metals and alloys, and on the methods of their measurement. Task efforts comprise studies of synchrotron radiation research for materials characterization, metallurgical processing, wear and mechanical properties, chemical metallurgy, corrosion and protection of metals, electrodeposition, and nondestructive characterization. The work herein described includes three cooperative data programs with American professional societies and industry: the American Society for Metals-NBS Alloy Phase Diagram Program, the National Association of Corrosion Engineers-NBS Corrosion Data Program, and the American Iron and Steel Institute-NBS Steel Sensor Program. New facilities include specialized hardware for the National Synchrotron Light Source, Hot Isostatic Pressing apparatus, gas atomizer for rapidly solidified powder production, a 300 kV transmission electron microscope, and a thermal wave measurement system. The scientific publications, invited talks, committee participation, and other professional interactions of the 95 full-time and part-time permanent members of the Metallurgy Division and its 30 guest researchers (in 1984) are identified.

12. KEY WORDS *(Six to twelve entries; alphabetical order; capitalize only proper names; and separate key words by semicolons)*

corrosion; electrodeposition; mechanical properties; metallurgy; nondestructive characterization; phase diagrams; processing; wear; x-ray characterization

13. AVAILABILITY

☒ Unlimited
☐ For Official Distribution. Do Not Release to NTIS
☐ Order From Superintendent of Documents, U.S. Government Printing Office, Washington, D.C. 20402.
☒ Order From National Technical Information Service (NTIS), Springfield, VA. 22161

14. NO. OF PRINTED PAGES

170

15. Price

$16.00